STRATEGIES, TACTICS, AND TOOLS TO ACHIEVE

CHEMICAL SYNTHESES OF CIS-CLERODANE TERPENOIDS

Qinda Ye

Submitted in partial fulfillment of the
requirements for the degree of
Doctor of Philosophy
in the Graduate School of Arts and Sciences

COLUMBIA UNIVERSITY

2015

ABSTRACT

Strategies, Tactics, and Tools to Achieve Chemical Syntheses of *cis*-Clerodane Terpenoids

Qinda Ye

The clerodane diterpenoids are a large group of secondary metabolites that display an array of biological activities and structural diversity. This dissertation details our efforts to synthesize clerodane natural products through a unified design and the use of a key synthetic intermediate.

Thus, Chapter 1 will serve to introduce this unique and interesting class of terpenoids, beginning with their proposed biosynthesis. This section will be followed by a highlight of their diverse biological activities. Lastly, a select collection of representative total syntheses will be described to provide a sense of the state of the art in accessing their molecular complexity.

Next, Chapter 2 will begin with our design of a two-phase approach towards the clerodane family, followed by an introduction of scaparvin A as an excellent example of a target with complex architecture and multiple oxygenated functional groups worthy of synthetic and biological study. In addtion, a detailed retrosynthetic analysis of scaparvin A will be described based on our global strategy for accessing the family.

Then, we will focus our discussion in Chapter 3 on the efficient construction of the common intermediate, while two modes of directed C–H oxidation to deliver the requisite oxidation state will be covered in Chapter 4. Finally, efforts of late-stage modification towards

scaparvin A and related compounds will be summarized in Chapter 5, culminating in a near complete synthesis of scaparvin A as well as a completed total synthesis of scaparvin C.

TABLE OF CONTENTS

List of Figures

List of Schemes

ACKNOWLEDGEMENTS

I would like to thank the following people and organizations for their support during my five-year graduate study:

Professor Scott Snyder for being a mentor and a source of scientific inspiration, as well as always being supportive throughout the research.

The Snyder group for giving me a welcoming and enlightened environment to carry out my research.

Dr. Adel ElSohly for helping to train me as an organic chemist, and for your constant inspiring conversation.

Dr. Myles Smith for being a great lab-mate for four and half years.

Pei Gan and Alison Gao for being wonderful lab-mates, and friends.

Professor Breslow, Professor Danishefsky, and Professor Lambert for serving on my committee, and for discussions about chemistry.

Dr. John Decatur, Dr. Yasuhiro Itagaki, and Dr. Xiangming Kong for support and expertise in helping with spectroscopic analysis.

Alix, Carol and Dani for your help over the years.

My family for all your love and for always being supportive even when you are thousands of miles away.

CHAPTER 1

THE CLERODANE TERPENOIDS: BACKGROUND, BIOSYNTHESIS, BIOLOGICAL ACTIVITIES, AND PREVIOUS TOTAL SYNTHESES

1.1 Introduction

The clerodane diterpenoids (general structure **1**, Figure 1) are a large group of secondary metabolites that have long been known within the scientific community.[1] The structure of clerodin (**2**), the inaugural member of the clerodane series, was elucidated by Barton in 1961,[2] and its absolute stereochemistry was revised in 1979.[3] In the ensuing decades, over one thousand diterpenoids and nor-diterpenoids with the clerodane carbon framework have been separated and identified, and these compounds often show a variety of interesting biological activities, including antifeedant, antitumor, antifungal, antibiotic, and anti-pepticulcer properties.[1a,4]

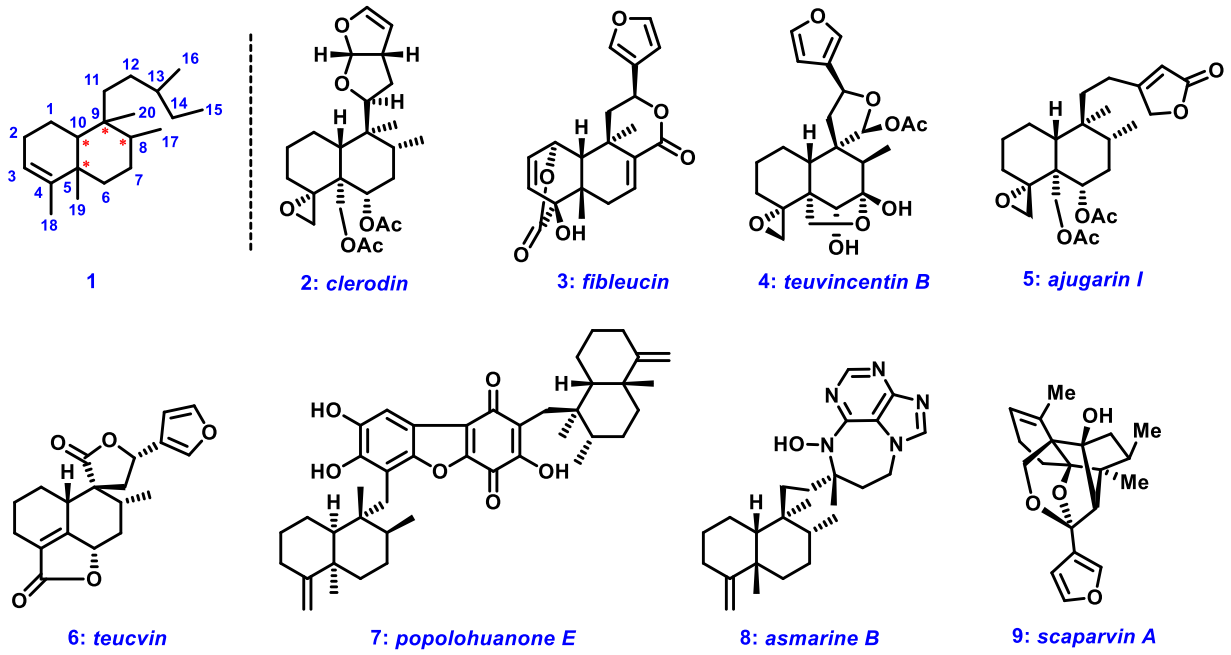

Figure 1. The diverse structures of representative clerodane terpenoids.

Structurally, most clerodane diterpenoids have four contiguous stereogenic centers on a decalin skeleton as shown in **1**. This unique structural feature, along with their diverse biological activities, have attracted intense synthetic studies and total synthesis efforts.[5] Globally, this opening chapter will serve to introduce this unique and interesting class of terpenoids, beginning

with their proposed biosynthesis. This section will be followed by a highlight of their diverse biological activities. Finally, a select collection of representative total syntheses will be described to provide a sense of the state of the art in accessing their molecular complexity.

1.2 Biosynthesis of the Clerodane Terpenoids

Biosynthetically, the clerodane terpenoids appear to be related to the labdanes via a series of methyl and hydride shifts (Scheme 1). The formation of the labdane carbon backbone itself can be rationalized by a cyclases-catalyzed cyclization[6] of geranylgeranyl diphosphate (**10**).[7] Sequentially, the labdadienyl cation formed (**11**) could be converted into naturally occurring labdanes through several oxidative steps, shown as grindelic acid (**12**).

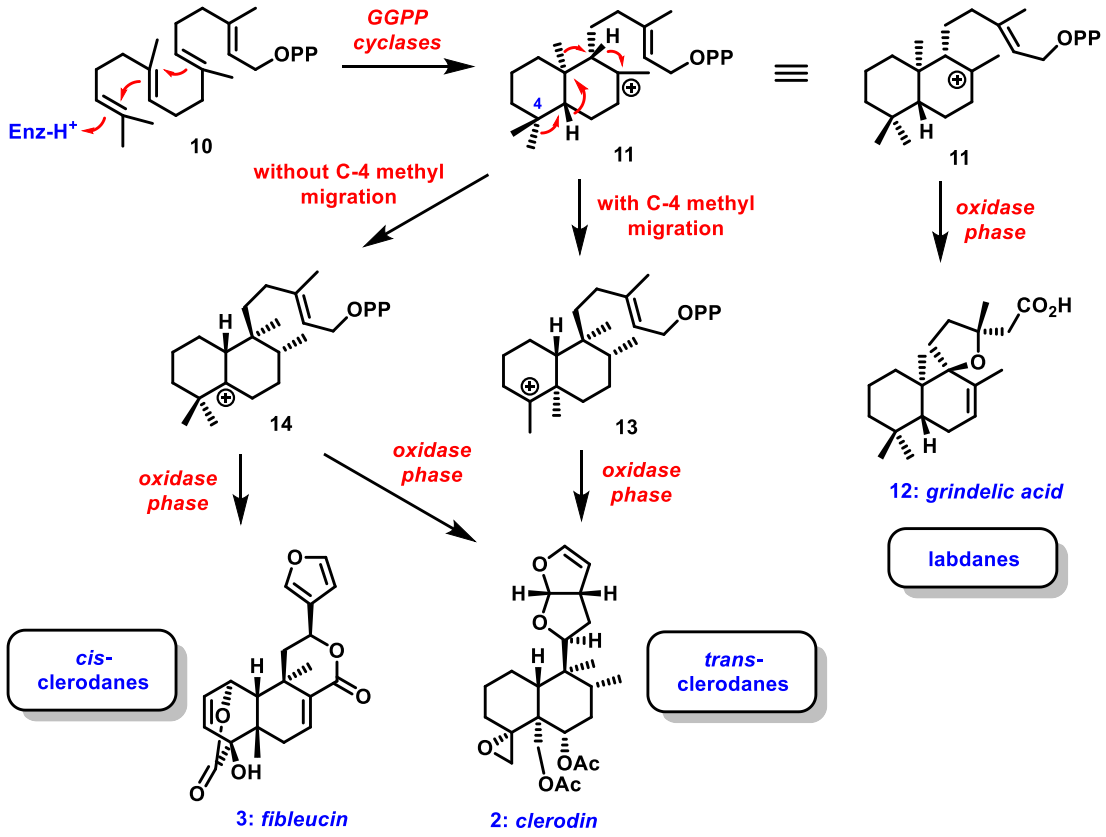

Scheme 1. Proposed biosynthesis for the clerodane diterpenoids.

However, when the rearrangement of labdadienyl cation (**11**) proceeds in a concerted manner up to the shift of 4α-methyl group, clerodane terpenoids with a *trans*-ring fusion (shown as clerodin **2**) will be resulted after an oxidase phase. By contrast, the wide occurrence of *cis*-clerodanes (shown as fibleucin, **3**[8]) suggests the intervention of a stepwise process with a "pause" at intermediate **14**, which then leads to either *cis*- or *trans*- products, dependant upon which of the C-4 methyl groups migrates.

The other variation of relative stereochemistry within the class is associated with the stereogenic center at C-8 (Figure 2). In most cases, the C_1-unit groups at C-8 and C-9 are *cis* as predicted from the biosynthesis, while a *trans* configuration exists in a small percentage of the naturally occurring clerodane diterpenoids (as in **4** and **15**).

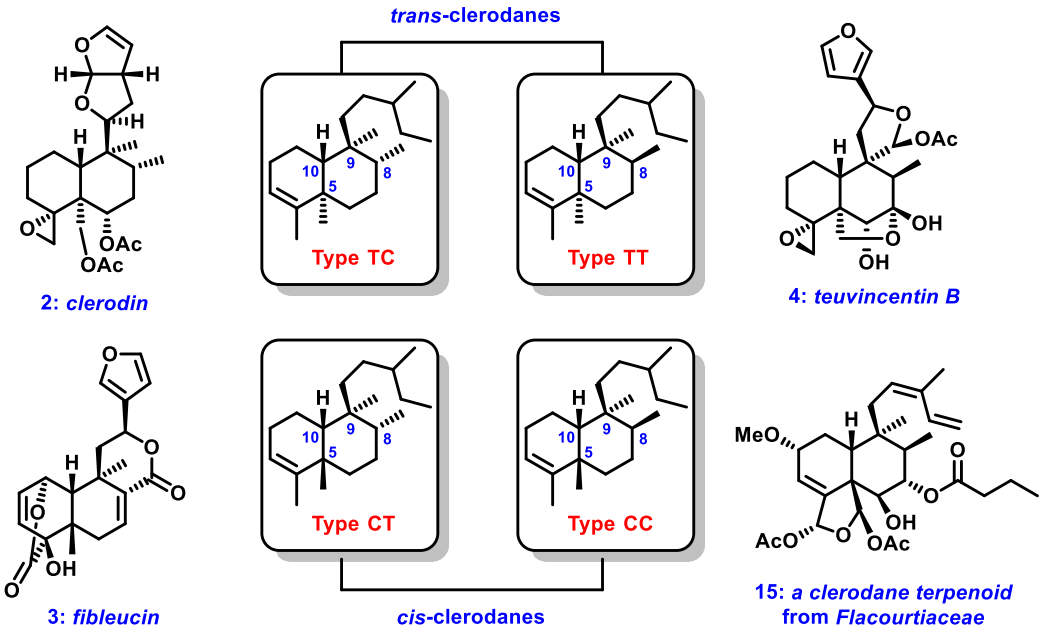

Figure 2. Stereochemical variety in clerodane terpenoids.

Thus, four types of the clerodane carbon skeleton (Figure 2) are distinguished with respect to the configuration of ring fusion and the substitution at the C-8 and C-9 positions (Types TC, TT, CC, and CT). As for the absolute configuration, the compounds are classified into two classes, *neo*- (as illustrated) and *ent-neo*-clerodanes (reversed).[3]

1.3 Biological Activity of the Clerodane Terpenoids

Only a small percentage of the clerodanes have been reported to exhibit any biological activity. However, even fewer members have been shown to have no activity in the tests carried out, thus rendering the majority as simply untested or unreported in terms of functional properties.[1a] The reported biological activities range from antifeedant, antitumor, antifungal, and

antibiotic to anti-pepticulcer activity.[1a,4] In this section, a number of clereodane natural products with unique biological activities will be highlighted.

The insect antifeedant activities of the clerodane diterpenoids is by far the most extensively studied biological property,[9] with an emphasis placed on the safety aspects of natural insect antifeedants in relation to mammalian life. Significant activity is sometimes displayed at low concentrations, and more importantly, that activity could be directed specifically against a narrow group of insect pests, leaving beneficial insects and other species unharmed.

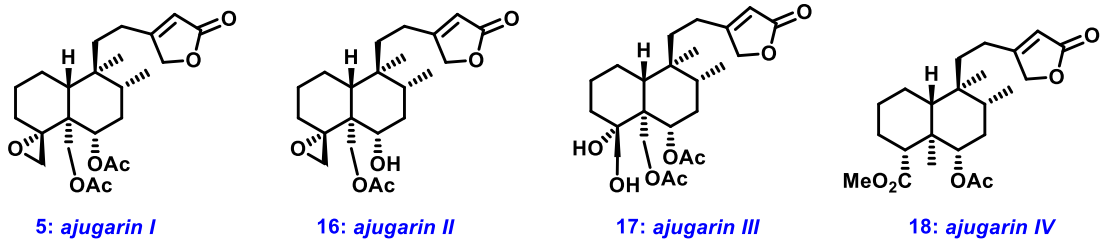

Figure 3. The structures of ajugarins I-IV.

For instance, of the compounds obtained from the *Ajuga genus* (Labiatae), ajugarins I-III[10] (**5**, **16**, **17**, Figure 3) show antifeedant activity towards the African army worm and African desert locust (*Schisticerea gregaria*), whilst ajugarin IV[11] (**18**) acts as an insecticide against *Bombyx mori*.[12]

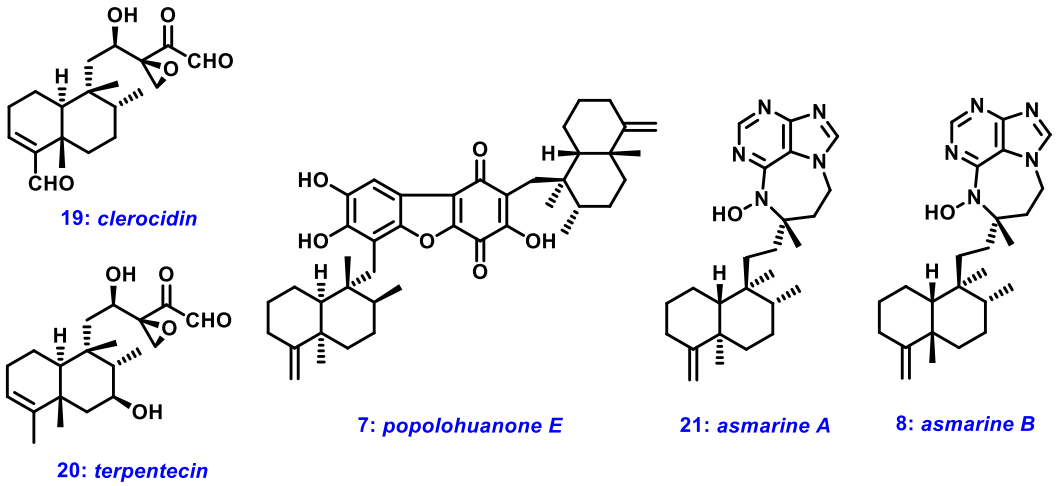

Figure 4. The structures of clerodanes with antitumor activities.

Biological evaluation of clerodane terpenoids in the recent decades has revealed many compounds with appealing antitumor activities. For example, clerocidin (**19**)[13] and terpentecin (**20**)[14], potent antibiotics, also displays impressive antitumor activities involving topoisomerase II mediated DNA cleavage.[15] Popolohuanone E (**7**), an oxidatively-dimerized arenarol derivative, acts as a potent inhibitor of topoisomerase II, and is also proved to be selectively cytotoxic to human non-small cell lung cancer cell line.[16] In addition, asmarines A (**21**) and B (**8**) have been found to have cytotoxic activities against a variety of cancer cells, including P-388 murine leukemia, A-549 human lung carcinoma, HT-29 human colon carcinoma and MEL-28 human melanoma.[17]

Noteworthy, too, is the fact that many clerodanes exhibit other interesting biological properties, providing opportunities to better understand biological processes in more general terms. For instance, teucvin (**6**)[18], isolated from the *Mallotus* (Euphorbiaceae) and *Teucrium* (Labiatae) genera, has been shown to be amoebicidal and can act as a root development

inhibitor,[19] while agelasine A (**22**) and B (**23**) have been reported as Na,K-ATPase inhibitors[20] which have *trans*- and *cis*-clerodane moieties respectively.

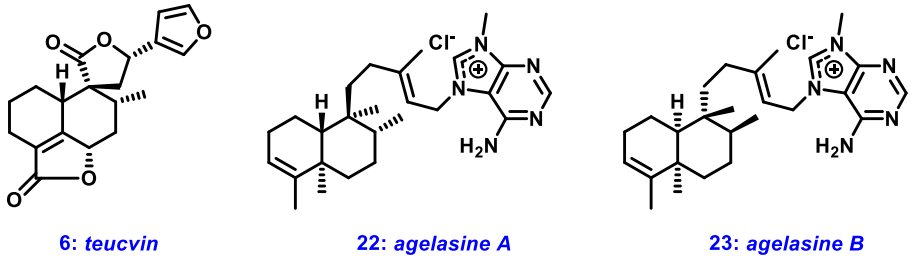

Figure 5. The structures of teucvin, agelasine A and B.

Indeed, to have such a range of activities within a given class is impressive, and argues strongly that a comprehensive codification of structure-activity relationships could be of broad value in the design of even more potent and selective materials. Therefore, the clerodane family has attracted substantial attention from synthetic chemists.

1.4 Selected Total Syntheses of Clerodane Terpenoids

Prior to 1980s, synthetic efforts towards the clerodane class were relatively limited, in spite of a rapid increase in numbers of isolated natural products. By contrast, a large body of work has appeared during the last thirty-five years, driven largely, we believe, by their complex structures and promising biological activities as noted above.

In 2000, Tokoroyama published a thorough and detailed review[5] summarizing the syntheses of clerodane and related terpenoids. So far, the key question addressed in most syntheses of clerodanes is how to construct the decalin framework with the contiguous

stereogenic centers. Herein, only a select collection of total syntheses will be presented, focusing our discussion on classic disconnection strategies and recent developments to form the characteristic decalin ring of the class. Although a few other important synthetic studies in the clerodane realm have been conducted,[21] their discussion will be deferred to later chapters in the cases where they are relevant to key design considerations of our own approach.

*1.4.1 Total Synthesis of (–)-Ilimaquinone (**24**)*[22]

The Wieland–Miescher type of diketone (**25**)[23] is a versatile synthon which has been employed predominantly in the total synthesis of terpenoids and steroids. Either optically pure enantiomer is available via amino acid-assisted asymmetric cyclization and subsequent product recrystallization.[24] Following the first total synthesis of clerodane diterpenoid by Kakisawa in 1979,[25] Wieland–Miescher diketone of type **25** has been widely utilized as starting material for the synthesis of this family. As an example, the Samadi synthesis of (–)-ilimaquinone (**24**), achieved in 1998, will be discussed below.[22]

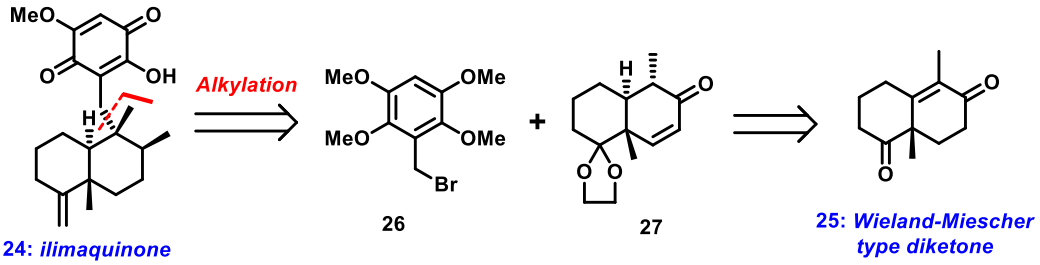

Scheme 2. Key strategic disconnections employed in the Samadi synthesis of ilimaquinone (**24**).

The marine natural product ilimaquinone (**24**)[26] was demonstrated to inhibit the toxicity of ricin and diphteria toxin,[27] to reversibly disrupt the Golgi complex,[28] and to provoke the loss

of the gap junction plaques and inhibition of intercellular communication in BICR-MIRk and NRK cells.[29] Thus, ilimaquinone appears as a valuable tool for the investigation of some important biological processes. In this vein, the Samadi group aimed to install the quinine moiety (**26**) by alkylation of enone (**27**), a material that, in turn, could be traced back to Wieland–Miescher diketone (**25**).

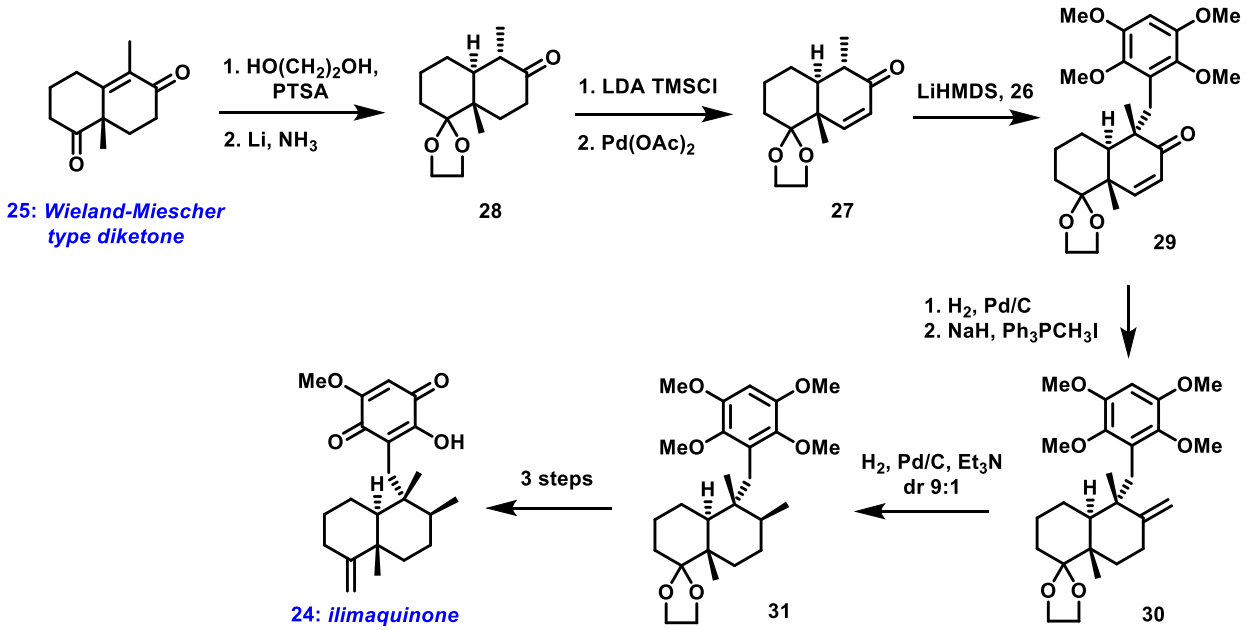

Scheme 3. The Samadi synthesis of ilimaquinone (**24**).

In the event, Wieland–Miescher diketone (**25**, Scheme 3) was selectively protected as its monoketal derivative, followed by Birch reduction of the double bond to give the saturated ketone **28** as a single isomer. Ketone **28**, in turn, was then converted into the corresponding enone (**27**) via Saegusa oxidation. Next, coupling of **27** through its lithium dienolate in the presence of benzyl bromide **26** cleanly furnished addition product **29** as a single isomer. The product of catalytic hydrogenation of **29** was subsequently submitted to Wittig olefination to give *exo* olefin **30**. Finally, hydrogenation of olefin **30** over Pd/C in Et_3N afforded compound **31**

with 9:1 d.r., which afforded 10 step synthesis of ilimaquinone (**24**) from Wieland–Miescher diketone (**25**).

*1.4.2 Total Syntheses of (±)-Mamanuthaquinone (**32**)[30] and (±)-Teucvin (**6**)[31]*

In spite of limited application of intramolecular Diels–Alder reactions with the class, two types of intermolecular Diels–Alder strategies have been widely employed in the stereoselective construction of clerodane and related skeletons (Scheme 4).

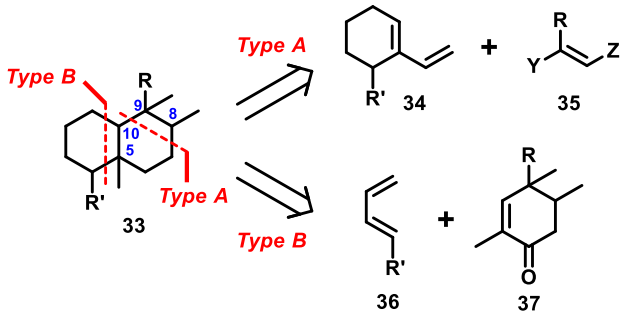

Scheme 4. Two types of disconnections employed in Diels-Alder strategies.

For the first approach, termed as type A, an intermolecular Diels–Alder reaction using 1-vinylcyclohexene derivatives of type **34** as the diene component would simultaneous establish three stereogenic centers at C-8, C-9, and C-10. While the task for the introduction of an angular substituent at C-5 remains to be fulfilled for the synthesis of clerodanes, the present method particularly suits the synthesis of isolabdane-type compounds.

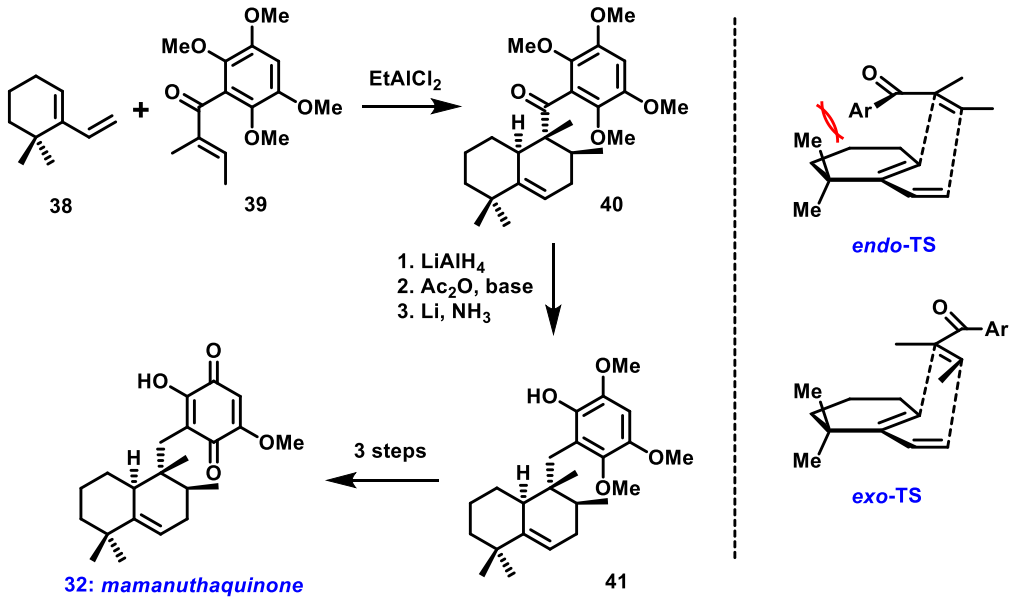

Scheme 5. The Danishefsky synthesis of mamanuthaquinone (**32**).

In the course of total synthesis of (±)-mamanuthaquinone (**32**),[30] the Danishefsky group investigated the stereoselectivity of a Diels–Alder reaction between vinylcyclohexene **38** and enone **39**. When mediated by $EtAlCl_2$, this cycloaddition afforded a single diastereomer in the form of **40**. In this case, the *endo* mode of the reaction is highly disfavored due to repulsion of the sterically demanding aroyl group with the dimethyl quaternary carbon on the diene (Scheme 5). With cycloadduct **40** in hand, a reduction/acylation/Birch reduction sequence gave phenol **41**, which in turn provided mamanuthaquinone (**32**) via several routine chemical transformations.

By contrast, the type B method, which utilizes cyclohexenone or benzoquinone derivatives in the form of **37** (Scheme 4) as the dienophile component, generally allows the establishment of C-5 and C-10 stereogenic centers.

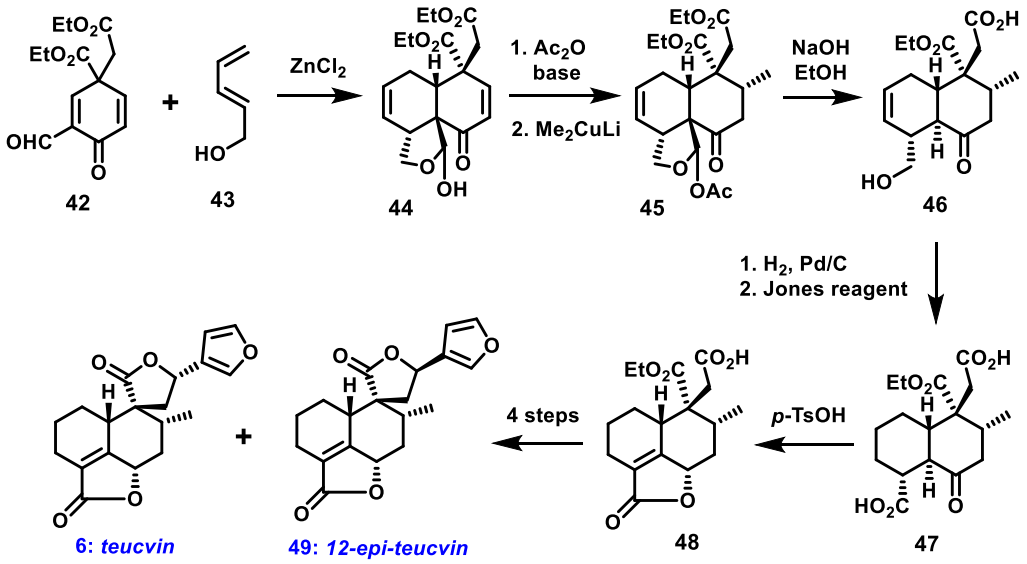

Scheme 6. The Liu synthesis of teucvin (**6**).

In the total synthesis of (±)-teucvin (**6**),[31] the Liu group showcased a $ZnCl_2$–catalyzed Diels–Alder reaction of dienophile **42** and diene **43**. This reaction occurred in a completely facial and stereoselective (*endo*) manner, as a result of concomitant intramolecular hemiacetal formation. Subsequent acylation of cycloadduct **44**, followed by conjugate addition, afforded compound **45** which was, in turn, deformylated under the condition of NaOH in EtOH. Then, catalytic hydrogenation of **46** followed by Jones oxidation provided acid **47**. Next, the γ-lactone ring was introduced by a sequence of enol lactone ring formation and double bond isomerization. Under thermodynamic–controlled conditions (*p*-TsOH in refluxing benzene), the more stable epimer **48** was obtained as the sole product. Finally, continuation of the synthesis from **48** resulted in the production of teucvin (**6**) in four further steps alongside its epimer (**49**).

*1.4.3 Total Synthesis of (±)-Linaridial (**50**)*[32]

In 1987, the Tokoroyama group published the first total synthesis of linaridial (**50**)[32] through a route which centered upon the use of the Hosomi–Sakurai reaction to construct the decalin core with diastereocontrol at three contiguous carbon (Scheme 7).

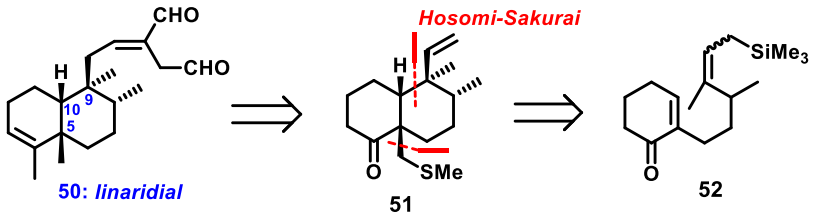

Scheme 7. Key strategic disconnections employed in the Tokoroyama synthesis of linaridial (**50**).

In the key event, the cyclization of allylsilane substrate **52** in the presence of $TiCl_4$ and chloromethyl methyl sulfide ($ClCH_2SMe$) was found to afford a single diastereomer of product in the form of **53** under perfect dual stereo-regulation, an outcome which can be explained in terms of orientation and folding-strain stereocontrols (Scheme 8). From an orientation perspective on stereocontrol, antiperiplanar transition state (TS) **54** should be favored over synclinal TS **55** if a chair-like conformation is assumed to be preferred. The folding-strain stereocontrol is concerned with diastereofacial selection with regard to the C-8 position. Of the two possible diastereomeric foldings (**54** and **56**), **54**, with the pseudo-equatorial methyl group, would be more stable than **56** in view of its 1,3-allylic repulsion and gauche interaction.

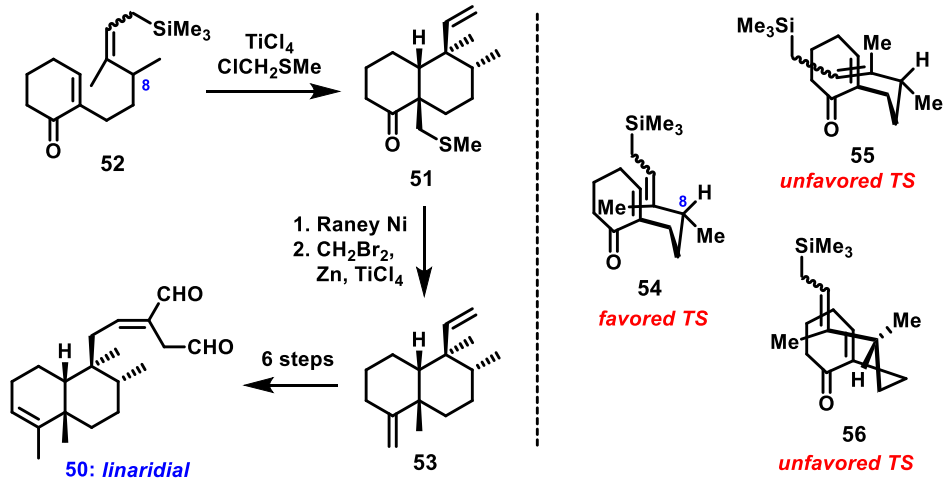

Scheme 8. The Tokoroyama synthesis of linaridial (**50**).

Next, with decalin **51** in hand, reductive removal of the methylthio group in **51**, followed by methylenation using the Nozaki procedure, worked excellently to yield diene **53**. From here, the total synthesis of linaridial **50** was achieved in six additional steps.

1.4.4 Total Synthesis of (±)-Maingayic acid (57)[33]

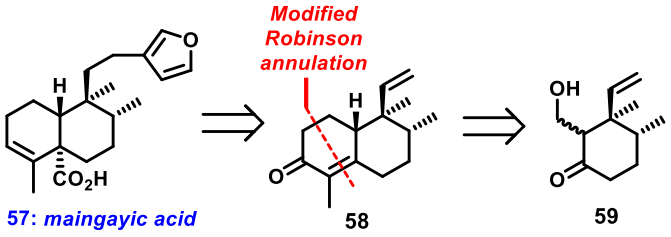

Scheme 9. Key strategic disconnections employed in the Tokoroyama synthesis of maingayic acid (**57**).

Robinson-type annulation reactions have also been widely used to assemble the decalin skeleton of the clereodane terpenoids. For instance, Tokoroyama and co-workers' total synthesis

of (±)-maingayic acid (**57**, Scheme 9) featured a modified Robinson annulation protocol of compound **59** which could be readily obtained from commercially available starting materials.[33]

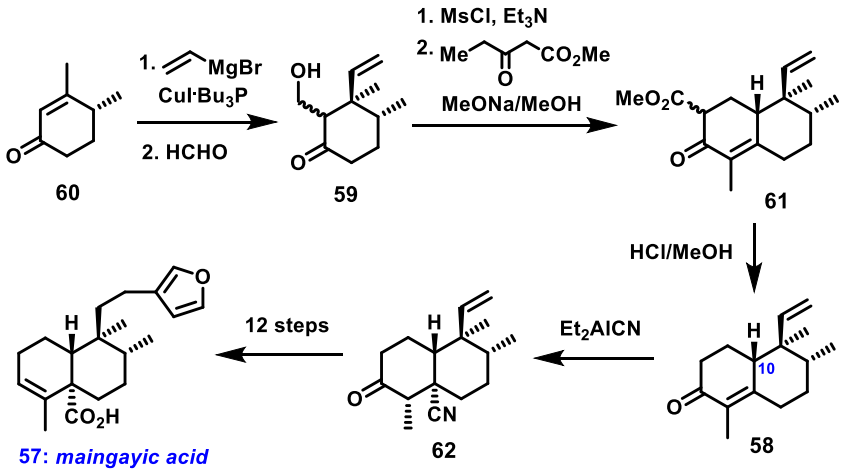

Scheme 10. The Tokoroyama synthesis of maingayic acid (**57**).

In the forward sense, stereoselective conjugate addition of vinyl cuprate to enone **60** and subsequent modified Robinson annulation afforded compound **58**. The stereogenic center at the ring junction (C-10) is favorably introduced under thermodynamic control. Next, hydrocyanation of **58** yielded *trans*-addtion product **62**, from which a total synthesis of maingayic acid **57** was accomplished.

*1.4.5 Total Synthesis of (–)-Solidagolactone (**63**)*[34]

In a recent example of a total synthesis of the clerodane natural products, the Overman group aimed to employ a radical 1,6-addition to install the side chain at the C-9 position. As additional key disconnections, they planned to complete the decalin framework of **64** through an enantioselective conjugate addition/intramolecular alkylation sequence.

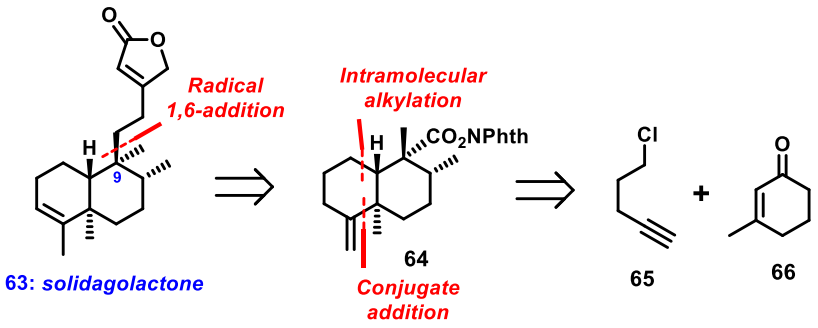

Scheme 11. Key strategic disconnections employed in the Overman synthesis of solidagolactone (**63**).

In the actual synthesis, beginning with the readily available alkyne **65** and enone **66**, Nickel-catalyzed hydroalumination, followed by catalytic enantioselective conjugate addition of the resulting internal vinylaluminum intermediate using Hoveyda's silver-NHC complex, gave **67** with high enantio-enrichment. Chlorohexanone **67** was then cyclized into decalone **68**. This material was then methylated and converted into nitrile **69** upon base-promoted reaction with *p*-toluenesulfonylmethyl isocyanide (TosMIC). From **69**, they were able to reach (*N*-acyloxy)phthalimide **64**, which when exposed to visible light in the presence of $Ru(bpy)_3(BF_4)_2$, the Hantzsch ester, and vinylbutenolide, afforded the desired coupling product in high yield as a single diastereomer. This critical operation which had stereoselection at C-9 is reasoned by coupling of the tertiary radical with radical acceptor from the less-hindered equatorial face (**71**). From here, straightforward double bond isomerization of the resulting product using $RuCl_3$ then completed an impressive synthesis of solidagolactone (**63**).

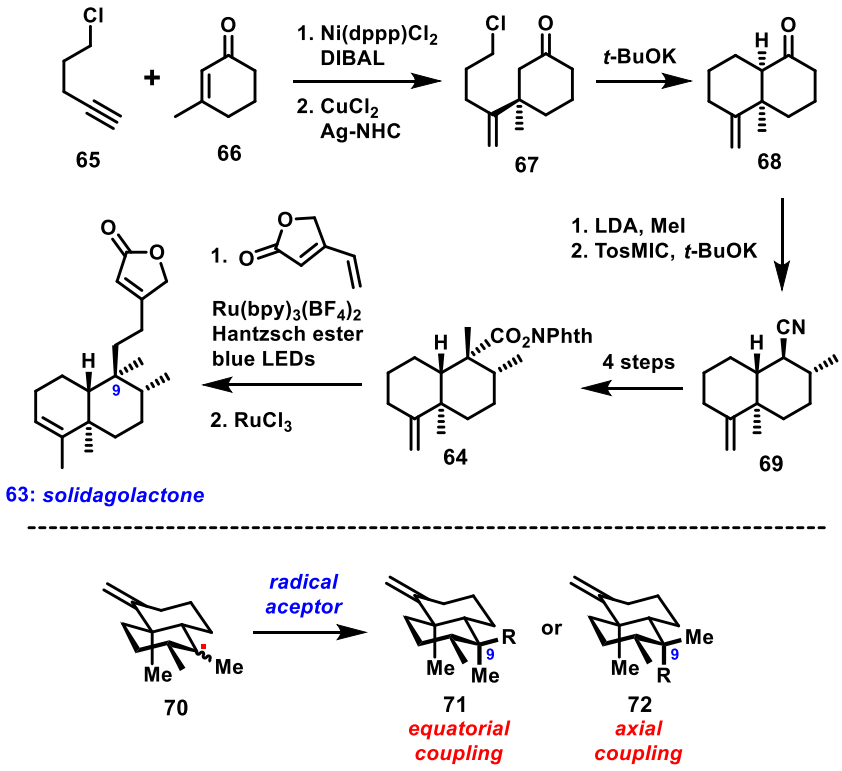

Scheme 12. The Overman synthesis of solidagolactone (**63**).

1.5 Conclusions

Chemists have rallied over the last several decades to produce many appealing synthetic solutions to the clerodane family of natural products. The interest in these materials has strongly been driven by the rich diversity of structure and biological activities that this family holds, as well as the opportunity for synthetic innovation, principally focused on the stereoselective construction of the decalin framework. As will be seen in the following chapters, it was these attractive features that drew our attention to the clerodane terpenoids as compelling targets for total synthesis, and afforded the opportunity to develop a number of strategies and tactics distinct from those defined in this chapter which we hope will have broad applicability.

1.6 References

(1) (a) Merritt, A. T.; Ley, S. V. *Nat. Prod. Rep.* **1992**, *9*, 243. (b) Rodríguez-Hahn, L.; Esquivel, B.; Cárdenas, J. In *Fortschritte der Chemie organischer Naturstoffe / Progress in the Chemistry of Organic Natural Products*; Herz, W., Kirby, G. W., Moore, R. E., Steglich, W., Tamm, C., Eds.; Springer Vienna, 1994; Vol. 63. (c) Silva, L.; Gomes, A. C.; Rodilla, J. M. L. *Nat. Prod. Commun.* **2011**, *6*, 497.

(2) Barton, D. H. R.; Cheung, H. T.; Cross, A. D.; Jackman, L. M.; Martin-Smith, M. *J. Chem. Soc. (Resumed)* **1961**, 5061.

(3) Rogers, D.; Unal, G. G.; Williams, D. J.; Ley, S. V.; Sim, G. A.; Joshi, B. S.; Ravindranath, K. R. *J. Chem. Soc., Chem. Commun.* **1979**, 97.

(4) Coll, J.; Tandron, Y. A. *Phytochem. Rev.* **2007**, *7*, 25.

(5) Tokoroyama, T. *Synthesis* **2000**, 611.

(6) Barrero, A. F.; Sånchez, J. F.; Cuenca, F. l. G. *Phytochemistry* **1988**, *27*, 3676.

(7) Sun, T. P.; Kamiya, Y. *The Plant Cell* **1994**, *6*, 1509.

(8) Ito, K.; Furukawa, H. *J. Chem. Soc. D: Chem. Commun.* **1969**, 653.

(9) Klein Gebbinck, E. A.; Jansen, B. J. M.; de Groot, A. *Phytochemistry* **2002**, *61*, 737.

(10) (a) Kubo, I.; Lee, Y.-W.; Balogh-Nair, V.; Nakanishi, K.; Chapya, A. *J. Chem. Soc., Chem. Commun.* **1976**, 949. (b) Kubo, I.; Kido, M.; Fukuyama, Y. *J. Chem. Soc., Chem. Commun.* **1980**, 897.

(11) Kubo, I.; Klocke, J. A.; Miura, I.; Fukuyama, Y. *J. Chem. Soc., Chem. Commun.* **1982**, 618.

(12) Kato, N.; Takahashi, M.; Shibayama, M.; Munakata, K. *Agric. Biol. Chem.* **1972**, *36*, 2579.

(13) Mccullough, J. E.; Muller, M. T.; Howells, A. J.; Maxwell, A.; Osullivan, J.; Summerill, R. S.; Parker, W. L.; Wells, J. S.; Bonner, D. P.; Fernandes, P. B. *J Antibiot* **1993**, *46*, 526.

(14) Isshiki, K.; Tamamura, T.; Takahashi, Y.; Sawa, T.; Naganawa, H.; Takeuchi, T.; Umezawa, H. *J Antibiot* **1985**, *38*, 1819.

(15) Kawada, S.-z.; Yamashita, Y.; Fujii, N.; Nakano, H. *Cancer Research* **1991**, *51*, 2922.

(16) Carney, J. R.; Scheuer, P. J. *Tetrahedron Lett.* **1993**, *34*, 3727.

(17) Yosief, T.; Rudi, A.; Stein, Z.; Goldberg, I.; Gravalos, G. M. D.; Schleyer, M.; Kashman, Y. *Tetrahedron Lett.* **1998**, *39*, 3323.

(18) Fujita, E.; Uchida, I.; Fujita, T.; Masaki, N.; Osaki, K. *J. Chem. Soc., Chem. Commun.* **1973**, 793.

(19) Rojasgarciduenas, M.; Dominguez, X. A. *Turrialba* **1976**, *26*, 10.

(20) Nakamura, H.; Wu, H.; Ohizumi, Y.; Hirata, Y. *Tetrahedron Lett.* **1984**, *25*, 2989.

(21) (a) Liu, X.; Lee, C.-S. *Org. Lett.* **2012**, *14*, 2886. (b) Ley, S. V.; Simpkins, N. S.; Whittle, A. J. *J. Chem. Soc., Chem. Commun.* **1983**, 503.

(22) Poigny, S.; Guyot, M.; Samadi, M. *J. Org. Chem.* **1998**, *63*, 5890.

(23) Wieland, P.; Miescher, K. *Helv. Chim. Acta* **1950**, *33*, 2215.

(24) Hajos, Z. G.; Parrish, D. R. *J. Org. Chem.* **1974**, *39*, 1615.

(25) Takahashi, S.; Kusumi, T.; Kakisawa, H. *Chem. Lett.* **1979**, *8*, 515.

(26) Luibrand, R. T.; Erdman, T. R.; Vollmer, J. J.; Scheuer, P. J.; Finer, J.; Clardy, J. *Tetrahedron* **1979**, *35*, 609.

(27) Nambiar, M. P.; Wu, H. C. *Exp. Cell Res.* **1995**, *219*, 671.

(28) Takizawa, P. A.; Yucel, J. K.; Veit, B.; Faulkner, D. J.; Deerinck, T.; Soto, G.; Ellisman, M.; Malhotra, V. *Cell* **1993**, *73*, 1079.

(29) Bruner, S. D.; Radeke, H. S.; Tallarico, J. A.; Snapper, M. L. *J. Org. Chem.* **1995**, *60*, 1114.

(30) Yoon, T.; Danishefsky, S. J.; de Gala, S. *Angew. Chem. Int. Ed. Engl.* **1994**, *33*, 853.

(31) Liu, H.-J.; Zhu, J.-L.; Chen, I. C.; Jankowska, R.; Han, Y.; Shia, K.-S. *Angew. Chem. Int. Ed.* **2003**, *42*, 1851.

(32) Tokoroyama, T.; Tsukamoto, M.; Asada, T.; Iio, H. *Tetrahedron Lett.* **1987**, *28*, 6645.

(33) Tokoroyama, T.; Fujimori, K.; Shimizu, T.; Yamagiwa, Y.; Monden, M.; Iio, H. *Tetrahedron* **1988**, *44*, 6607.

(34) Müller, D. S.; Untiedt, N. L.; Dieskau, A. P.; Lackner, G. L.; Overman, L. E. *J. Am. Chem. Soc.* **2015**, *137*, 660.

CHAPTER 2

DESIGN OF A GENERAL SYNTHETIC APPROACH TOWARDS THE CLERODANE TERPENOIDS: SCAPARVIN A

2.1 Introduction

As can be gleaned from the examples laid out in Chapter 1, the clerodane class of terpenoids presents an array of intriguing structures for which many creative synthetic solutions have been reported over the last four decades.[1] However, the majority of synthetic efforts to date only target a single molecule or a series of closely related natural products. Furthermore, the scarcity of total syntheses of multiply oxygenated clerodanes provides great potential to develop a general synthetic approach, which could easily divert to structurally distinct clerodanes with a broad range of oxidation levels. As such, coupled with interests in the unexplored biological activities, we decided to initiate a synthetic program seeking to deliver clerodane natural products with a wide scope of carbon frameworks and functionalities through a unified design and the use of a key synthetic intermediate.

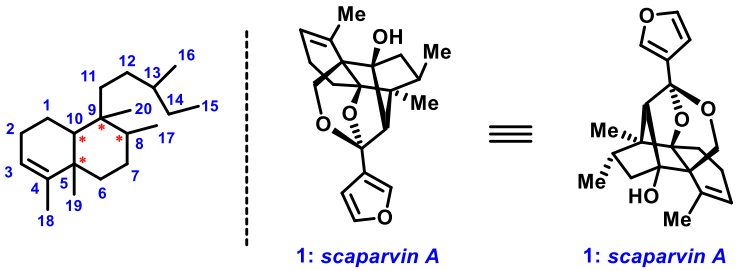

Figure 1. Scaparvin A (**1**) shown in two orientations.

This chapter will begin with our design of a two-phase approach towards the clerodane family, followed by an introduction of scaparvin A (**1**)[2] as an excellent example of a target with complex architecture and multiple oxygenated functional groups worthy of synthetic and biological study. Finally, a detailed retrosynthetic analysis of scaparvin A (**1**) will be described based on our global strategy for accessing the family.

2.2 Our Design of Synthetic Approach towards Clerodane Terpenoids

Given the biosynthesis noted in Section 1.2, natural production of clerodane terpenoids involves both a cyclase phase and a subsequent oxidase phase employing bicyclic compound **6** (or *ent*-**6**) as a common precursor to deliver *cis*-clerodanes with a high degree of structural diversity (Scheme 1). Considering the large number of structurally distinct molecules synthesized in Nature, this divergent oxidase phase process is extremely efficient if Nature's synthesis at this stage is meant to be controlled. Unfortunately, in any event, such chemo- and stereoselective oxidations are generally beyond the current capabilities of chemical synthesis. As such, a step-by-step emulation of these oxidation sequences is likely difficult, if not impossible, to execute in a laboratory setting.

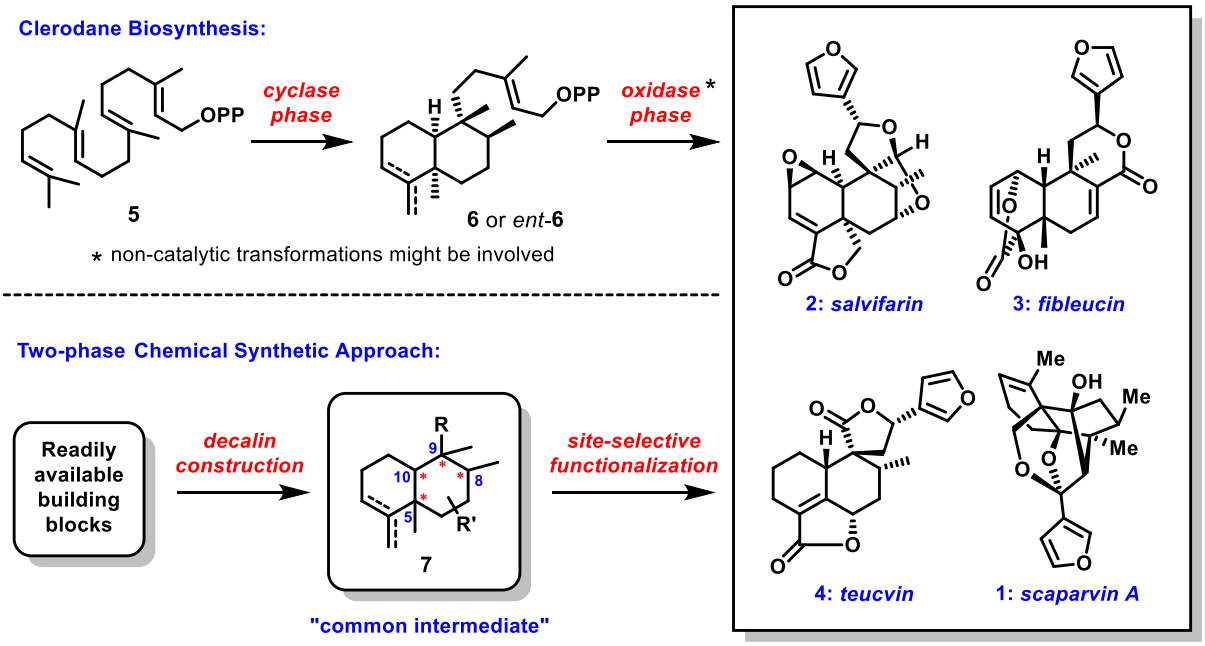

Scheme 1. Biosynthesis and two-phase chemical synthetic approach towards clerodane terpenoids.

However, we envision that a similar two-phase chemical synthetic approach could be achieved if a properly functionalized "common intermediate" in the form of **7** could be

synthesized (Scheme 1). The first phase focuses on the construction of the carbon skeleton, a problem which is mainly solved as it has been investigated in previous synthetic studies from other teams. The second phase, the more challenging part of the design, should involve one or several key site-selective chemical transformations that could utilize tools largely fueled by an immense resurgence of C–H functionalization in the past two decades, as well as new reactions and reagents to accomplish previously unachievable oxidation events.[3] The groups labeled as R within **7**, then, are likely key to unlocking this second phase of synthesis.

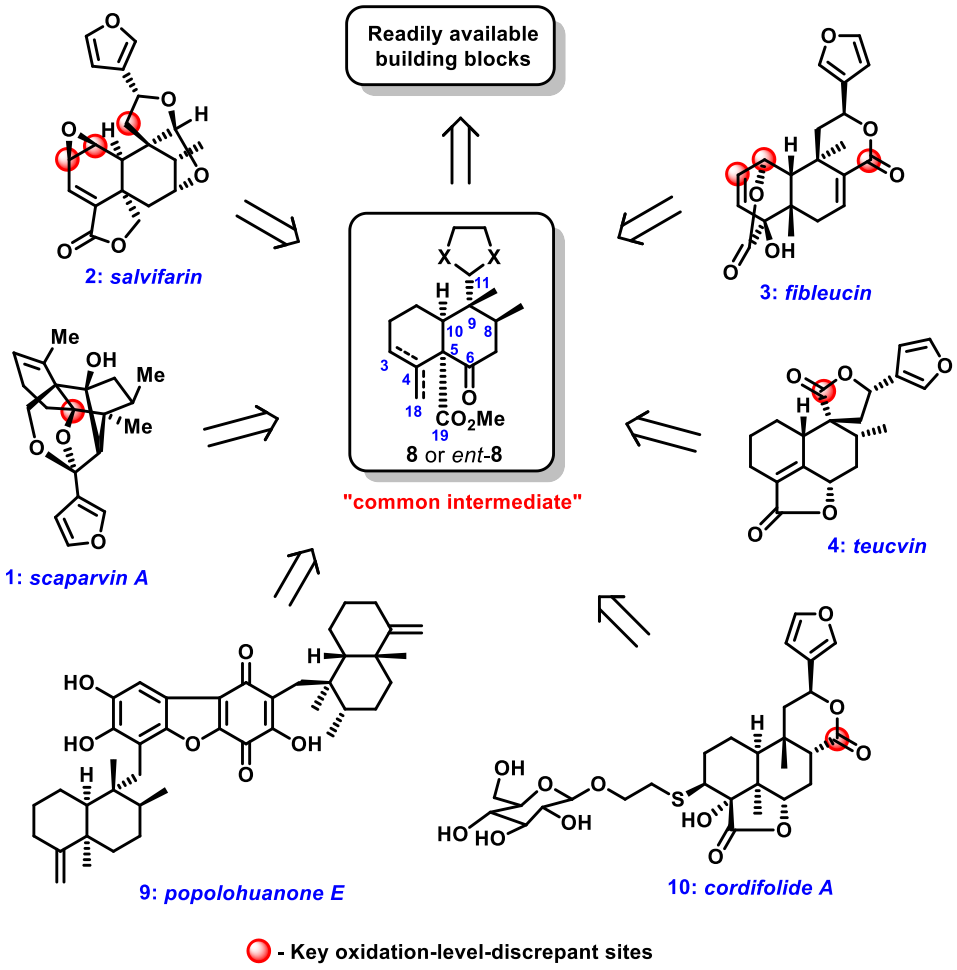

Scheme 2. Outline of the two-phase approach towards clerodane terpenoids.

After careful examination of the general oxidative patterns of *cis*-clerodanes, we believe that an ideal candidate of the "common intermediate" in this approach could be compound **8** (or *ent*-**8**) with four contiguous stereocenters to dedicate following diastereoselectivity, and more importantly, proper functional groups such as a C3–C4 double bond and oxygen-based functional groups at C-6, C-11, and C-19 to facilitate further site-selective modifications. As shown in Scheme 2, a series of *cis*-clerodanes, shown here as scaparvin (**1**)[2], salvifarin (**2**)[4], fibleucin (**3**)[5], teucvin (**4**)[6], popolohuanone E (**9**)[7] and cordifolide A (**10**)[8], could likely be derived from "common intermediate" **8** (or *ent*-**8**) if suitable site-selective synthetic transformations are developed and applied to solve the highlighted oxidation level discrepancies between these natural products and the "common intermediate" **8** (or *ent*-**8**).

Globally, this proposed two-phase approach can also serve as a platform to test the reactivity and selectivity of the existing C–H functionalization protocols in complex structural settings, and in turn afford insights to further optimize, revamp, and develop new methods. Additionally, from the viewpoint of chemical biology, this approach could not only allow access to naturally-occurring compounds, but also unnatural analogs to investigate structure-activity relationships in a systematic manner. Thus, we decided to investigate the feasibility of this approach, starting by an attempt to achieve a total synthesis of scaparvin A (**1**).

2.3 Introduction of Scaparvin A (1)

Scaparvin A (**1**, Figure 2) was isolated in 2010 by Lou and co-workers along with four related *cis*-clerodanes, scaparvins B-E (**11**-**14**), from the epilithic liverwort *Scapania parva* Steph.

Its unique structure was assigned through a combination of advanced 1D and 2D NMR techniques, buttressed by CD and HRMS data.

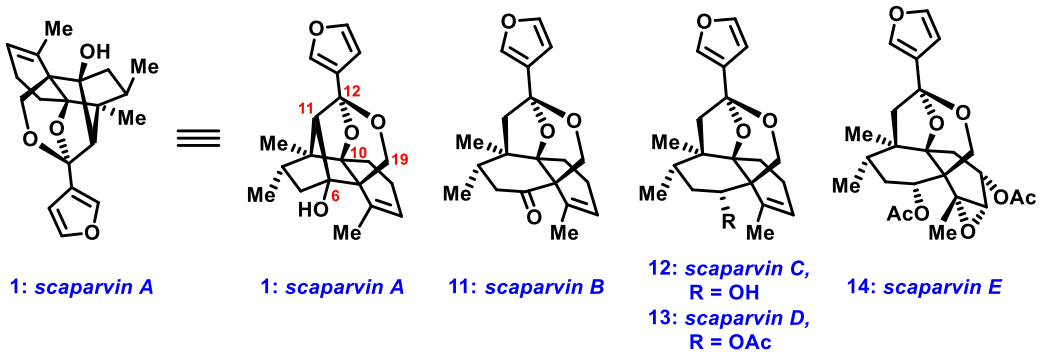

Figure 2. Structures of Scaparvin A-E (**1**, **11**-**14**).

Structurally, scaparvin A (**1**) features a novel cage structure bridged with a distinct C-6/C-11 bond and intramolecular ketal at C-12, with seven contiguous stereocenters along the ring system (5 of which are fully substituted and 2 of which are quarternary). It is worth noting that there are four oxygenated carbons (C-6, C-10, C-12, and C-19) located within a very congested space, which makes the structure quite synthetically challenging in terms of potential functional group manipulation. Hence, we believe scaparvin A (**1**) could serve as an exceptionally suitable target to justify our global synthetic logic, with the other scaparvins as possible targets of opportunity as well, differing largely with the absence of the C6–C11 bond that completes the cage of **1**.

2.4 Retrosynthetic Analysis of Scaparvin A (1) from Common Intermediate (8)

Based on our global strategy as described in broad terms in Section 2.2, scaparvin A (**1**) could be derived from a diol precursor such as **15**, which in turn could arise from C6–C11 bridge

formation of ketoaldehyde **16**. This key chemical transformation was envisioned to be accomplished through either an aldol reaction or a Pinacol coupling/oxidation protocol. Comparing **16** with "common intermediate" **8**, the tertiary C–H bond at C-10 required to be oxidized selectively over the sterically more accessible C–H bond at C-8, and allylic C–H bonds at C-2 and C-18. It was hoped that this key event could be accomplished with **17**. Finally, the preoxidized compound **17** could be traced back to "common intermediate" **8** through several straightforward functional group manipulations.

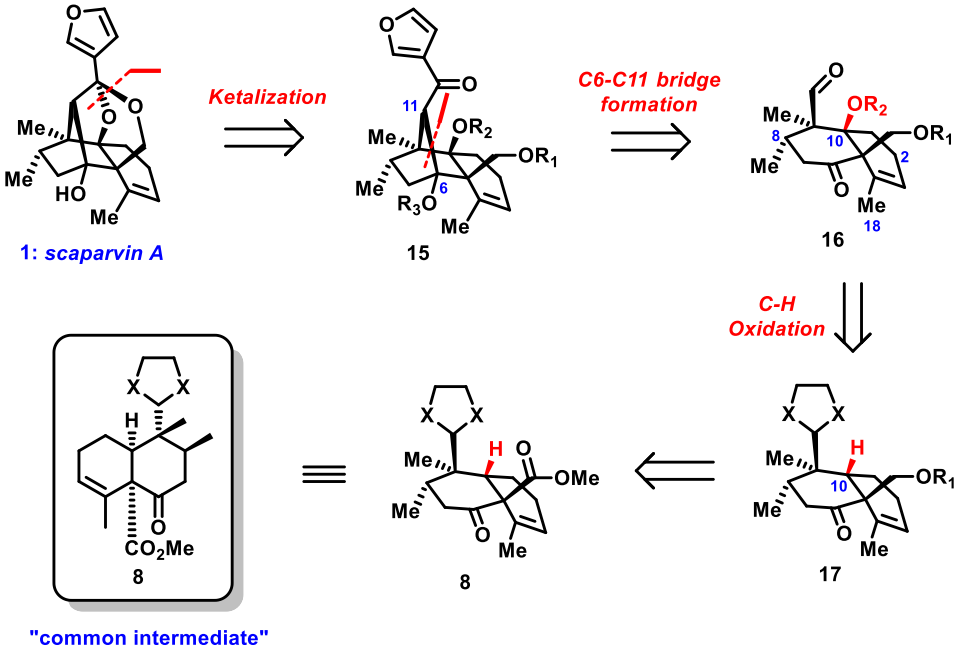

Scheme 3. Preliminary retrosynthetic analysis of scaparvin A (**1**) from common intermediate (**8**).

2.5 Conclusion

As detailed in the above sections, we have designed a two-phase approach towards *cis*-clerodane terpenoids, with scaparvin A (**1**) serving as an example to highlight the key synthetic

challenges. As will be described in the ensuing chapters, a number of strategies and tactics have been developed to address these problems. We will focus our discussion in Chapter 3 on the efficient construction of "common intermediate" **8**, while two modes of directed C–H oxidation at C-10 will be covered in Chapter 4. Finally, efforts of late-stage modification towards scaparvin A (**1**) and related compounds will be summarized in Chapter 5, culminating in a near complete synthesis of **1** as well as a completed total synthesis of scaparvin C (**12**).

2.6 References

(1) Tokoroyama, T. *Synthesis* **2000**, 611.

(2) Guo, D.-X.; Zhu, R.-X.; Wang, X.-N.; Wang, L.-N.; Wang, S.-Q.; Lin, Z.-M.; Lou, H.-X. *Org. Lett.* **2010**, *12*, 4404.

(3) (a) Godula, K.; Sames, D. *Science* **2006**, *312*, 67. (b) Davies, H. M. L.; Manning, J. R. *Nature* **2008**, *451*, 417. (c) Giri, R.; Shi, B.-F.; Engle, K. M.; Maugel, N.; Yu, J.-Q. *Chem. Soc. Rev.* **2009**, *38*, 3242. (d) Ishihara, Y.; Baran, P. S. *Synlett* **2010**, *2010*, 1733. (e) Lyons, T. W.; Sanford, M. S. *Chem. Rev.* **2010**, *110*, 1147. (f) Mkhalid, I. A. I.; Barnard, J. H.; Marder, T. B.; Murphy, J. M.; Hartwig, J. F. *Chem. Rev.* **2010**, *110*, 890. (g) Chen, M. S.; White, M. C. *Science* **2007**, *318*, 783. (h) Breslow, R. *Acc. Chem. Res.* **1980**, *13*, 170. (i) Barton, D. H. R.; Doller, D. *Acc. Chem. Res.* **1992**, *25*, 504. (j) Gutekunst, W. R.; Baran, P. S. *Chem. Soc. Rev.* **2011**, *40*, 1976. (k) Newhouse, T.; Baran, P. S. *Angew. Chem. Int. Ed.* **2011**, *50*, 3362.

(4) Eguren, L.; Fayos, J.; Perales, A.; Savona, G.; Rodríguez, B. *Phytochemistry* **1984**, *23*, 466.

(5) Ito, K.; Furukawa, H. *J. Chem. Soc. D: Chem. Commun.* **1969**, 653.

(6) Fujita, E.; Uchida, I.; Fujita, T.; Masaki, N.; Osaki, K. *J. Chem. Soc., Chem. Commun.* **1973**, 793.

(7) Carney, J. R.; Scheuer, P. J. *Tetrahedron Lett.* **1993**, *34*, 3727.

(8) Pan, L.; Terrazas, C.; Lezama-Davila, C. M.; Rege, N.; Gallucci, J. C.; Satoskar, A. R.; Kinghorn, A. D. *Org. Lett.* **2012**, *14*, 2118.

CHAPTER 3

CONCISE SYNTHESIS OF A COMMON INTERMEDIATE

FOR THE CIS-CLERODANE TERPENOIDS

3.1 Introduction

Given the global synthetic logic described in Chapter 2, compound **1** (Scheme 1) could serve as a common precursor for the synthesis of the *cis*-clerodane terpenoids, represented here by scaparvin A (**2**). Thus, our first task was to develop an efficient method to construct the decalin system stereoselectively, keeping in mind that gram-scale quantities of that common intermediate **1** would be ideal to truly fuel the next stage of studies towards **2** as well as other targets.

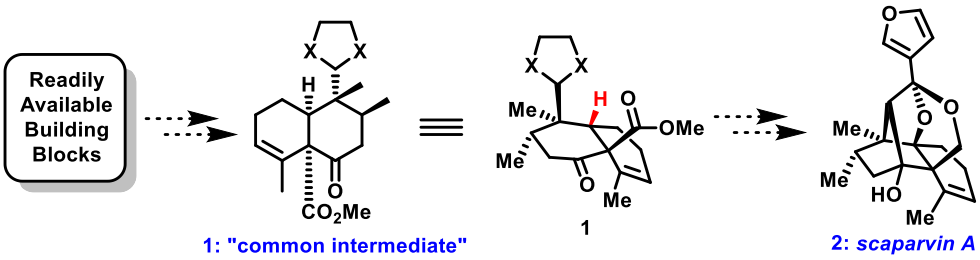

Scheme 1. Common intermediate (**1**) as a precursor of scaparvin A (**2**).

This chapter will detail the evolution of our synthetic approach to **1**, beginning with a failed pyrone Diels–Alder strategy that could not deliver the core. That discussion will be followed by our attempts to assemble its characteristic framework empowered by an intramolecular Conia-ene reaction. Finally, approaches to obtain optically pure **1** will be illustrated as well.

3.2 Pyrone Diels–Alder Approach to Common Intermediate

The Diels–Alder reaction is particularly useful in synthetic organic chemistry as a reliable method for forming six-membered systems with good control over both regio- and

stereochemical properties in how its two partners are merged.[1] Among diene components, the 2-pyrone hetero-cycle has been widely exploited to assemble the [2.2.2]-bicyclic lactone motif characteristic in general terms of the desired decalin framework needed for synthesis.[2] Thus, mindful of our aforementioned goal to deliver **1** in a concise, efficient, and scalable fashion, we were drawn to the notion that its stereochemically rich decalin framework could arise from a pyrone Diels–Alder reaction shown in Scheme 2 using an α,β-unsaturated cyclohexanone or quinone as a coupling partner.

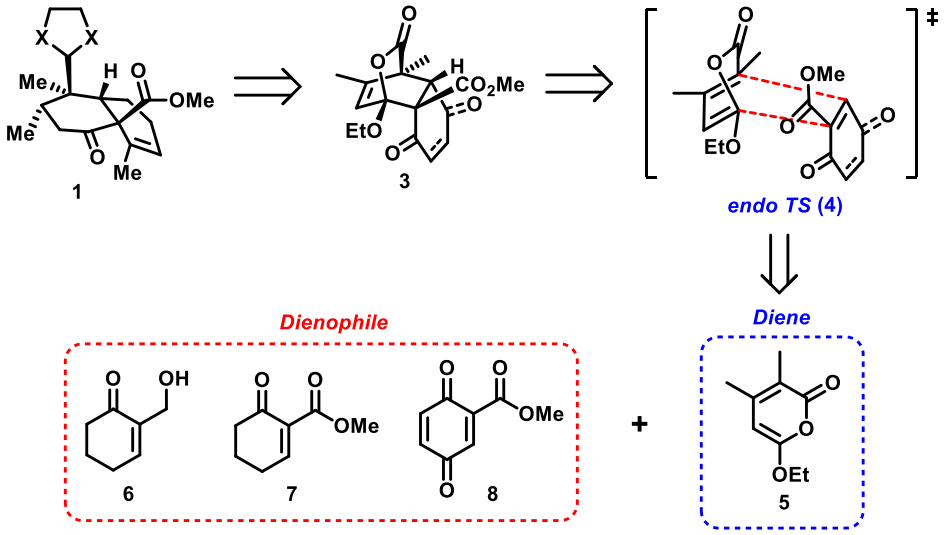

Scheme 2. Retrosynthetic analysis of common intermediate by using pyrone Diels-Alder reaction.

More specifically, common intermediate **1** could retrosynthetically be derived from a bridged lactone precursor **3**, which in turn could be traced back to pyrone **5** and dienopile (**6**, **7**, or **8**) through an *endo* selective [4+2]-cycloaddtion, assuming that the transformation could be achieved at a temperature low enough such that the resultant product would not decompose through a retro [4+2]-cycloadditon expelling CO_2. Finally, both Diels–Alder components would be readily obtained from commercially available starting materials.

In the forward sense, our studies began with the preparation of pyrone **5** (Scheme 3). As shown, a rhodium-catalyzed cyclopropenation of 2-butyne (**9**) with ethyl diazoacetate (**10**) gave cycloadduct **11** in 83% yield which, upon treatment of $[Rh(CO)_2Cl]_2$ under a CO atmosphere, afforded pyrone **5** through a sequence that likely involves oxidative addition, carbonyl insertion, 1,3-migration, and reductive elimination.[3] It is worth noting that these two catalytic reactions could be carried out with relatively low catalyst loadings and that we could readily obtain diene **5** on multigram scale.

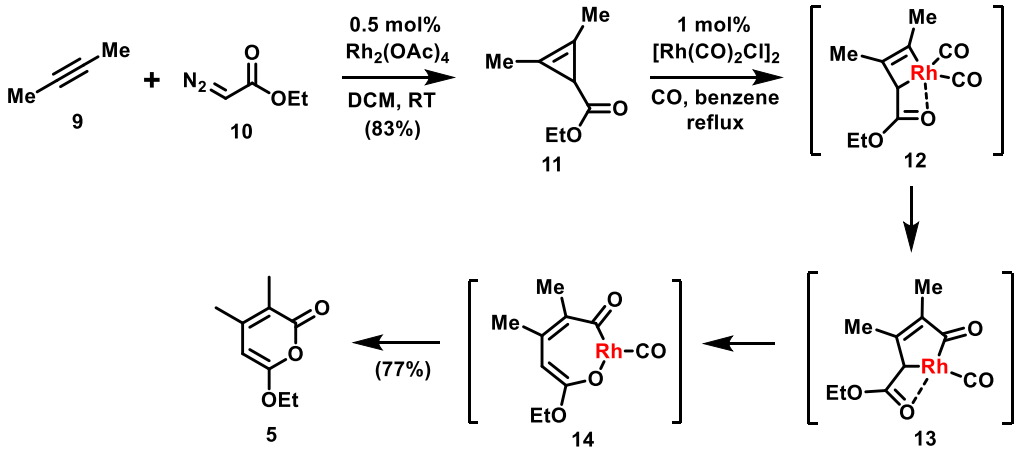

Scheme 3. Synthesis of pyrone **5.**

As for the dienophile partner, we decided to examine compounds **6**, **7**, and **8** for the following reasons. First, the electron-withdrawing groups in the dienophiles could dedicate to regioselectivity of the normal demand Diels–Alder reaction, given that with pyrone dienes there is little opportunity to tune regioselectivity or reactivity through other standard techniques such as Lewis acid catalysts since complexation can occur with both components. Second, particularly for **8**, π-π stacking between the planar quinone motif with pyrone **5** might accelerate the reaction, as well as reinforce the desired *endo* selectivity.

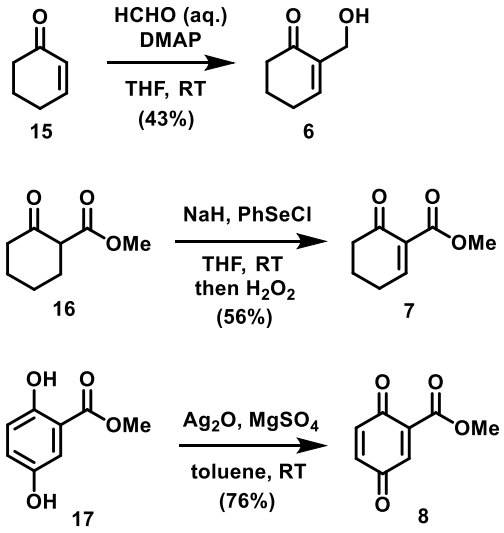

Scheme 4. Syntheses of dienophiles **6**, **7**, and **8**.

The syntheses of the dienophiles proved to be very straightforward (Scheme 4). A Baylis–Hillman reaction of commercially available cyclohexenone (**15**) afforded dienophile **6**,[4] while **7** was obtained from ketoester **16** via α-selenenylation followed by oxidative selenoxide elimination.[5] A silver(I)-mediated oxidation of hydroquinone **17** delivered quinone **8** smoothly in 76% yield.

With both the diene and dienophiles in hand, we then turned our attention to investigating the proposed Diels–Alder reaction, starting with cycloadditions promoted by thermal activation. Unfortunately, these attempts only gave uncharacterizable mixtures of by-products at high temperatures (100–150 °C), while no conversion was observed at lower temperatures (50–80 °C).

Scheme 5 illustrates our rationale for this unsuccessful Diels–Alder reaction. The sterically demanding, fully substituted carbons at C-5, C-6, and C-9, along with the partially aromatic nature of pyrones (caluculated to be ca. 30% as aromatic as benzene),[6] likely require significant thermal activation to participate in the [4+2] cycloaddition. However, the subsequent

entropy-driven loss of CO_2 will be dramatically accelerated at such high temperatures, which could quickly consume transient oxabicyclooctene **3**. In order to overcome the low reactivity and suppress the loss of CO_2, reactions performed under high pressure (~300 psi) at lower temperatures were also tested, but again showed disappointing results.

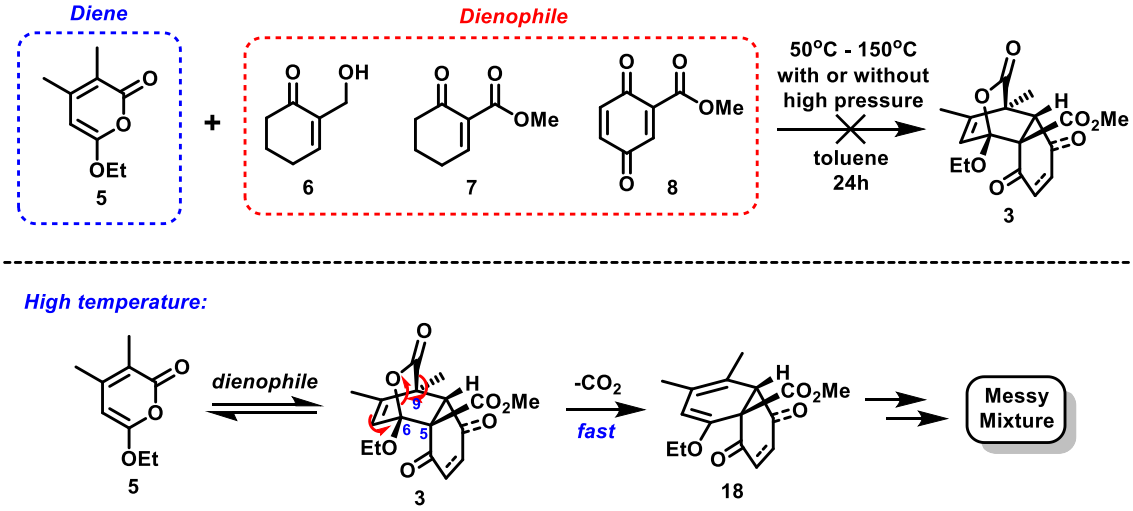

Scheme 5. Diels-Alder reaction of **5** under thermal conditions and rationale for the failure.

In light of this outcome, we sought to improve the reactivity of our dienophile by using Lewis acids, aiming to lower the reaction temperature. However, despite much experimentation using various Lewis acids (Scheme 6), the desired Diels–Alder products were not observed. Indeed, this outcome affording complex mixtures of by-products is not that surprising, especially when strong Lewis acids (e.g. $TiCl_4$, $SnCl_4$, BF_3•OEt_2) were used. For instance, Lewis acids might not only be confused in terms of promoting the [4+2] cycloaddition based on which partner they complexed with, but if the reaction had occurred, they might also assist in ring opening of the partially-strained [2.2.2]-bicyclic lactone. Scheme 6 showcases a possible reaction pathway by which product **3** could have reacted further if formed.

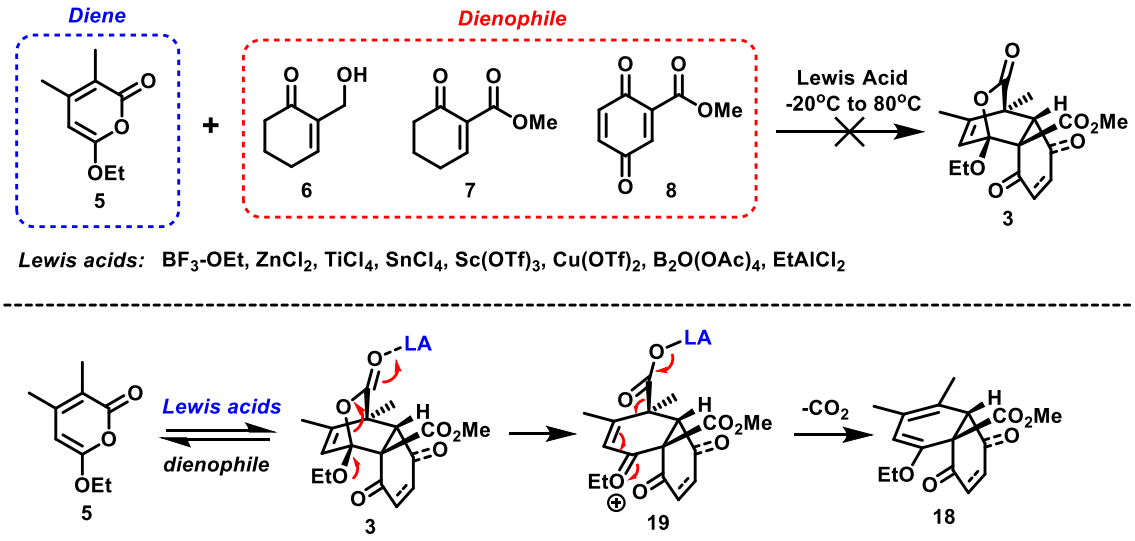

Scheme 6. Diels-Alder reaction of **5** under Lewis acid promoted conditions and rationale for the failure.

Thus, we drew the conclusion that the proposed pyrone Diels–Alder reaction shown above is likely challenging to reduce to practice, mainly due to sterically demanding nature of the reaction and the labile [2.2.2] bicyclic motif. At this juncture, we elected to redesign our retrosynthetic analysis of common intermediate **1**, using alternative strategic disconnections to forge its key bonds and stereocenters.

3.3 Conia-Ene Approach to Common Intermediate

The key lesson learned from the failed pyrone Diels–Alder strategy is that it might be difficult to intermolecularly assemble the requisite highly substituted decalin system in a single step. Thus, we switched to an approach that would construct it in a stepwise manner, but still hopefully in a modicum of operations as predicted by the Conia-ene approach highlighted in Scheme 7. Here, initial disconnection of the C4–C5 bond in the common intermediate shown here in protected form as **20** led back to alkyne **21**, a material bearing all the carbon atoms of the

final decalin system. This material (**21**), in turn, could potentially arise from enone **22** through a Cu-mediated conjugate addition, while this resultant compound could be further traced back to ketoaldehyde **23**. Finally, compound **23** was seen as the product of Diels–Alder reaction between tiglic aldehyde **24** and Rawal's diene **25**[7]. And, if that Diels–Alder reaction could be achieved asymmetrically, then an enantiospecific synthesis could result if the initial chiral centers present in **23** assisted in directing the formation of all the remaining chirality centers in a stereoselective manner.

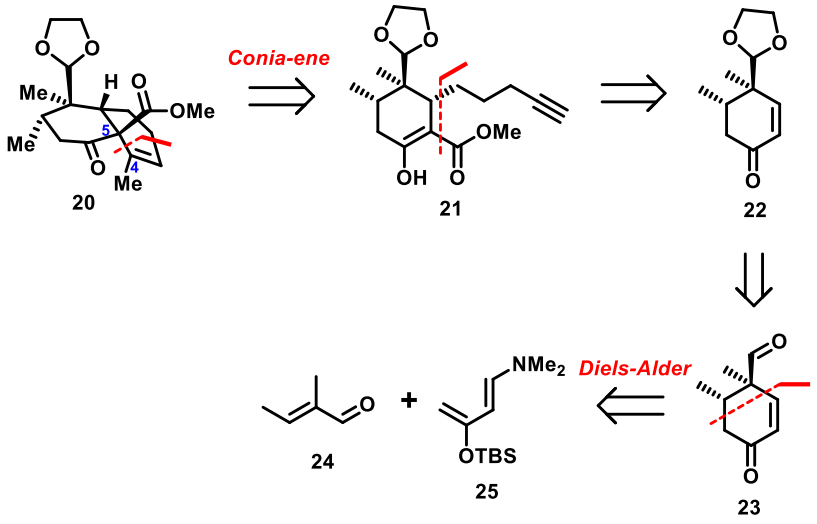

Scheme 7. Retrosynthetic analysis of common intermediate (protected as **20**) by using Conia-ene reaction.

With this plan in mind, we set about testing the initial Rawal-type Diels–Alder reaction. In the event, mixing tiglic aldehyde **24** with a slight excess of Rawal's diene **25** and heating in THF at 50 °C for 12 h, followed by treatment with ethylene glycol under acidic conditions, led exclusively to the thermodynamically stable acetal **22**. Next, the resulting enolate from the Cu-mediated conjugate addition was quenched by Mander's reagent[8] (noting that other reagents such as $ClCO_2Me$ mainly afforded O-acylated products) to afford alkyne **26** in 55% yield and with 5:1 dr. At this stage, it proved challenging to assign the configuration of the newly formed C-10

stereocenter because **26** exists as a tautomeric mixture of enol and ketone forms, complicating NMR analysis. As such, we elected to carry the major diastereomer forward to the Conia-ene reaction, hoping we could determine the stereochemistry from the decalin system formed.

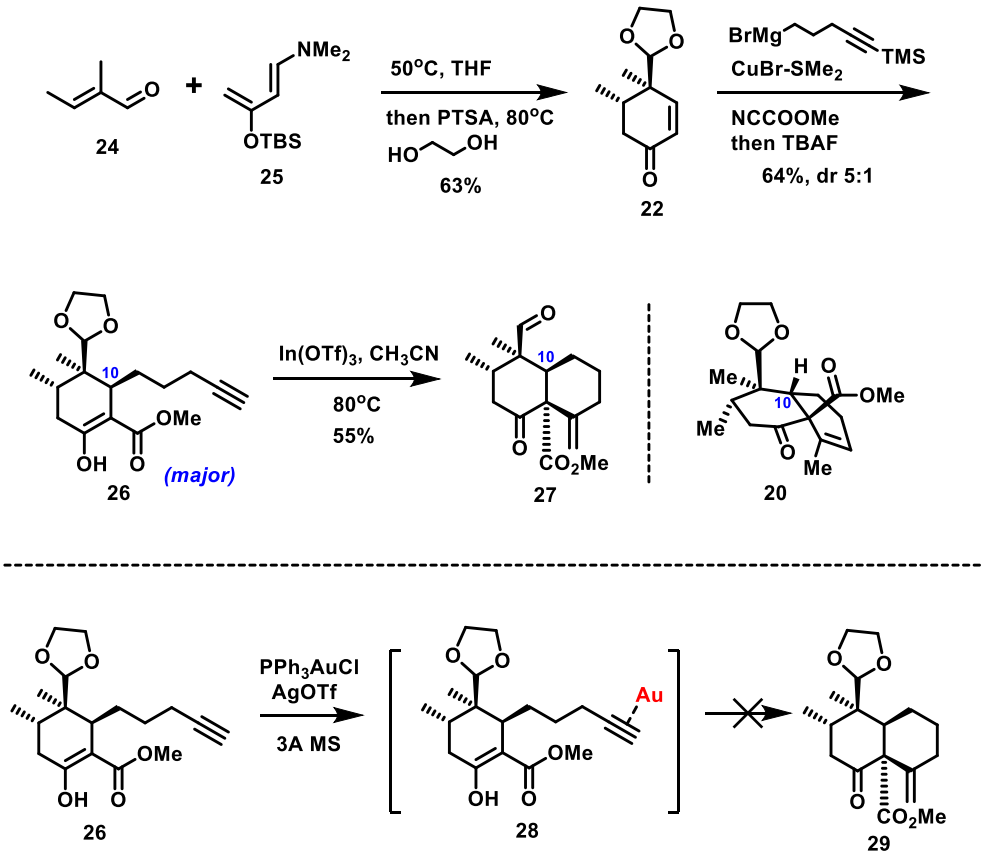

Scheme 8. Synthesis of bicycle **27.**

In that key step, despite extensive failures to effect the Conia-ene reaction under gold catalysis,[9] we were pleased to find that $In(OTf)_3$ could serve as an effective Lewis acid to promote the desired transformation. Indeed, upon aqueous work-up, ketoaldehyde **27** was the only isomer observed, the stereochemistry of which was assigned through a combination of NOSEY and other 2D NMR to that as drawn.

The generation of the undesired stereochemistry within product **27** versus target **20** suggests that the conjugate addition of **22** occurred from the β-face. In order to understand and potentially invert the facial selectivity, conformational analysis of enone **22** (as shown in Scheme 9) indicates that **22** should exist predominantly as conformer **31** with methyl and acetal group at pseudo-equatorial positions. If so, then axial attack of the organocopper reagent will result in the undesired stereomer as observed.

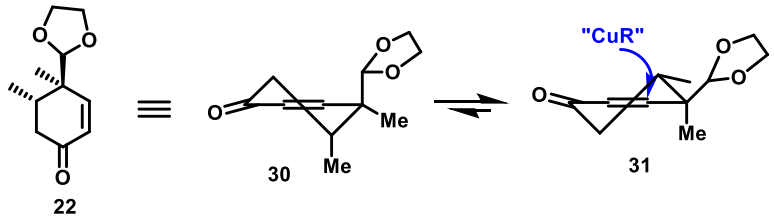

Scheme 9. Conformational analysis of conjugate addtion of enone **22.**

In order to overcome this innate facial selectivity, one reasonable solution is to introduce a bulky group that could block the preferred face of attack within the cyclohexenone system, forcing the conjugate addition proceed from the alternate side. For example, in the Ley total synthesis of insect antifeedant ajugarin I, 1,3-dithiolane moiety was reported to be capable of controlling the facial selectivity during a Cu-mediated conjugate addition.[10] In this case, the complexation between dithiolane moiety and copper (I) species acts as a "bulky" group to prevent nucleophilic attack from the β-face irrespective of which chair conformer is attacked by the nucleophile (Scheme 10).

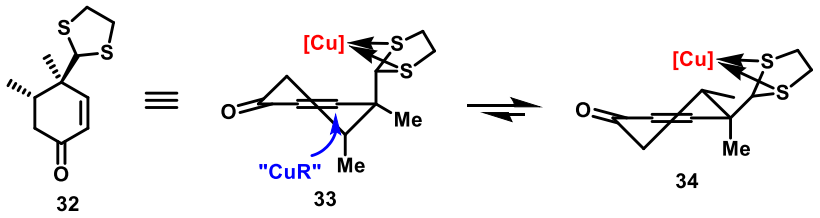

Scheme 10. Conformational analysis of conjugate addtion of enone **32.**

To probe this tactic, we simply needed to switch the protecting group of the C-11 aldehyde to dithiolane moiety. Again, starting from Diels–Alder product **35** (Scheme 11), treatment with a stoichiometric amount of 1,2-ethanedithiol and silica gel that had been pre-treated with thionyl chloride was able to selectively protect the C-11 aldehyde and afford **32** in 73% yield. It is worth mentioning that other conditions to effect this protection using Lewis acids or protic acids, in contrast to thioacetalization, usually gave a mixture of compounds (**32**, **38**, **39**, and other by-products), due to irreversible C-S bond formation and overprotection.

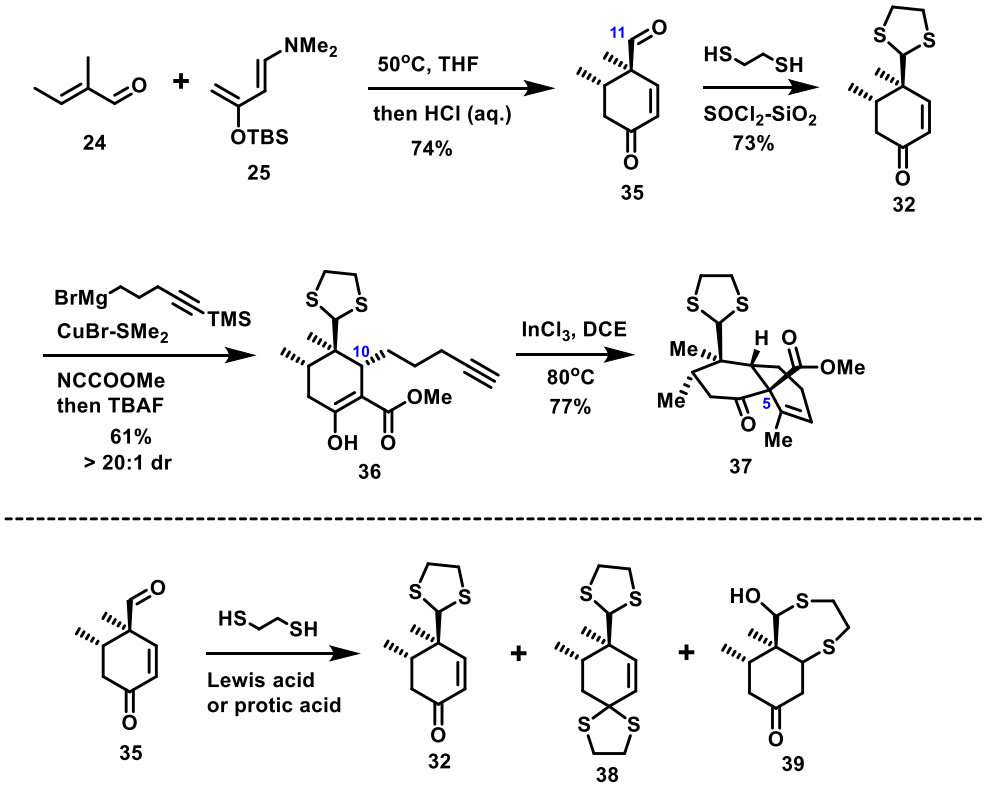

Scheme 11. Synthesis of common intermediate proctected as **37**.

Subjecting **32** to the same conjugate addition conditions pleasingly delivered the desired C-10 epimer in the form **36**, which was then cyclized to *cis*-decalin bicycle **37** under the Conia-ene reaction conditions. Here, in this key event, $InCl_3$ was found to be the optimal In(III)-based Lewis acid to effectively promote the double bond migration of the resulting Conia-ene product, affording *endo*-olefin **37** in 77% yield. Notably, over 10 grams of common intermediate **37** have been prepared through this concise route (4 steps from Rawal's diene **25**), thereby providing ample material supplies to fuel the next phase of studies.

3.4 Enantioselective Synthesis of Common intermediate

Having successfully developed a reliable racemic route towards **37** as described in the previous section, we next set our sights on an enantioselective preparation to this common intermediate. Based on the synthetic route noted above, the initial chiral centers (C-8, and C-9) were generated during the Diels–Alder reaction; as such, a straightforward idea is to incorporate enantiomeric control in the Diels–Alder reaction.

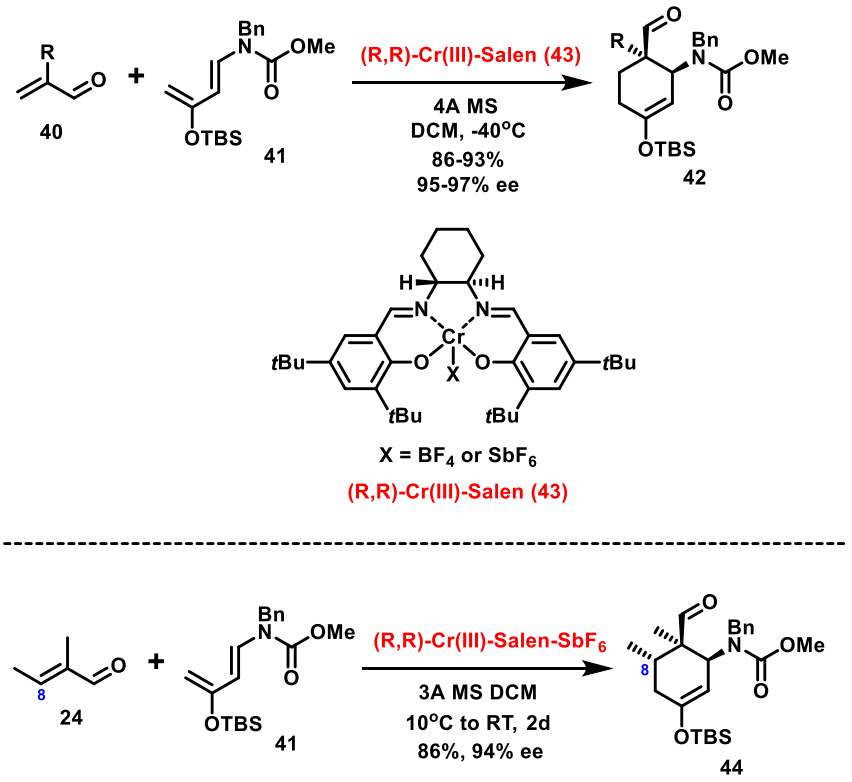

Scheme 12. Enantioselective Rawal's Diels-Alder reaction to afford compound **44.**

In 2000, the Rawal group described a highly enantioselective Diels–Alder reaction of their diene as catalyzed by Cr(III) salen complex (Scheme 12).[11] Comparing the structures of acrolein substrates (**40**) with tiglic aldehyde **24**, we expected that **24** might have lower reactivity due to the steric hindrance at C-8 position, and consequently might require higher temperature or

stronger Lewis acids that might be less effective in terms of final enantiocontrol. To our delight, a small screen of the reaction conditions (temperature, solvent and counterion of the catalyst) revealed that using the catalyst possessing a SbF_6^- counterion at slightly higher concentration (2.0 M) in CH_2Cl_2 gave optimal yield and enantiomeric excess (86%, 94% ee) and reasonable reaction time (2 d).

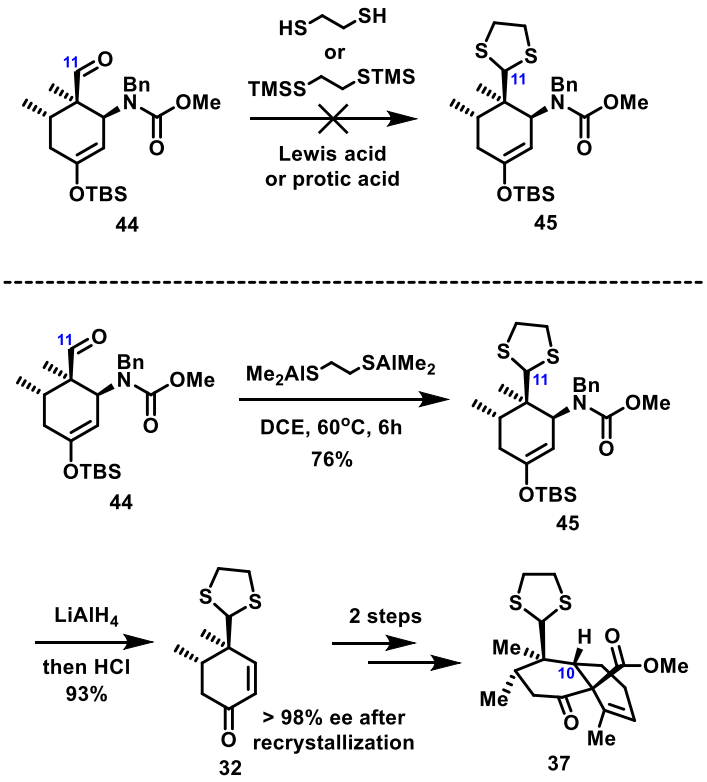

Scheme 13. Synthesis of intermediate **32** from cycloadduct **44**.

Encouraged by this crucial result, we next set to convert **44** into **32**, the intermediate previously formed in the racemic route. After numerous unsuccessful attempts of thioacetal formation promoted by Lewis acids or protic acids (because of vinyl ether cleavage and further reactions), the required dithiolane moiety was accomplished by employment of a neutral reagent $Me_2AlSCH_2CH_2SAlMe_2$ (3 equiv, prepared *in situ* from ethanedithiol and Me_3Al, developed by the Corey group).[12] Subsequent reduction of carbamate **45** provided optically pure enone **32**

upon acidic work-up. After recrystallizing this material using Et_2O/hexanes as solvent, a step which served to enhance the level of enantioselectivity to >98%, we were then able to advance it to common intermediate **37** using the chemistry described previously for the racemic route.

3.5 Conclusion

As detailed in this chapter, we have developed a concise stereoselective synthesis of the common intermediate **37** which proceeded in 4 step (5 steps for enantioselective route) from Rawal's diene (**25** or **41**), highlighting the power and utility of Rawal's Diels–Alder reaction. Additional key elements were a facially selective conjugate addition as controlled by dithiolane moiety and an $InCl_3$-promoted Conia-ene reaction to rapidly assemble the remaining compounets of the decalin core.

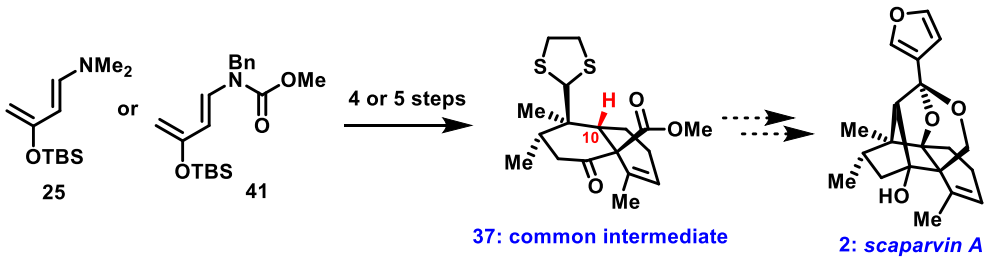

Scheme 14. Synthesis of common intermediate **37**, a precursor of scaparvin A (**2**).

With sufficient quantities of common intermediate **37** prepared, we were set to proceed to the next phase of our synthetic plan, namely modification of **37** into various scaparvin terpenoids, efforts which will be discussed in the following chapters.

3.6 References

(1) Nicolaou, K. C.; Snyder, S. A.; Montagnon, T.; Vassilikogiannakis, G. *Angew. Chem. Int. Ed.* **2002**, *41*, 1668.

(2) Afarinkia, K.; Vinader, V.; Nelson, T. D.; Posner, G. H. *Tetrahedron* **1992**, *48*, 9111.

(3) Cho, S. H.; Liebeskind, L. S. *J. Org. Chem.* **1987**, *52*, 2631.

(4) Ciganek, E. In *Organic Reactions*; John Wiley & Sons, Inc., 2004.

(5) Reich, H. J.; Renga, J. M.; Reich, I. L. *J. Am. Chem. Soc.* **1975**, *97*, 5434.

(6) Bird, C. W. *Tetrahedron* **1986**, *42*, 89.

(7) Kozmin, S. A.; Rawal, V. H. *J. Org. Chem.* **1997**, *62*, 5252.

(8) Mander, L. N.; Sethi, S. P. *Tetrahedron Lett.* **1983**, *24*, 5425.

(9) Kennedy-Smith, J. J.; Staben, S. T.; Toste, F. D. *J. Am. Chem. Soc.* **2004**, *126*, 4526.

(10) Ley, S. V.; Simpkins, N. S.; Whittle, A. J. *J. Chem. Soc., Chem. Commun.* **1983**, 503.

(11) Huang, Y.; Iwama, T.; Rawal, V. H. *J. Am. Chem. Soc.* **2000**, *122*, 7843.

(12) (a) Snyder, S. A.; Corey, E. J. *J. Am. Chem. Soc.* **2006**, *128*, 740. (b) Corey, E. J.; Beames, D. J. *J. Am. Chem. Soc.* **1973**, *95*, 5829.

3.7 Experimental Section

General Methods: All reactions were carried out under an argon atmosphere with dry solvents under anhydrous conditions, unless otherwise stated. Dry methylene chloride (CH_2Cl_2), diethyl ether (Et_2O), tetrahydrofuran (THF), benzene and toluene were obtained by passing commercially available pre-dried, oxygen-free formulations through activated alumina columns; triethylamine (Et_3N) was distilled from KOH; dichloroethane (DCE), acetonitrile (CH_3CN) and methanol (MeOH) were purchased in anhydrous form from Sigma-Aldrich and used as received. Yields refer to chromatographically and spectroscopically (^1H and ^{13}C NMR) homogeneous materials, unless otherwise stated. Reagents were purchased at the highest commercial quality and used without further purification, unless otherwise stated. Reactions were magnetically stirred and monitored by thin-layer chromatography (TLC) carried out on 0.25 mm E. Merck silica gel plates (60F-254) using UV light and an aqueous solution of cerium ammonium sulfate and ammonium molybdate and heat as visualizing agents. Preparative TLC was carried out on 0.50 mm E. Merck silica gel plates (60F-254). SiliCycle silica ge (60 A, academic grade, particle size 40-63 μm) was used for flash column chromatography. NMR spectra were recorded on Bruker DRX-300, DRX-400, DRX-500 and DRX-700 instruments and calibrated using residual undeuterated solvent as an internal reference. The following abbreviations are used to explain multiplicities: s = singlet, d = doublet, t = triplet, q = quartet, m = multiplet, br = broad, app = apparent. IR spectra were recorded on a Perkin-Elmer Spectrum Two FT-IR spectrometer. High resolution mass spectra (HRMS) were recorded in the Columbia University Mass Spectral Core facility on a JOEL HX110 mass spectrometer using FAB (Fast Atom Bombardment).

Enone 32. To a solution of (E)-1-dimethylamino-3-*tert*-butyldimethylsiloxy-1,3-butadiene (**25**, 58.7 g, 259 mmol, 1.2 equiv) in THF (200 mL) at 23 °C was added tiglic aldehyde (**24**, 20.8 mL, 216 mmol, 1.0 equiv). The stirred reaction was then heated to 50 °C for 16 h. After cooling down to 23 °C, the reaction was quenched by 2 M HCl solution (200 mL) and further stirred for 5 h at this temperature. The reaction contents were then transferred to a separatory funnel, diluting with EtOAc (300 mL) and saturated aqueous $NaHCO_3$ (300 mL). The organic layer was separated and the aqueous layer was extracted with EtOAc (3 × 100 mL). The organic layers were combined, dried with $MgSO_4$, filtered and concentrated. The resulting crude product was purified by flash column chromatography (silica gel, hexanes/EtOAc, 10:1 to 4:1) to give cycloadduct **35** (24.2 g, 74% yield) as a yellow oil.

A portion of this product (**35**, 17.0 g, 112 mmol, 1.0 equiv) was dissolved in benzene (1.5 L) and cooled to 0 °C. SiO_2-$SOCl_2$ (40 g) was added in one portion, followed by addition of 1,2-ethanedithiol (9.4 mL, 112 mmol, 1.0 equiv). After 10 min, the ice-water bath was removed and the reaction mixture was allowed to warm to 23 °C for 16 h. Upon completion, the reaction contents were filtered through Celite (rinsing with EtOAc) and transferred to a separatory funnel. After washing with saturated aqueous $NaHCO_3$ (400 mL), the organic layer was separated and the aqueous layer was extracted with EtOAc (3 × 200 mL). The organic layers were combined, dried with $MgSO_4$, filtered and concentrated. The resulting crude product was purified by flash column chromatography (silica gel, hexanes/EtOAc, 20:1 to 8:1) to give enone **32** (17.0 g, 73% yield) as a yellow oil. **32**: R_f = 0.53 (silica gel, hexanes/EtOAc, 4:1); ^{1}H NMR (400 MHz, $CDCl_3$) δ 7.12 (d, *J* = 10.3 Hz, 1 H), 6.01 (d, *J* = 10.3 Hz, 1 H), 4.89 (s, 1 H), 3.33–3.12 (m, 4 H), 2.45–2.20 (m, 3 H), 1.15 (s, 3 H), 1.00 (d, *J* = 6.5 Hz, 3 H); ^{13}C NMR (100 MHz, $CDCl_3$) δ 199.0, 155.3, 129.0, 61.6, 44.2, 42.2, 39.0, 38.8, 37.4, 18.9, 15.3.

Alkyne 36. Magnesium turnings (10.2 g, 425 mmol, 5 equiv) was weighed directly into a flame-dried flask, whereafter a solution of 1-bromo-5-(trimethylsilyl)-4-pentyne (46.5 g, 212 mmol, 2.5 equiv) in Et_2O (500 mL) was slowly added at 23 °C over 1 h. After vigorous stirring for an additional 4 h, the resultant solution of Grignard reagent was slowly transferred into a vigorously-stirred suspension of CuBr-SMe_2 (21.8 g, 106 mmol, 1.2 equiv) in Et_2O (200 mL) at –78 °C through a cannula. The reaction contents were slowly warmed to –60 °C over 1 h, and then cooled to –78 °C. A solution of enone **32** (17.2 g, 82.7 mmol, 1.0 equiv) in Et_2O (200 mL) was added dropwise, and the reaction contents were slowly warmed to 23 °C over 10 h. After cooling to –78 °C again, HMPA (150 mL) and Mander's reagent (20.2 mL, 254 mmol, 3 equiv) were added dropwise, and the reaction contents were slowly warmed to 23 °C over 16 h. Upon completion, the reaction mixture was diluted with MeOH (200 mL) and filtered through a pad of Celite (rinsing with Et_2O). To the resulting filtrate was added a solution of TBAF in THF (1.0 M, 300 mL). The resulting solution was stirred at 23 °C for 10 h before being quenched with a mixture of NH_4OH (50 mL) and saturated aqueous NH_4Cl (300 mL). The reaction contents were then transferred to a separatory funnel, diluting with hexanes (500 mL) and water (500 mL). The organic layer was separated and the aqueous layer was extracted with EtOAc (3 × 400 mL). The organic layers were combined, dried with $MgSO_4$, filtered and concentrated. The resulting crude product was purified by flash column chromatography (silica gel, hexanes/EtOAc, 50:1 to 15:1) to give alkyne **36** (17.8 g, 61% yield) as a yellow oil. **36**: R_f = 0.58 (silica gel, hexanes/EtOAc, 10:1); ^{1}H NMR (400 MHz, $CDCl_3$) δ 12.34 (s, 1 H), 4.84 (s, 1 H), 3.77 (s, 3 H), 3.25–3.07 (m, 4 H), 2.62 (dd, *J* = 7.3, 18.8 Hz, 1 H), 2.48 (m, 1 H), 2.14 (dt, *J* = 2.6, 7.0 Hz, 2 H), 2.08–1.85 (m, 4 H), 1.65–1.53 (m, 2 H), 1.30 (m, 1 H), 1.22 (s, 3 H), 1.10 (d, *J* = 7.3 Hz, 3 H); ^{13}C NMR (100

MHz, $CDCl_3$) δ 173.1, 170.6, 101.0, 84.5, 68.2, 64.2, 51.5, 44.5, 41.7, 39.2, 38.4, 35.2, 34.3, 32.8, 29.4, 19.6, 18.6, 15.6.

Common Intermediate 37. To a suspension of $InCl_3$ (7.2 g, 32.5 mmol, 1.0 equiv) in DCE (300 mL) at 23 °C was added a solution of alkyne **36** (11.5 g, 32.5 mmol, 1.0 equiv) in DCE (200 mL). The stirred reaction was then heated to 80 °C for 16 h. After cooling down to room temperature, the reaction was quenched by saturated aqueous $NaHCO_3$ (300 mL) and further stirred for 30 min at this temperature. The reaction contents were then filtrated through a pad of Celite (rinsing with CH_2Cl_2), and transferred to a separatory funnel. The organic layer was separated and the aqueous layer was extracted with CH_2Cl_2 (3 × 100 mL). The organic layers were combined, dried with $MgSO_4$, filtered and concentrated. The resulting crude product was purified by flash column chromatography (silica gel, hexanes/EtOAc, 20:1 to 5:1) to give common intermediate **37** (8.86 g, 77% yield) as a yellow oil. **37**: R_f = 0.41 (silica gel, hexanes/EtOAc, 4:1); ^{1}H NMR (400 MHz, $CDCl_3$) δ 5.85 (br, 1 H), 4.76 (s, 1 H), 3.78 (s, 3 H), 3.34–3.12 (m, 4 H), 3.08 (dd, *J* = 3.0, 13.3 Hz, 1 H), 2.84 (dd, *J* = 6.2, 17.8 Hz, 1 H), 2.36 (m, 1 H), 2.17–1.97 (m, 4 H), 1.58 (m, 2 H), 1.11 (m, 1 H), 0.96 (d, *J* = 6.6 Hz, 3 H), 0.95 (s, 3 H); ^{13}C NMR (100 MHz, $CDCl_3$) δ 207.9, 173.3, 129.4, 128.5, 65.1, 65.1, 52.4, 44.9, 44.3, 43.7, 38.5, 38.4, 36.8, 25.3, 24.8, 20.6, 16.3, 15.5.

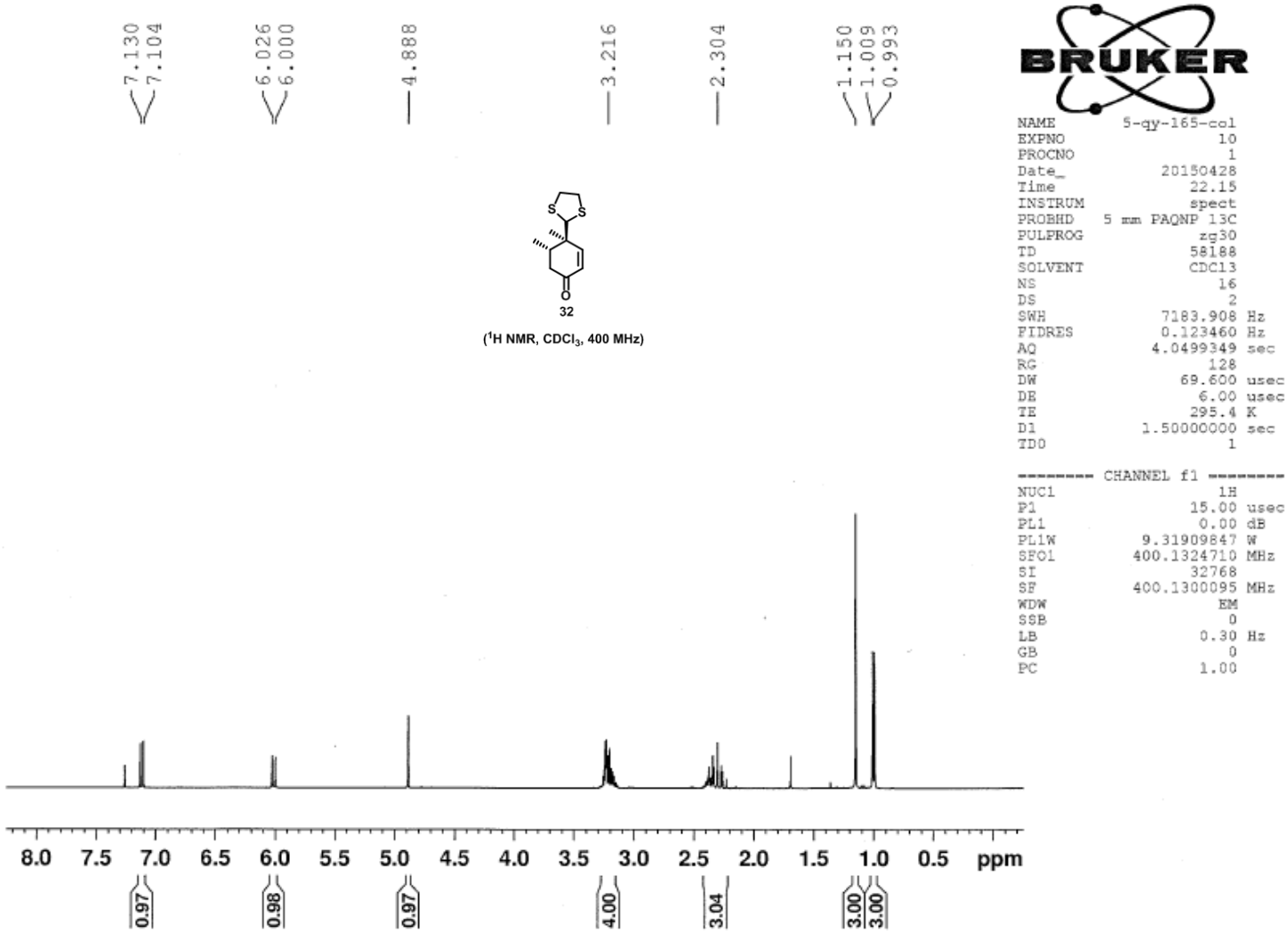
7.130
7.104
6.026
6.000
4.888
3.216
2.304
1.150
1.009
0.993
32
(¹H NMR, CDCl₃, 400 MHz)
NAME 5-qy-165-col
EXPNO 10
PROCNO 1
Date_ 20150428
Time 22.15
INSTRUM spect
PROBHD 5 mm PAQNP 13C
PULPROG zg30
TD 58188
SOLVENT CDCl3
NS 16
DS 2
SWH 7183.908 Hz
FIDRES 0.123460 Hz
AQ 4.0499349 sec
RG 128
DW 69.600 usec
DE 6.00 usec
TE 295.4 K
D1 1.50000000 sec
TD0 1
CHANNEL f1
NUC1 1H
P1 15.00 usec
PL1 0.00 dB
PL1W 9.31909847 W
SFO1 400.1324710 MHz
SI 32768
SF 400.1300095 MHz
WDW EM
SSB 0
LB 0.30 Hz
GB 0
PC 1.00
8.0 7.5 7.0 6.5 6.0 5.5 5.0 4.5 4.0 3.5 3.0 2.5 2.0 1.5 1.0 0.5 ppm
0.97
0.98
0.97
4.00
3.04
3.00
3.00

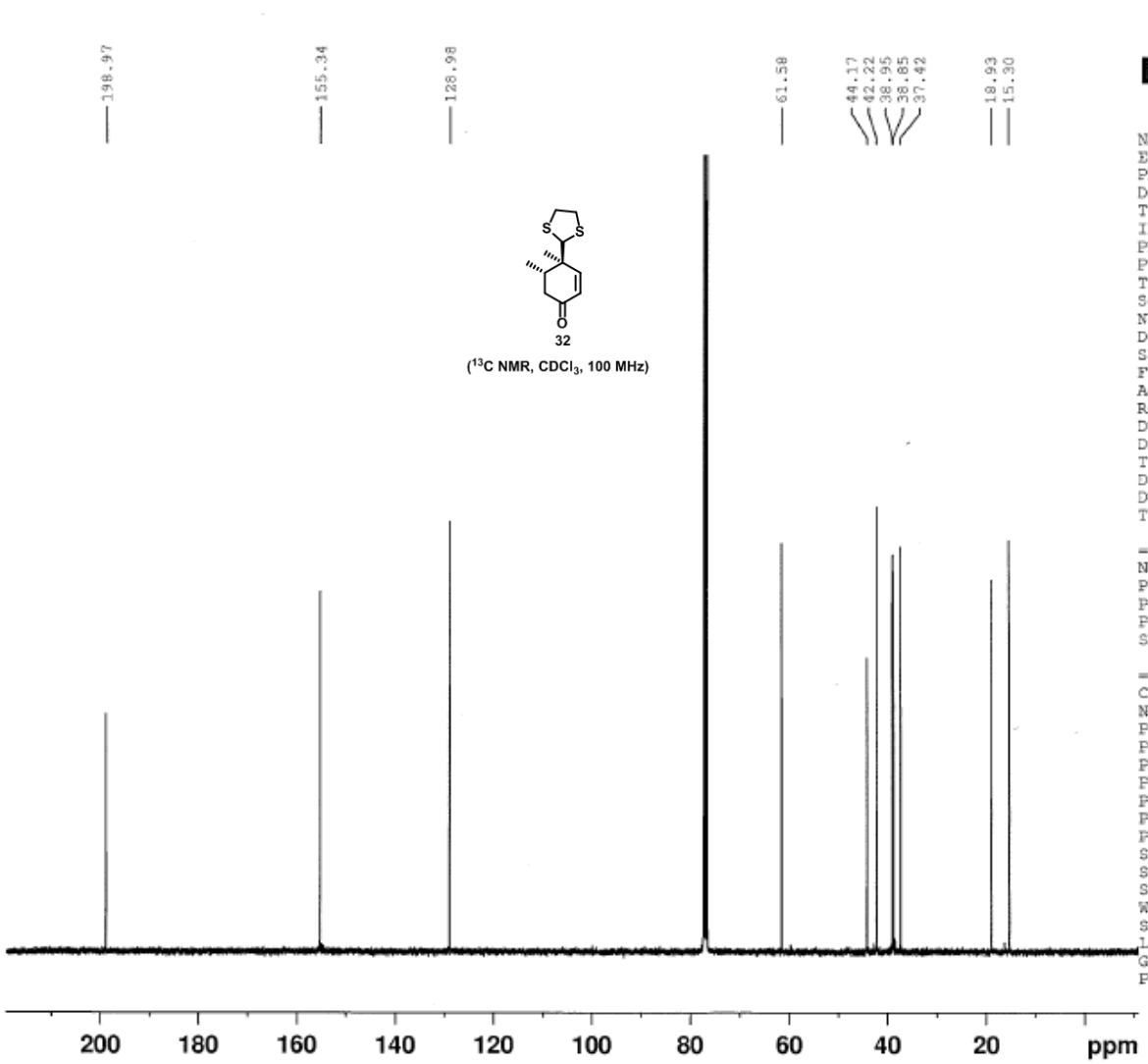

32

(^{13}C NMR, $CDCl_3$, 100 MHz)

BRUKER

NAME	5-qy-165-col	
EXPNO	11	
PROCNO	1	
Date_	20150429	
Time	1.09	
INSTRUM	spect	
PROBHD	5 mm PAQNP 13C	
PULPROG	zgpg30	
TD	65536	
SOLVENT	CDCl3	
NS	3000	
DS	4	
SWH	23980.814	Hz
FIDRES	0.365918	Hz
AQ	1.3664756	sec
RG	456.1	
DW	20.850	usec
DE	6.50	usec
TE	295.7	K
D1	2.00000000	sec
D11	0.03000000	sec
TD0	1	
======== CHANNEL f1 ========		
NUC1	13C	
P1	7.50	usec
PL1	-2.30	dB
PL1W	64.41350555	W
SFO1	100.6228298	MHz
======== CHANNEL f2 ========		
CPDPRG2	waltz16	
NUC2	1H	
PCPD2	90.00	usec
PL2	0.00	dB
PL12	15.56	dB
PL13	120.00	dB
PL2W	9.31909847	W
PL12W	0.25904420	W
PL13W	0.00000000	W
SFO2	400.1316005	MHz
SI	32768	
SF	100.6127748	MHz
WDW	EM	
SSB	0	
LB	1.00	Hz
GB	0	
PC	1.40	

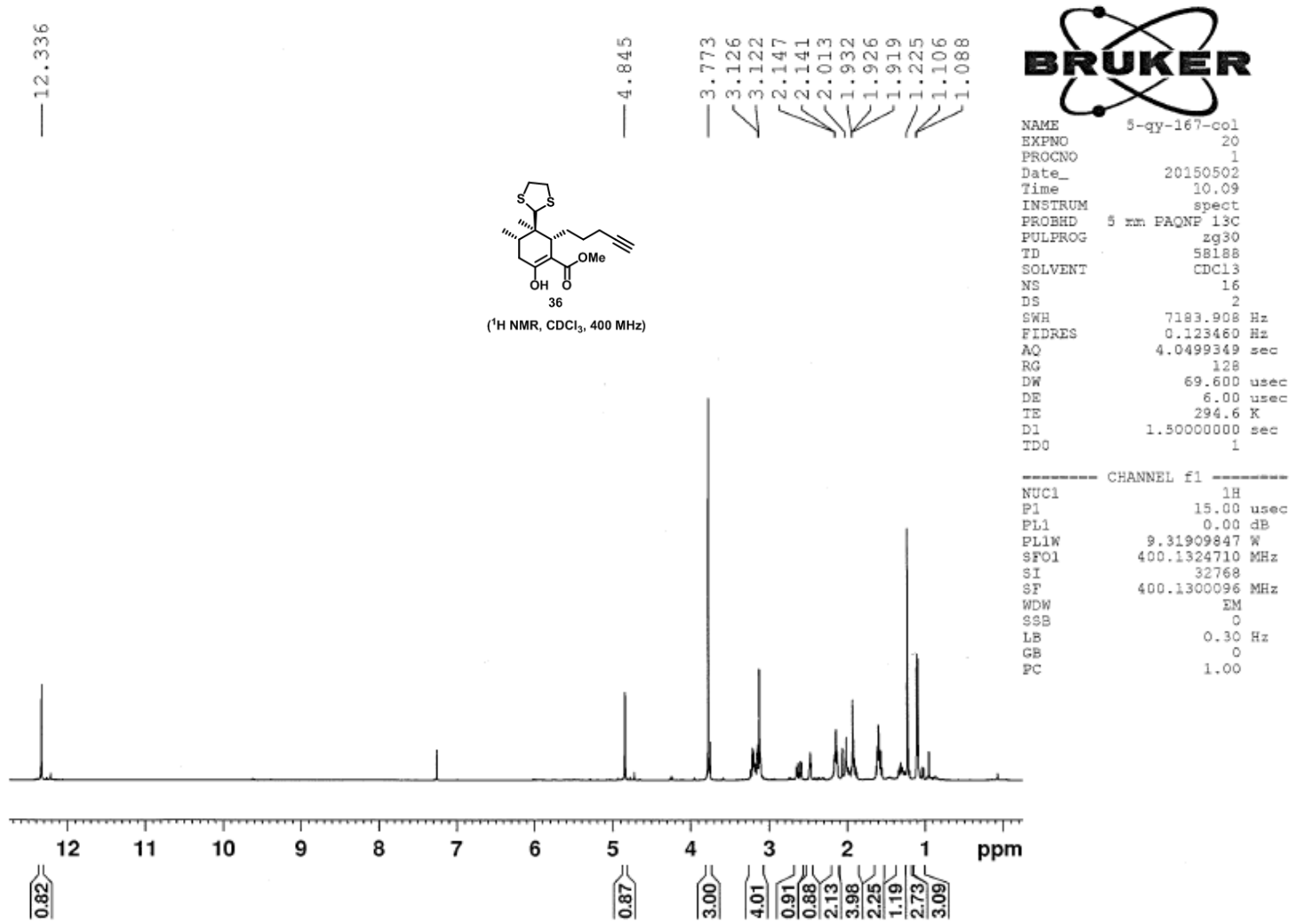
12.336
4.845
3.773
3.126
3.122
2.147
2.141
2.013
1.932
1.926
1.919
1.225
1.106
1.088
OMe
OH
O
36
(1H NMR, CDCl3, 400 MHz)
BRUKER
NAME 5-qy-167-col
EXPNO 20
PROCNO 1
Date_ 20150502
Time 10.09
INSTRUM spect
PROBHD 5 mm PAQNP 13C
PULPROG zg30
TD 58188
SOLVENT CDCl3
NS 16
DS 2
SWH 7183.908 Hz
FIDRES 0.123460 Hz
AQ 4.0499349 sec
RG 128
DW 69.600 usec
DE 6.00 usec
TE 294.6 K
D1 1.50000000 sec
TD0 1
CHANNEL f1
NUC1 1H
P1 15.00 usec
PL1 0.00 dB
PL1W 9.31909847 W
SFO1 400.1324710 MHz
SI 32768
SF 400.1300096 MHz
WDW EM
SSB 0
LB 0.30 Hz
GB 0
PC 1.00
12 11 10 9 8 7 6 5 4 3 2 1 ppm
0.82 0.87 3.00 4.01 0.91 0.88 2.13 3.98 2.25 1.19 2.73 3.09

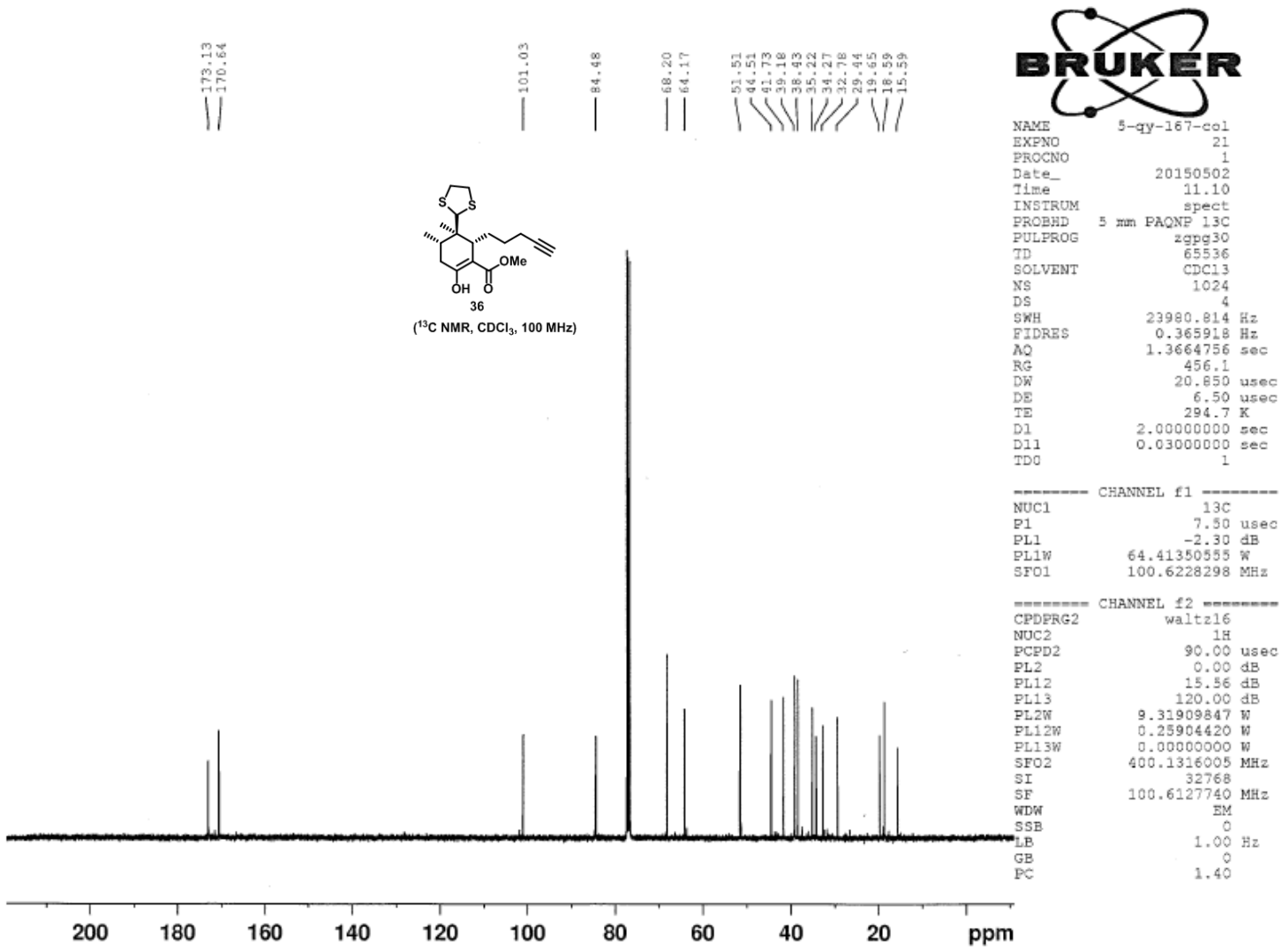

BRUKER

NAME	5-qy-167-col	
EXPNO	21	
PROCNO	1	
Date_	20150502	
Time	11.10	
INSTRUM	spect	
PROBHD	5 mm PAQNP 13C	
PULPROG	zgpg30	
TD	65536	
SOLVENT	CDCl3	
NS	1024	
DS	4	
SWH	23980.814	Hz
FIDRES	0.365918	Hz
AQ	1.3664756	sec
RG	456.1	
DW	20.850	usec
DE	6.50	usec
TE	294.7	K
D1	2.00000000	sec
D11	0.03000000	sec
TD0	1	
======== CHANNEL f1 ========		
NUC1	13C	
P1	7.50	usec
PL1	-2.30	dB
PL1W	64.41350555	W
SFO1	100.6228298	MHz
======== CHANNEL f2 ========		
CPDPRG2	waltz16	
NUC2	1H	
PCPD2	90.00	usec
PL2	0.00	dB
PL12	15.56	dB
PL13	120.00	dB
PL2W	9.31909847	W
PL12W	0.25904420	W
PL13W	0.00000000	W
SFO2	400.1316005	MHz
SI	32768	
SF	100.6127740	MHz
WDW	EM	
SSB	0	
LB	1.00	Hz
GB	0	
PC	1.40	

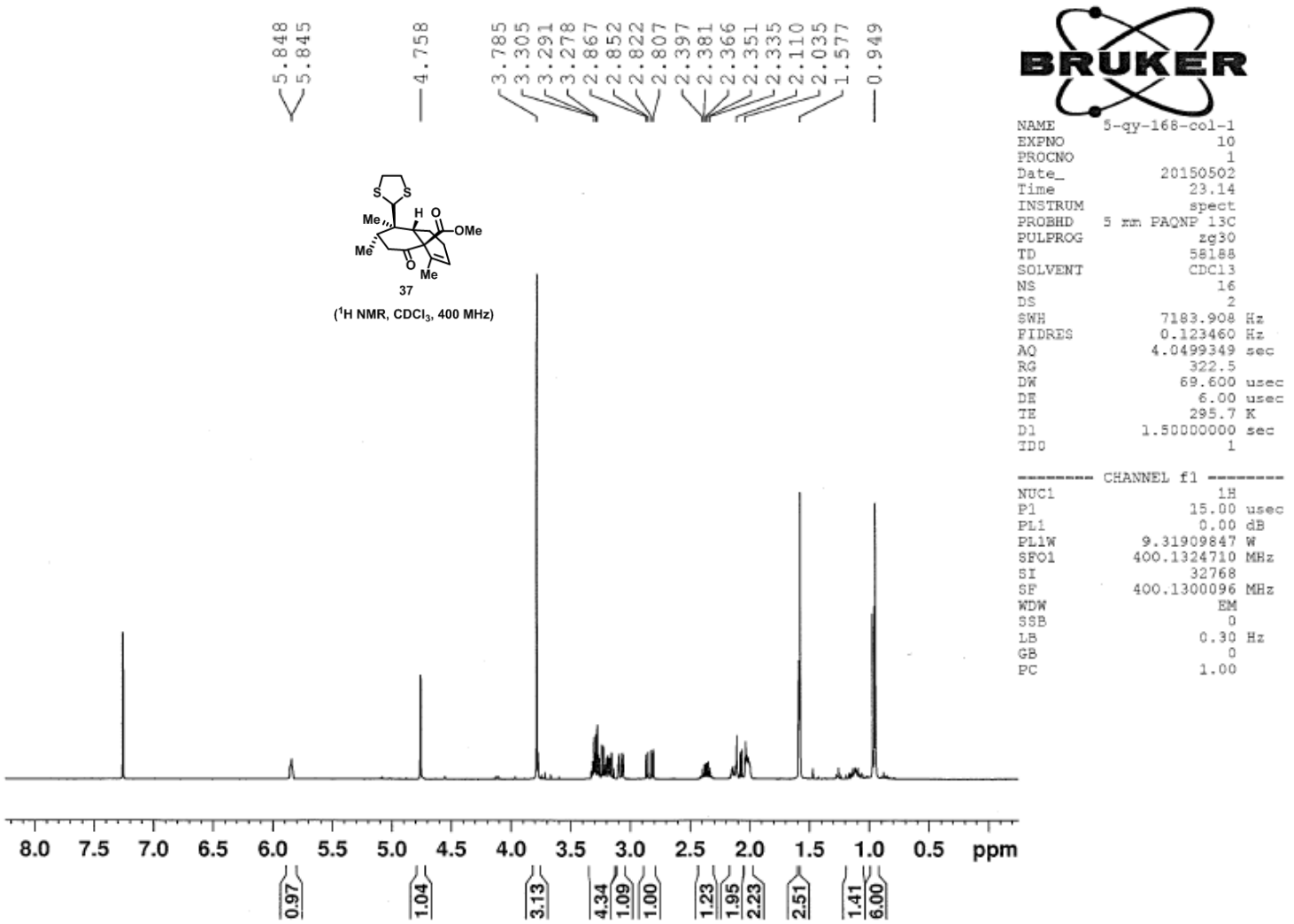
5.848
5.845
4.758
3.785
3.305
3.291
3.278
2.867
2.852
2.822
2.807
2.397
2.381
2.366
2.351
2.335
2.110
2.035
1.577
0.949
S
S
H
O
OMe
Me
Me
O
Me
37
(1H NMR, CDCl3, 400 MHz)
BRUKER
NAME 5-qy-168-col-1
EXPNO 10
PROCNO 1
Date_ 20150502
Time 23.14
INSTRUM spect
PROBHD 5 mm PAQNP 13C
PULPROG zg30
TD 58188
SOLVENT CDCl3
NS 16
DS 2
SWH 7183.908 Hz
FIDRES 0.123460 Hz
AQ 4.0499349 sec
RG 322.5
DW 69.600 usec
DE 6.00 usec
TE 295.7 K
D1 1.50000000 sec
TD0 1
CHANNEL f1
NUC1 1H
P1 15.00 usec
PL1 0.00 dB
PL1W 9.31909847 W
SFO1 400.1324710 MHz
SI 32768
SF 400.1300096 MHz
WDW EM
SSB 0
LB 0.30 Hz
GB 0
PC 1.00
8.0 7.5 7.0 6.5 6.0 5.5 5.0 4.5 4.0 3.5 3.0 2.5 2.0 1.5 1.0 0.5 ppm
0.97
1.04
3.13
4.34
1.09
1.00
1.23
1.95
2.23
2.51
1.41
6.00

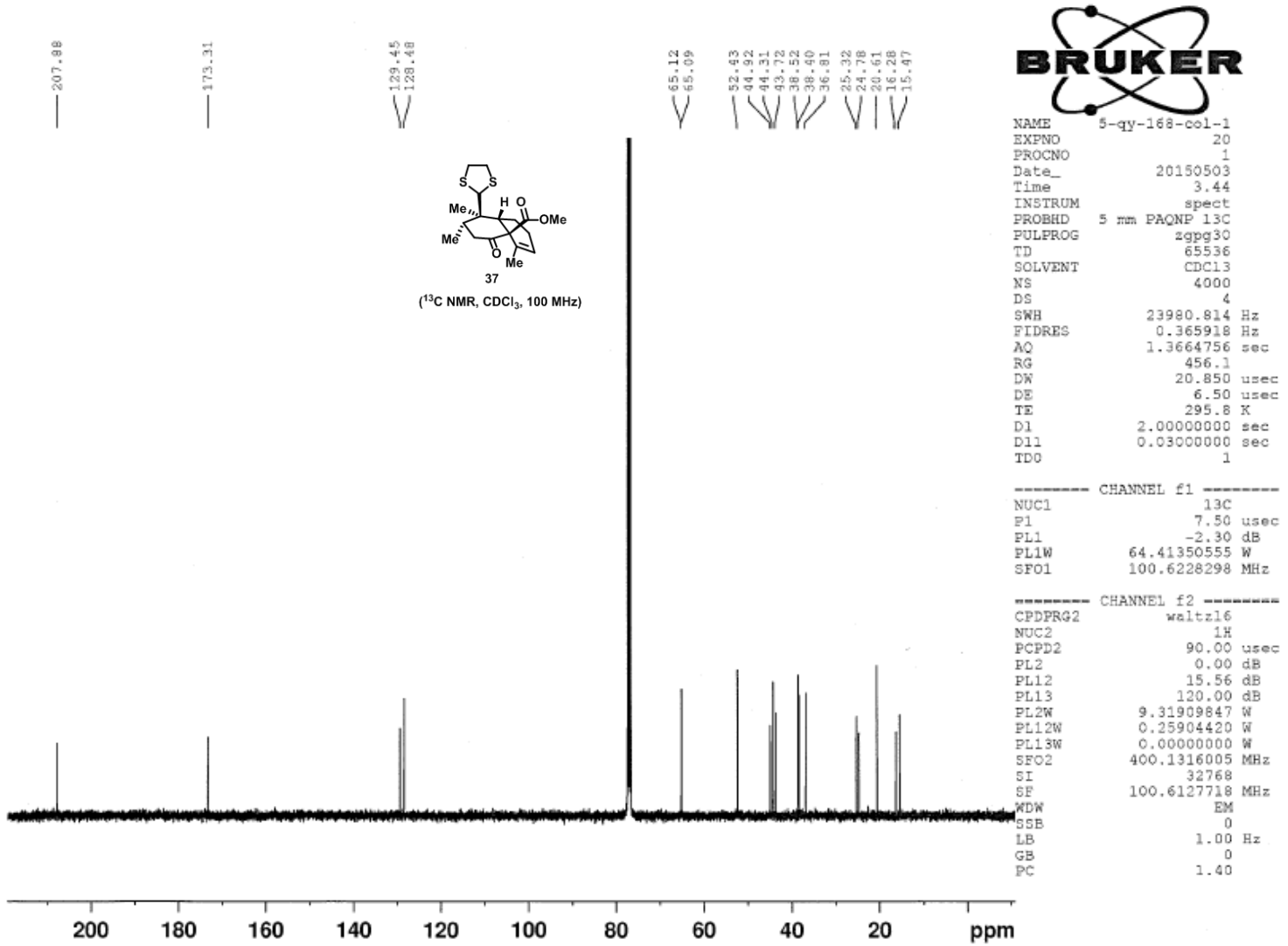


```
NAME          5-qy-168-col-1
EXPNO                     20
PROCNO                     1
Date_               20150503
Time                    3.44
INSTRUM                spect
PROBHD    5 mm PAQNP 13C
PULPROG             zgpg30
TD                      65536
SOLVENT                 CDCl3
NS                      4000
DS                         4
SWH                23980.814 Hz
FIDRES             0.365918 Hz
AQ                 1.3664756 sec
RG                     456.1
DW                    20.850 usec
DE                     6.50 usec
TE                    295.8 K
D1                 2.00000000 sec
D11                0.03000000 sec
TD0                        1

======== CHANNEL f1 ========
NUC1                      13C
P1                       7.50 usec
PL1                     -2.30 dB
PL1W            64.41350555 W
SFO1           100.6228298 MHz

======== CHANNEL f2 ========
CPDPRG2              waltz16
NUC2                      1H
PCPD2                 90.00 usec
PL2                    0.00 dB
PL12                  15.56 dB
PL13                 120.00 dB
PL2W             9.31909847 W
PL12W            0.25904420 W
PL13W            0.00000000 W
SFO2           400.1316005 MHz
SI                     32768
SF             100.6127718 MHz
WDW                       EM
SSB                        0
LB                      1.00 Hz
GB                         0
PC                      1.40
```

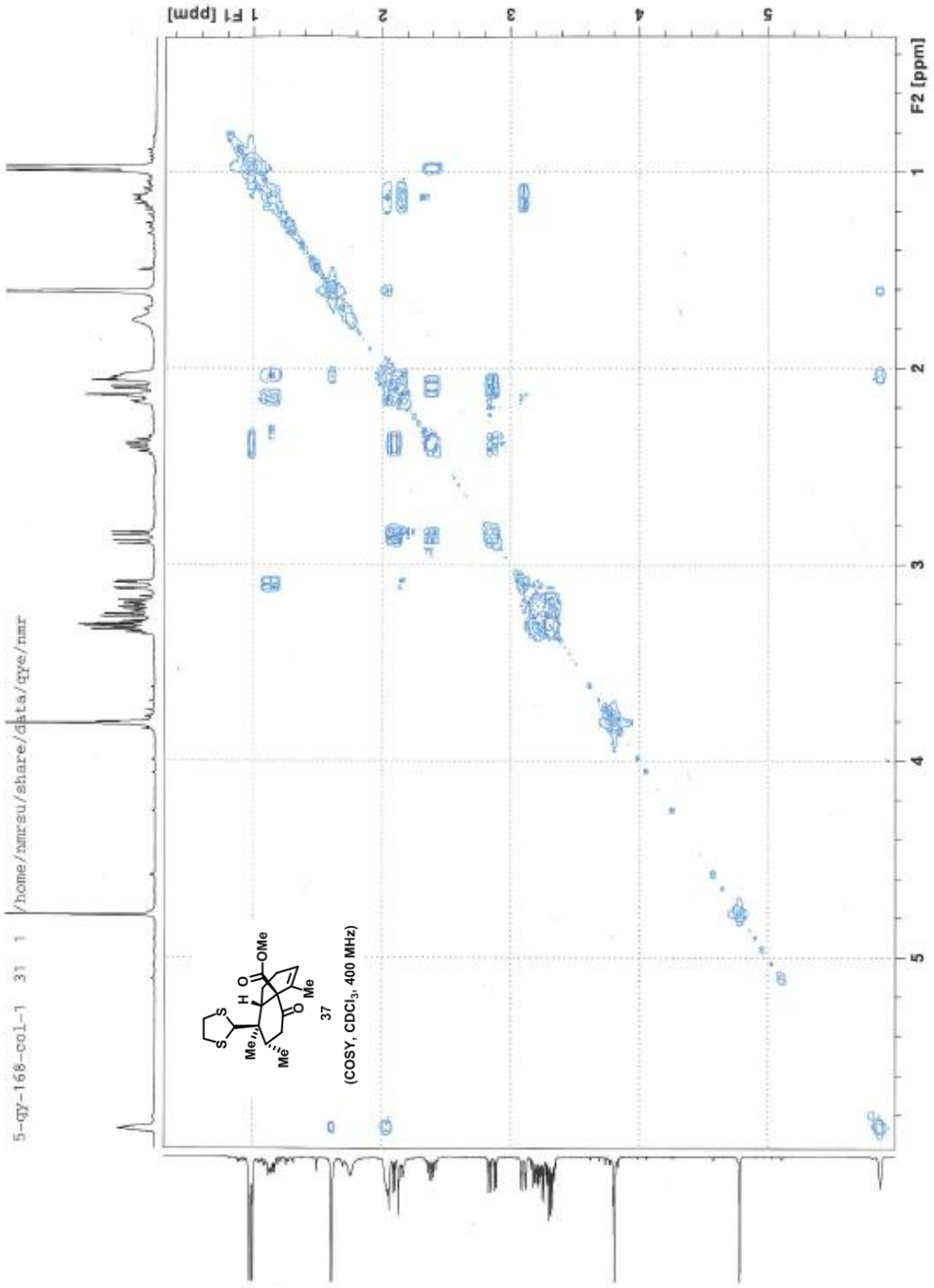
5-qy-168-col-1 31 1 /home/nmrsu/share/data/qye/nmr
F1 [ppm]
F2 [ppm]
1
2
3
4
5
OMe
H
O
Me
Me
Me
S
S
O
37
(COSY, CDCl3, 400 MHz)

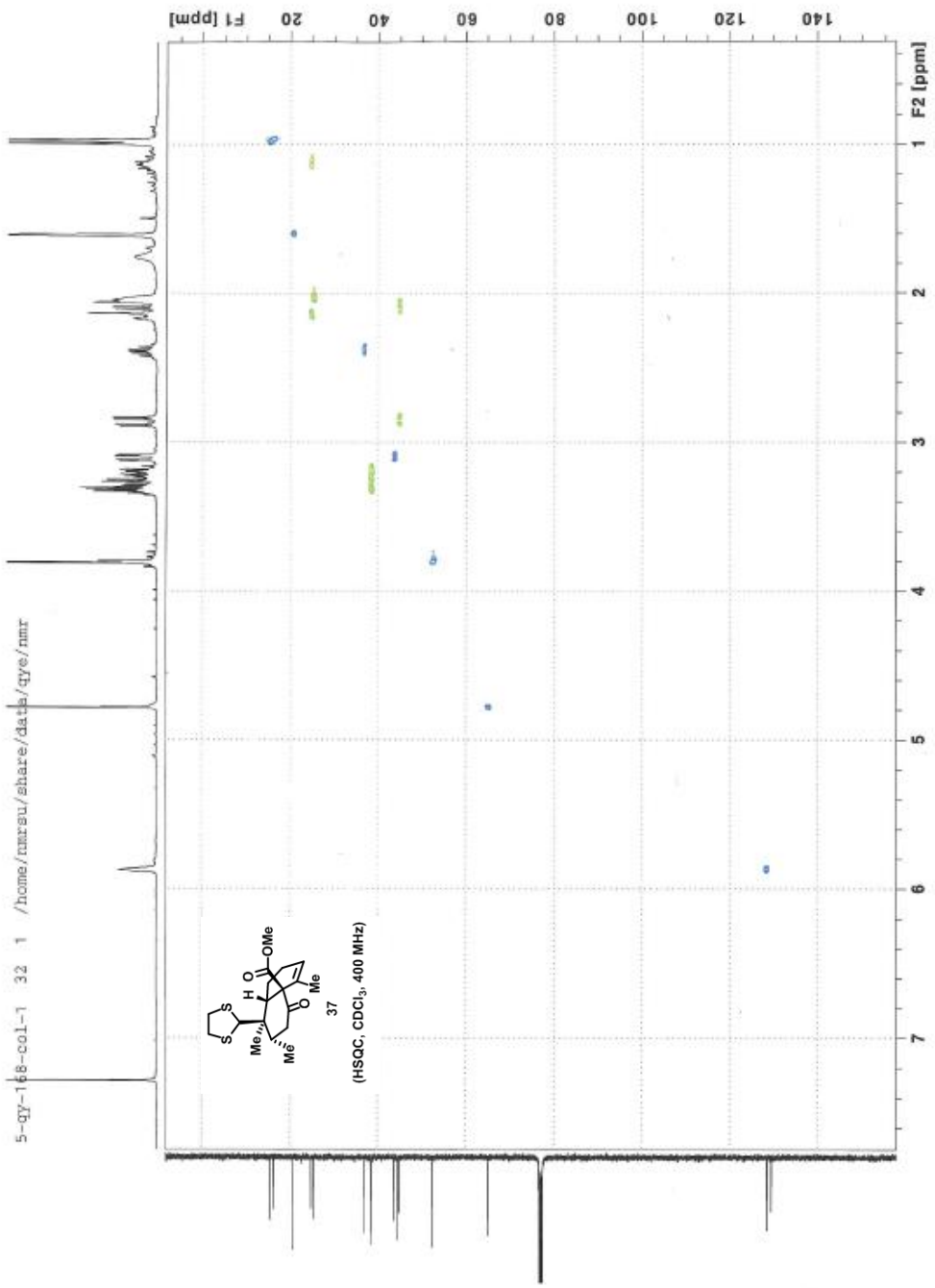
5-qy-1 66-col-1 32 1 /home/nmrsu/share/data/qye/nmr
F1 [ppm]
F2 [ppm]
OMe
Me
Me
Me
37
(HSQC, CDCl3, 400 MHz)

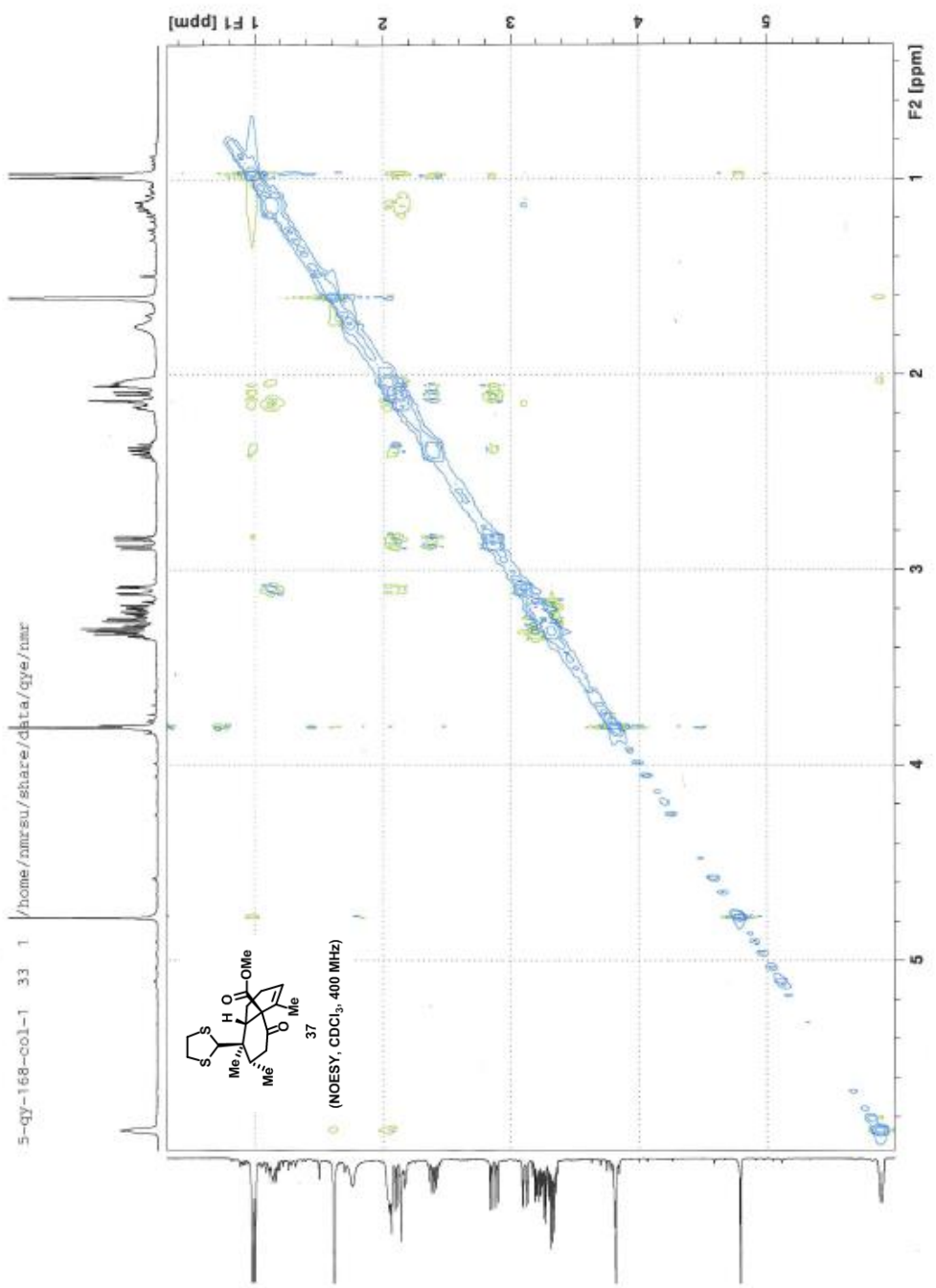
5-qy-168-col-1 33 1
/home/nmrsu/share/data/qye/nmr
F1 [ppm]
F2 [ppm]
1
2
3
4
5
OMe
O
H
S
S
Me
O
Me
Me
37
(NOESY, CDCl3, 400 MHz)

CHAPTER 4

EXPLORATION OF SITE-SELECTIVE C–H OXIDATION

AT THE C-10 POSITION

4.1 Introduction

With the gram scale synthesis of common intermediate **3** achieved, we then moved to the second phase of our studies, namely modification of the decalin framework to full scaparvin terpenoids (Scheme 1). Comparing the structure of common intermediate **3** with scaparvin A (**4**), in particular, the most challenging element of the transformations envisioned involves an oxidation at the C-10 position through some means of C–H oxidation. This chapter details the evolution of our approach for that site-selective oxidation, beginning with efforts to utilize a Hofmann–Loffler–Freytag strategy. That discussion will be followed by our attempts to facilitate a directed C–H oxidation using materials with a locked molecular conformation. Finally, some additional and critical optimizations of the overall synthetic route will be discussed as well.

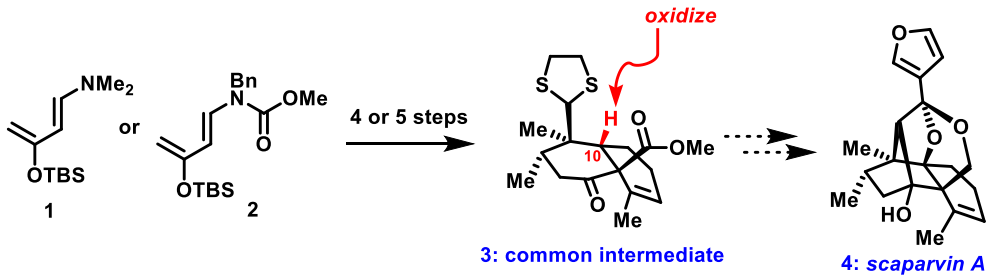

Scheme 1. Site-selective C-H oxdiation at C-10 postion of the common intermediate (**3**).

4.2 C-10 Oxidation via Hofmann–Loffler–Freytag Strategy

Given the retrosynthetic analysis of scaparvin A (**4**) presented in Chapter 2, we hoped that key intermediate **5** could serve to deliver several scaparvin terpenoids, including scaparvin A (**4**, Scheme 2). In order to obtain **5** from common intermediate **3**, the C-10 position must be oxidized selectively. However, achieving this chemical transformation was expected to be

difficult given the presence of the sterically more accessible tertiary C–H bond at C-8, as well as the more activated allylic C–H bonds at C-2 and C-18 within the molecule.

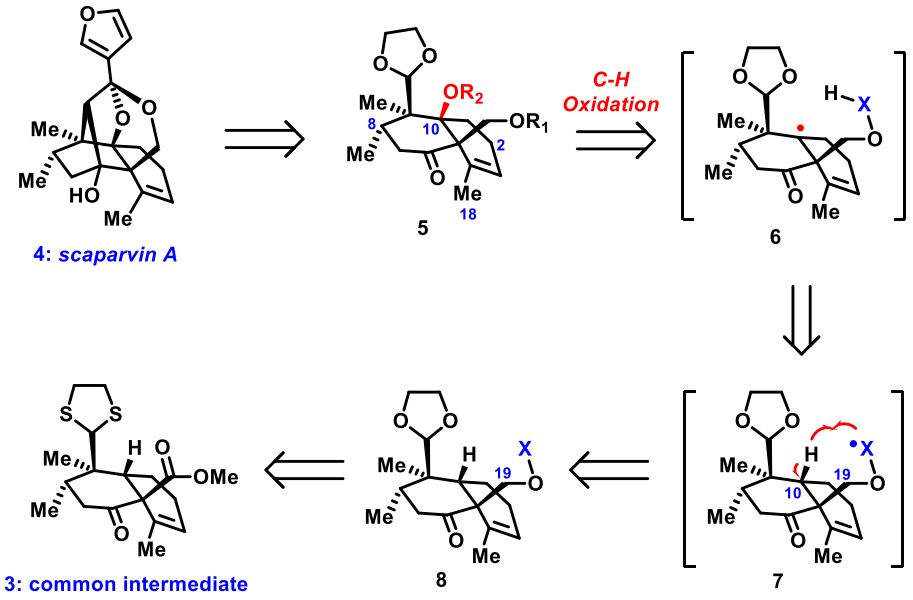

Scheme 2. Preliminary retrosynthetic analysis of scaparvin A (**1**) from common intermediate **3.**

Because the C–H bond at C-10 is neither sterically favored nor electronically favored, we envisioned that C–H oxidation chemistry effected in an intermolecular fashion would be unlikely to achieve the desired oxidation selectively over other potential reactive sites. By contrast, if a proper functional group within the structure could be exploited as a directing group, then the innate requirements of the reaction's cyclic transition state might provide the desired site-selectivity. For instance, when radical-generating functionality is installed at C-19 position, the resulting radical (**7**, Scheme 2) is expected to intramolecularly abstract the hydrogen at C-10 position through a cyclic transition state. Subsequent radical quenching of the resulting tertiary radical **6** could result in a formal C–H oxidation.

A thorough review of the literature afforded a promising precedent in the work of Baran[1] who reported a radical-mediated C–H oxidation using a trifluoroethyl carbamate moiety as a

directing group (Scheme 3). This Hofmann–Loffler–Freytag reaction is proposed to involve initial *N*-radical generation followed by hydrogen abstraction through a 7-membered ring transition state. The new radical species (**12**), in turn, delivered cyclic carbonate **14.** With this encouraging precedent, we sought to install a carbamate moiety to direct a C–H oxidation at the C-10 position in our molecule in a similar manner.

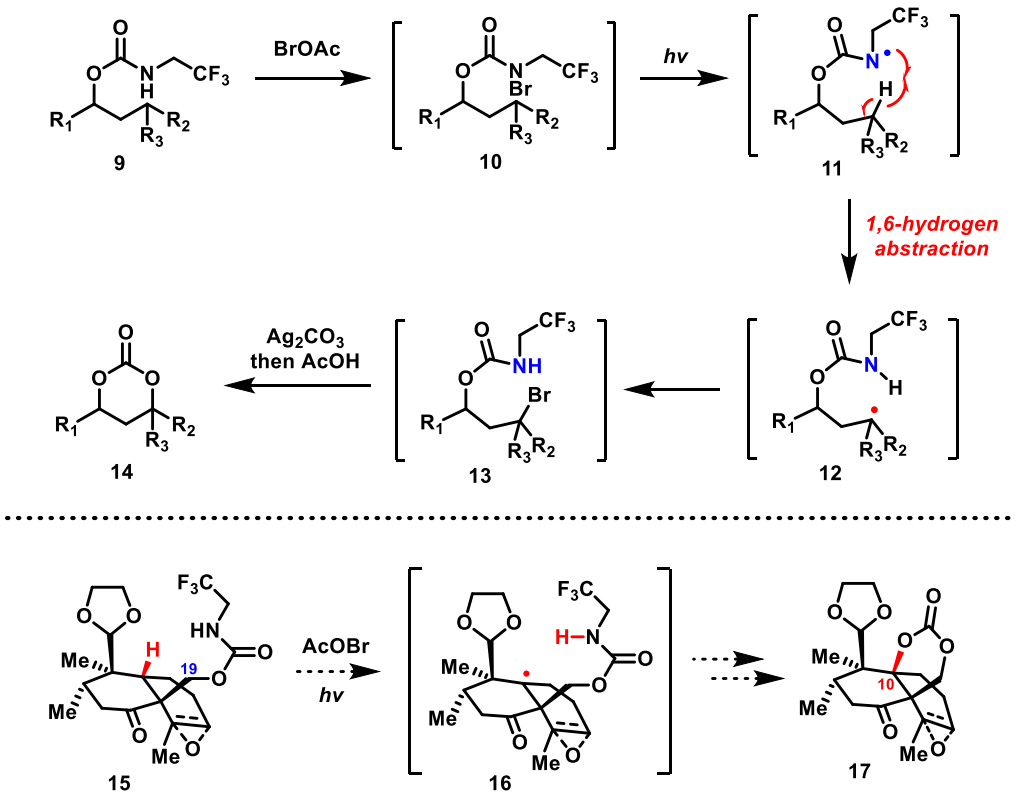

Scheme 3. Hofmann-Loffler-Freytag reaction using Baran's trifluoroethyl carbamate.

In order to test the feasibility of this protocol on the decalin framework, we first prepared the simplified *cis*-decalin **23** (Scheme 4) to serve as a model compound. Beginning with a $TiCl_4$-assisted Diels–Alder reaction of 1-cyclohexene-1-carboxaldehyde (**18**) with 2-methyl-1,3-butadiene (**19**), reduction of the resulting aldehyde **20** followed by carbamate formation afforded compound **22** smoothly. Following catalytic hydrogenation, the precursor for the Hofmann–

Loffler–Freytag reaction (**23**) was obtained quantitatively in 2.2:1 dr. In the key test, subjecting the major isomer of **23** to the Baran conditions using *N*-bromide formation and subsequent photolization, we pleasingly obtained the desired carbonate **25** in 41% yield following a terminating treatment with Ag_2CO_3 and AcOH.

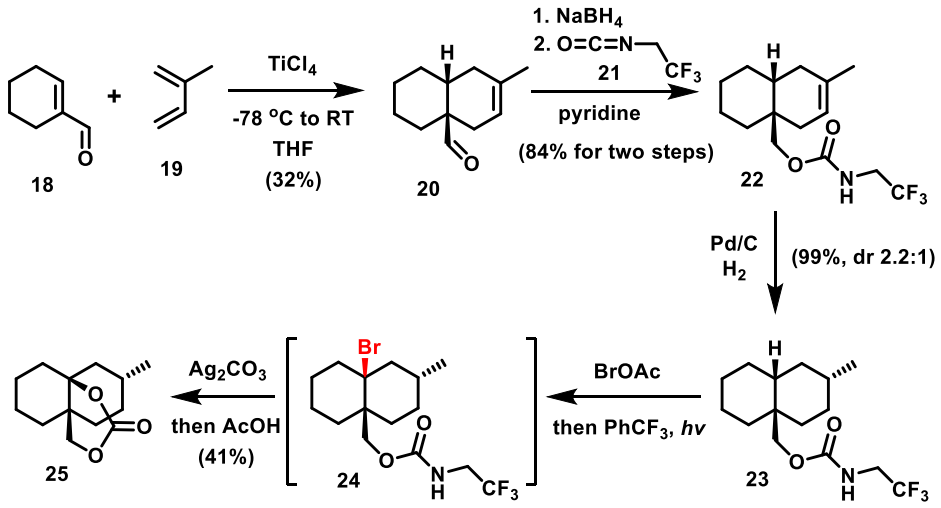

Scheme 4. Model study of Hofmann-Loffler-Freytag reaction using Baran's trifluoroethyl carbamate.

Encouraged by this crucial result, we then set about applying this radical-based C–H oxidation to fully functionalized materials for the scaparvin terpenoids (Scheme 5). Common intermediate **3** was therefore treated with $PhI(OTFA)_2$ and ethylene glycol, providing acetal **26**. Next, a selective reduction of the ketone group in **26**, followed by carbamate formation, successfully installed the directing group at the C-19 position. At this stage, given concerns of potential electrophilic additions involving the double bond under *N*-bromide formation conditions, an additional and alternative C–H oxidation precursor, epoxide **29** (dr = 1.4:1), was also synthesized through a standard *m*CPBA-induced epoxidation protocol.

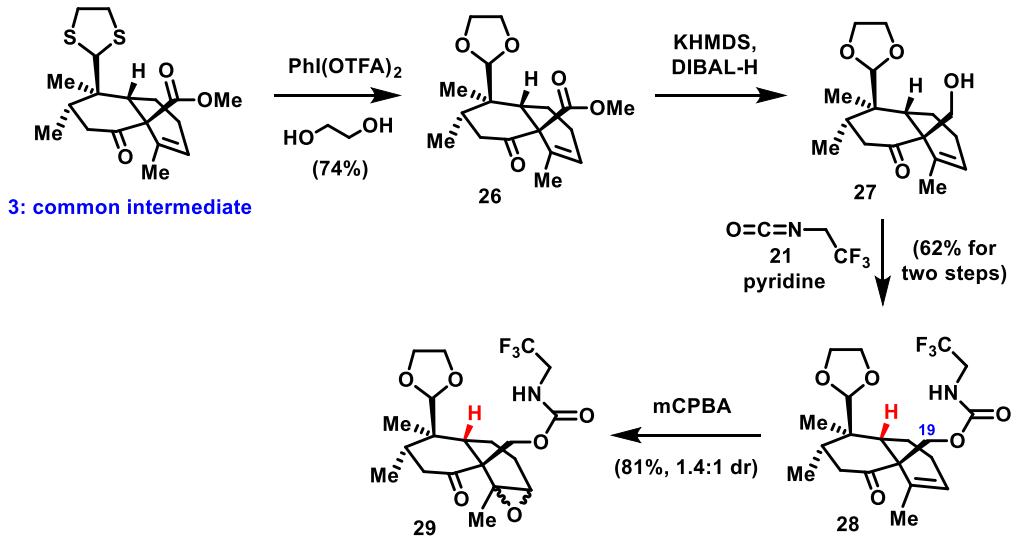

Scheme 5. Syntheses of the fully functionalized precursors (**29** and **28**) of Hofmann-Loffler-Freytag reaction.

Unfortunately, following extensive attempts to tune reaction conditions (involving standard changes of solvents, temperature, reaction time, etc.), the proposed Hofmann–Loffler–Freytag failed reaction to deliver the desired product (**17**, Scheme 6). Based on TLC analysis, the initial *N*-bromide formation step appeared to succeed, suggesting that *N*-radical **30** should be formed upon photo irradiation. However, the reaction ultimately afforded an uncharacterizable mixture of by-products in the end. Based on molecular models, the conformation of *N*-radical species might not be predisposed for success, as the productive conformer suffers from severe steric repulsion between the acetal group and the carbamate moiety. Given that the C5–C19 single bond is free to rotate, the highly reactive N-radical might prefer to exist as conformer **31**, which, in turn, could cause various side reactions either inter- or intramolecularly and thus explain the results obtained.

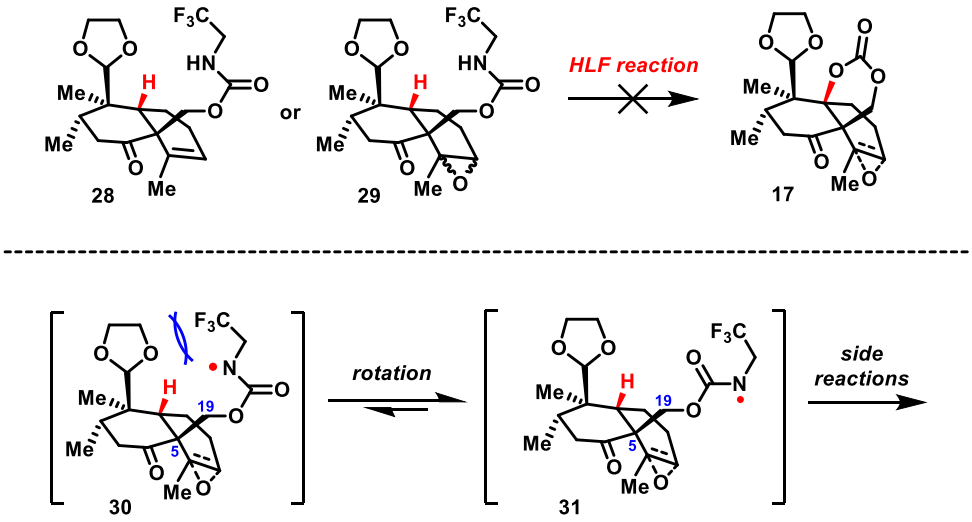

Scheme 6. Rationale for the failed Hofmann-Loffler-Freytag reaction.

Thus, we determined that achieving the needed C–H oxidation using C-19 functionality as a directing group is not likely to succeed, even with alternate protocols, based on the flexible molecular conformation of the framework in general terms. As a result, we needed to redesign our approach again to achieve a site-selective C-10 oxidation.

4.3 C-10 Oxidation Using a Rigid Bridge System

The key lesson we learned from the failed Hofmann–Loffler–Freytag strategy is that an effective directing group within our decalin framework should be conformationally locked. With this idea in mind, we revised our synthetic plan, aiming to construct the [2.2.1]-bridge system of the target first and then use functionality at the C-12 position to direct the C–H oxidation as shown in Scheme 7. The key concept here is that the C-12 moiety will be locked by the rigid carbon skeleton and in turn facilitate the directed C–H oxidation with this desired conformation.

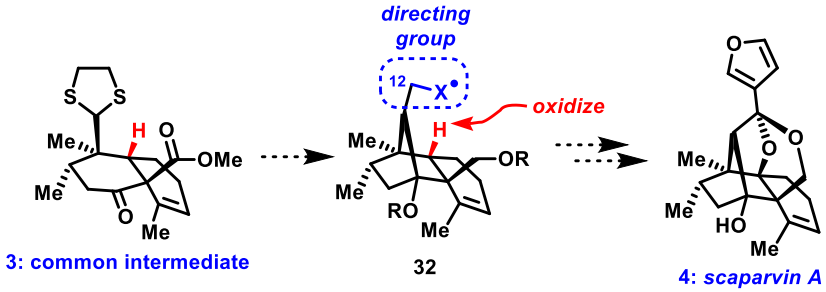

Scheme 7. Site-selective C-H oxidation with bridge system.

To identify the optimal directing group, we sought to utilize a simplified [2.2.1]-bicyclic structure as an initial model (Scheme 8). As shown, this material took several steps to prepare. Starting from Diels–Alder product **33**, subsequent double bond reduction, followed by a SmI_2-mediated Pinacol coupling[2], afforded [2.2.1]-bicycle **35**. This new material (**35**) was then oxidized to hydroxyl ketone **36** via Swern conditions[3]. It is worth mentioning that other oxidation conditions (such as Dess–Martin periodinane, IBX, TPAP/NMO, etc.) afforded oxidative cleavage products. After olefination of ketone **36** using a Wittig reaction,[4] the resulting tertiary alcohol (**37**) was protected as a TBS ether to afford **38**. Next, alcohol **39** was obtained as a mixture of diastereomers through a sequence of hydroboration and following oxidative work-up. In addition to alcohol **39**, compound **40** was also prepared as a potential C–H oxidation precursor with the carboxylic acid moiety would serve as the directing group.

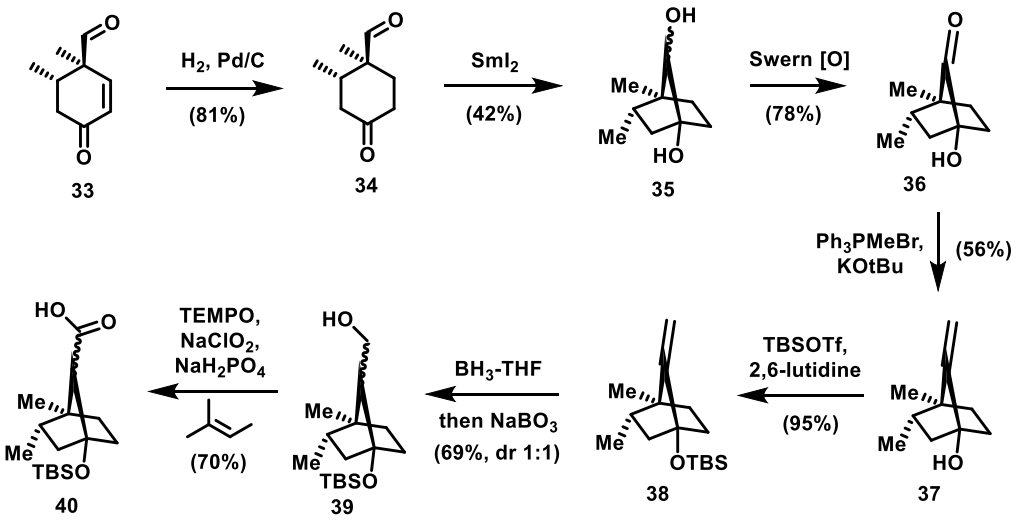

Scheme 8. Syntheses of the model compounds (**39** and **40**) for directed C-H oxidation.

With both **39** and **40** in hand, we then examined the C–H oxidation chemistry (Scheme 9). After several failed attempts, we were pleased to find the oxy-radical generated from **39** under Suárez condition[5] delivered C–H oxidation product **42** via a 1,5-hydrogen abstraction. Similarly, treatment of carboxylic acid **40** with the White-Chen catalyst [Fe(PDP)] and H_2O_2 also facilitated the desired tertiary C–H oxidation.[6] Although the yields were low in both cases in numerical terms, the overall outcome is actually fairly good, considering that only one epimer (i.e. half of the starting material) satisfies the three-dimensional requirements for a productive transition state. In deciding how to press forward, we believed that the potential of lactone moiety in **44** for further functionalization would be a far superior approach, as we sought to use this variant in our following studies.

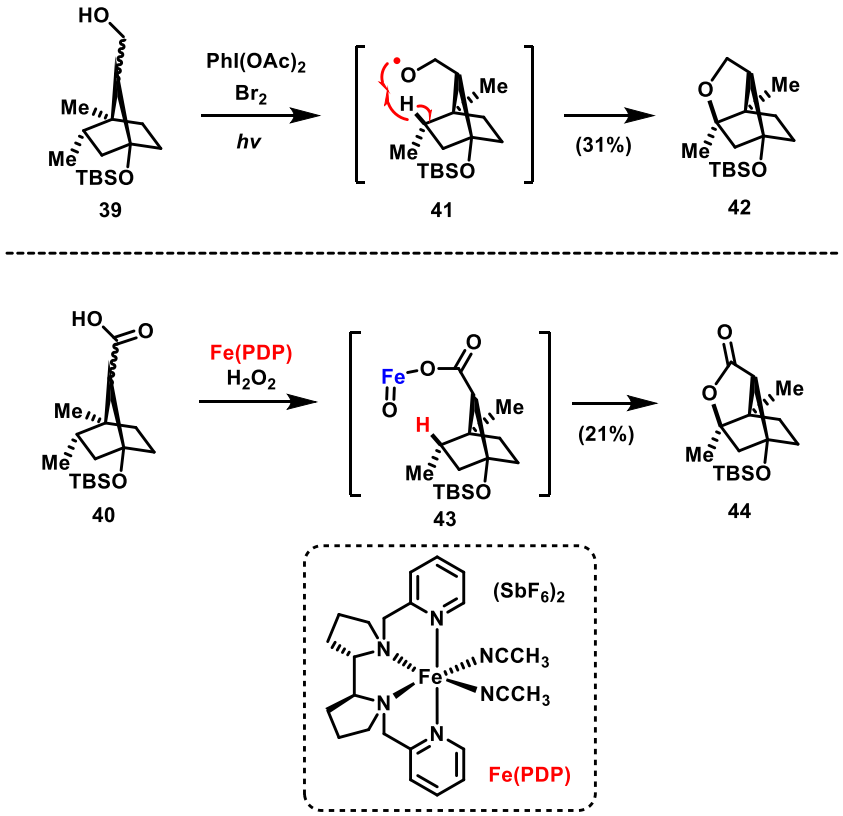

Scheme 9. Model studies of directed C-H oxidation.

Encouraged by this crucial result, we then headed to C–H oxidation of fully functionalized materials for the scaparvin terpenoids, beginning with construction of the bridge system. As shown in Scheme 10, oxidative deprotection of the dithiolane moiety on common intermediate **3** using $PhI(OTFA)_2$ provided ketoaldehyde **45**. Surprisingly, upon treatment with SmI_2, only ester migration product **46** was observed (a structure verified by X-ray crystallography), of which a plausible reaction pathway is showcased. The resulting ketyl radical anion **47**, instead of adding to the ketone group, seemingly preferred to attack the sterically more accessible ester group. Once [1.2.3]-bicycle **48** is formed, it could quickly undergo a retro-aldol type reaction to release the ring strain. Thus, upon acidic work-up, **46** is the major product formed.

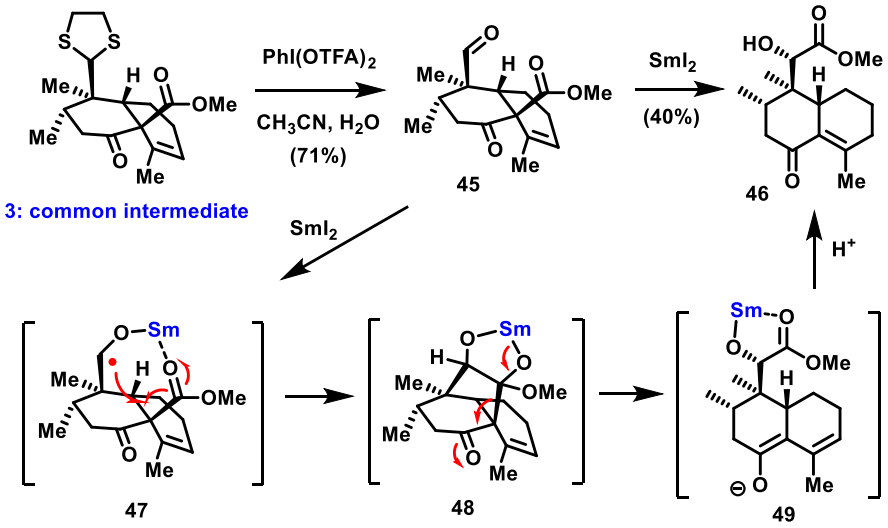

Scheme 10. Formation of the undesired ester migration product (**46**).

The solution to prevent this ester migration pathway proved very straightforward to achieve. Again starting from common intermediate **3**, selective reduction of ester group followed by TIPS protection and oxidative deprotection of dithiolane group afforded ketoaldehyde **50** smoothly. In this case, the ketone group is the only electrophilic site within the molecule, resulting a successful Pinacol coupling of **50** to deliver [2.2.1]-bicycle **51**.

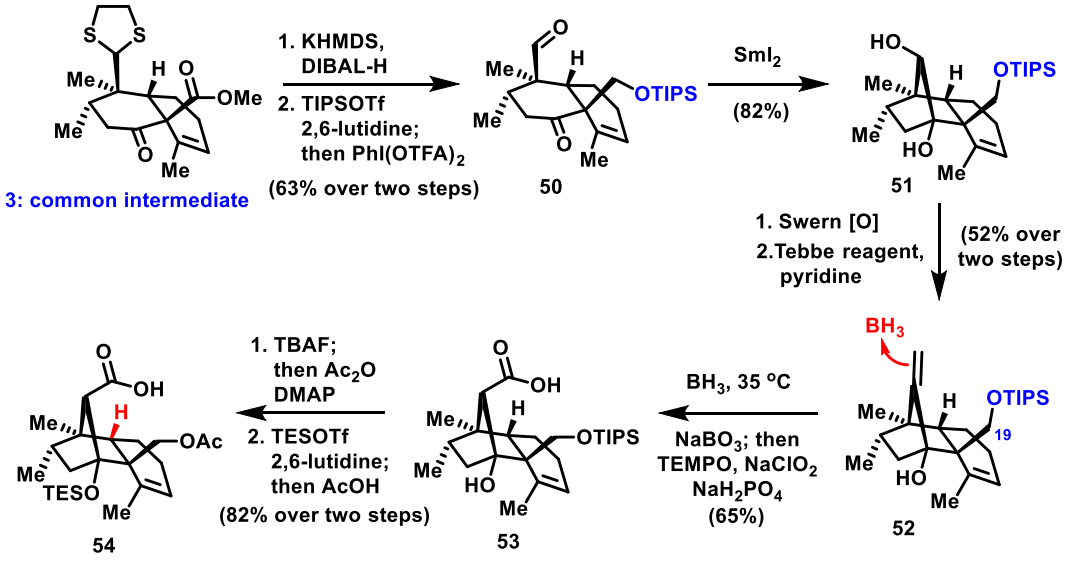

Scheme 11. Synthesis of the fully functionalized precursor **54** for directed C-H oxidation.

With this key bond now synthesized, the resultant 1,2-diol moiety was then oxidized to a hydroxy ketone using a standard Swern oxidation. After several unsuccessful attempts of olefinating the newly formed ketone, we identified that the Tebbe reagent could achieve the desired methylenation of this hindered ketone group.[7] Next, hydroboration of that new alkene **52**, followed by oxidative work-up, provided carboxylic acid **53** as a single diastereomer. In this substrate, the bulky TIPS group is crucial for regio- and facial-selectivity of the hydroboration step, which forces the borane species reacting from the opposite face. Other substrates with smaller functionalities at C-19 position, such as one with a TBS group, often resulted in complex mixtures of products and inferior yields of the desired carboxylic acid **53**. Finally, the fully functionalized C–H oxidation precursor (**54**) was obtained through several straightforward protecting group manipulations.

With **54** in hand, we first tested the directed C–H oxidation using the standard protocol reported by the White group.[6] Adding 15 mol% of Fe(PDP) and 3 equivalents of H_2O_2 in three equal portions to a solution of **54** in acetonitrile over 45 min gave **55** in 31% yield. In the event, the carboxylic acid moiety again proved to be an effective directing group for C-10 oxidation, while the tri-substituted double bond was epoxidized as well. Although **55** could be reduced back to alkene **56** by using Cp_2TiCl to extrude the epoxide oxygen atom, we felt it would be highly useful if a fully chemoselective C–H oxidation to deliver **56** in one step could be achieved, not only our own substrate, but for others as well where accessible and reactive olefins might be present.

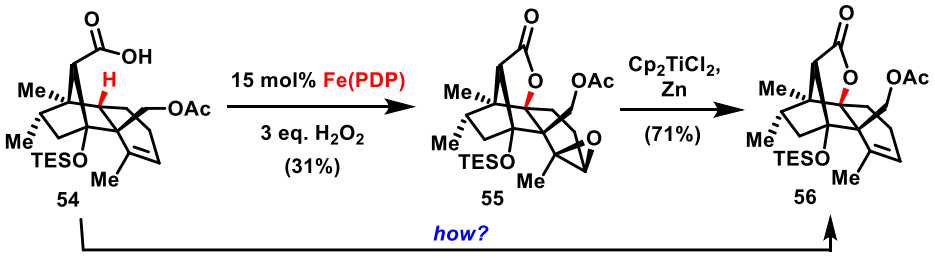

Scheme 12. Directed C-H oxidation of **54** using the standard White's protocol.

In order to improve the directed C–H oxidation, we considered in greater depth the reaction pathways by which the oxidation could have occurred (Scheme 13). On one hand, when the carboxylic acid moiety coordinates to Fe(PDP), it should only facilitate an intramolecular hydrogen abstraction to afford the desired product **56**. By contrast, any free iron-catalyst in the reaction media would be the likely culprit for catalyzing the epoxidation of olefin moiety. Based on this understanding of the mechanism, the key to suppress the epoxidation pathway is to limit the amount of free catalyst within the reaction mixture.

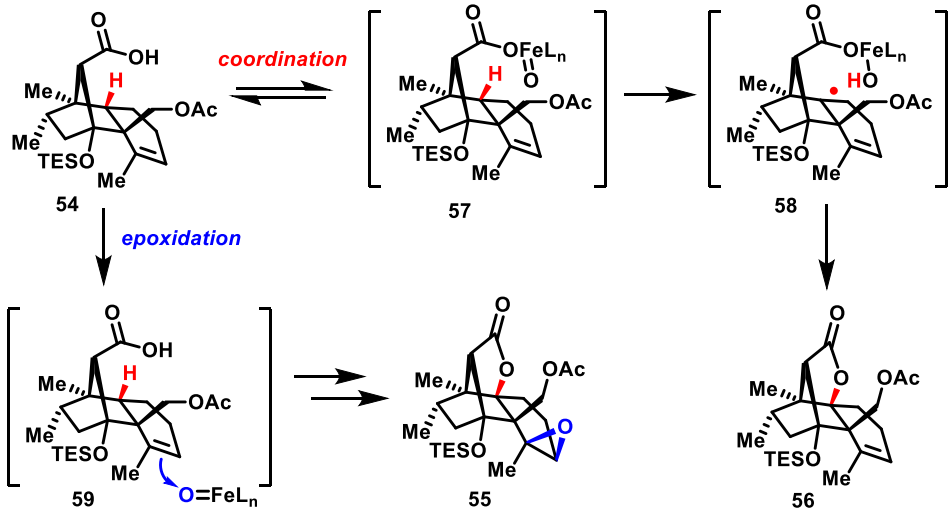

Scheme 13. Two reaction pathways of the directed C-H oxidation of **54.**

A small screen of conditions revealed that both catalyst loading and addition method play an important role in controlling the C–H oxidation. The optimal conditions involved slow and

simultaneous addition of 2 mol% Fe(PDP) in CH_3CN and 1.2 equivalent H_2O_2 in CH_3CN over 1 h using syringe pump into a solution of the substrate in CH_3CN, providing the desired C–H oxidation product **56** in 43% yield along with 28% epoxide **55**. Thus, although **56** could not be produced exclusively, overoxidation to **55** could be somewhat suppressed relative to our initial studies.

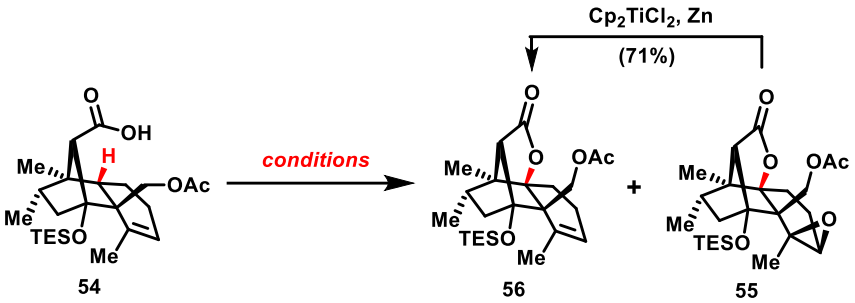

Entry	*Fe(PDP)*	*H_2O_2*	*addition methods*	*Yield of 56*	*Yield of 55*
1	15 mol%	3.0 eq.	added in 3 portions	trace	31%
2	15 mol%	1.2 eq.	added in 3 portions	7%	37%
3	5 mol%	1.2 eq.	added in 3 portions	18%	21%
4	2 mol%	1.2 eq.	added in 3 portions	31%	17%
5	2 mol%	1.2 eq.	slow addition using syringe pump	43%	28%

Scheme 14. Optimization of the directed C-H oxidation.

Given the challenge of this chemical transformation, the overall yield of 63% is proved sufficient to move forward for further studies, noting that additional modifications to the conditions, for example employing other metals, are the subject of current investigations as well.

4.4 Conclusion

As detailed in the above sections, we have accomplished a site-selective C-H oxidation at C-10 position, affording compound **56** as an advanced intermediate for scaparvin terpenoids. It required a total of 9 steps from common intermediate **3**, with key highlights of the developed approach being a SmI_2-mediated Pinacol coupling and a directed C–H oxidation using the White-Chen catalyst under optimized conditions which achieved high chemoselectivity over a reactive and accessible trisubstituted alkene as denoted in Scheme 15.

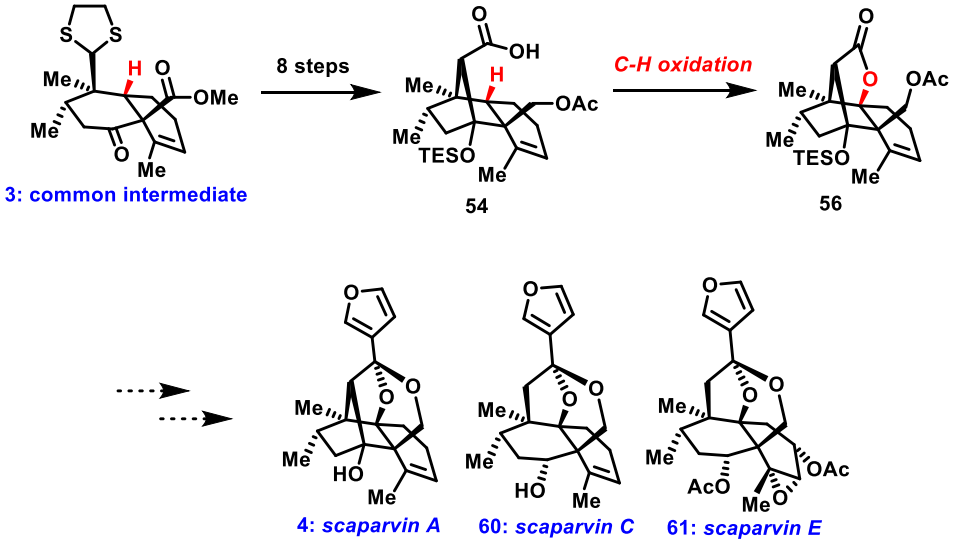

Scheme 15. Synthesis of advanced intermediate **56**, a precursor for scaparvin terpenoids.

With sufficient quantities of advanced intermediate **56** prepared, we then proceeded to the final phase of our synthetic plan, the completion of total syntheses of scaparvin terpenoids, studies that will be discussed in the following chapters.

4.5 References

(1) Chen, K.; Richter, J. M.; Baran, P. S. *J. Am. Chem. Soc.* **2008**, *130*, 7247.

(2) Molander, G. A.; Harris, C. R. *Chem. Rev.* **1996**, *96*, 307.

(3) Omura, K.; Swern, D. *Tetrahedron* **1978**, *34*, 1651.

(4) Wittig, G.; Schöllkopf, U. *Chem. Ber.* **1954**, *87*, 1318.

(5) González, C. C.; León, E. I.; Riesco-Fagundo, C.; Suárez, E. *Tetrahedron Lett.* **2003**, *44*, 6347.

(6) Bigi, M. A.; Reed, S. A.; White, M. C. *J. Am. Chem. Soc.* **2012**, *134*, 9721.

(7) Tebbe, F. N.; Parshall, G. W.; Reddy, G. S. *J. Am. Chem. Soc.* **1978**, *100*, 3611.

4.6 Experimental Section

General Methods: All reactions were carried out under an argon atmosphere with dry solvents under anhydrous conditions, unless otherwise stated. Dry methylene chloride (CH_2Cl_2), diethyl ether (Et_2O), tetrahydrofuran (THF), benzene and toluene were obtained by passing commercially available pre-dried, oxygen-free formulations through activated alumina columns; triethylamine (Et_3N) was distilled from KOH; dichloroethane (DCE), acetonitrile (CH_3CN) and methanol (MeOH) were purchased in anhydrous form from Sigma-Aldrich and used as received. Yields refer to chromatographically and spectroscopically (^1H and ^{13}C NMR) homogeneous materials, unless otherwise stated. Reagents were purchased at the highest commercial quality and used without further purification, unless otherwise stated. Reactions were magnetically stirred and monitored by thin-layer chromatography (TLC) carried out on 0.25 mm E. Merck silica gel plates (60F-254) using UV light and an aqueous solution of cerium ammonium sulfate and ammonium molybdate and heat as visualizing agents. Preparative TLC was carried out on 0.50 mm E. Merck silica gel plates (60F-254). SiliCycle silica ge (60 A, academic grade, particle size 40-63 μm) was used for flash column chromatography. NMR spectra were recorded on Bruker DRX-300, DRX-400, DRX-500 and DRX-700 instruments and calibrated using residual undeuterated solvent as an internal reference. The following abbreviations are used to explain multiplicities: s = singlet, d = doublet, t = triplet, q = quartet, m = multiplet, br = broad, app = apparent. IR spectra were recorded on a Perkin-Elmer Spectrum Two FT-IR spectrometer. High resolution mass spectra (HRMS) were recorded in the Columbia University Mass Spectral Core facility on a JOEL HX110 mass spectrometer using FAB (Fast Atom Bombardment).

Diol 51. To a solution of common intermediate (**3**, 8.0 g, 22.6 mmol, 1.0 equiv) in THF (50 mL) at –78 °C was added a solution of KHMDS in toluene (0.5 M, 72.3 mL, 1.6 equiv). The stirred reaction was then warmed to 0 °C for 30 min. A solution of DIBAL-H in toluene (1.0 M, 72.3 mL, 3.2 equiv) was added dropwise into the yellowish solution at the same temperature. Then, the reaction contents were slowly warmed to 23 °C over 16 h. Upon completion (determined by TLC analysis), the reaction was cooled to 0 °C and slowly quenched by a mixture of saturated aqueous NH_4Cl (50 mL) and saturated aqueous Rochelle's Salt (50 mL). After stirring for an additional 2 h at 23 °C, the reaction contents were then transferred to a separatory funnel, diluting with EtOAc (100 mL). The organic layer was separated and the aqueous layer was extracted with EtOAc (3 × 50 mL). The organic layers were combined, washed by saturated aqueous NaCl (50 mL), dried with $MgSO_4$, filtered and concentrated. The resulting crude product was directly used for the following step.

The crude alcohol product was dissolved in CH_2Cl_2 (500 mL) and cooled to 0 °C. 2,6-Lutidine (10.4 mL, 90.4 mmol, 4.0 equiv) was added into the resulting solution, followed by slow addition of TIPSOTf (12.1 mL, 42.5 mmol, 2.0 equiv). After 10 min, the ice-water bath was removed and the reaction mixture was allowed to warm to 23 °C for 16 h. Then, 10 mL MeOH was added into the reaction contents, which was concentrated to a viscous oil and further diluted with MeOH (50 mL) at 0 °C. $PhI(OTFA)_2$ (21.3g 49.7 mmol, 2.2 equiv) was added in one portion, and the resulting white mixture was further stirred for 6 h at 23 °C. Upon completion, the reaction was diluted with THF (500 mL) and quenched by 2 M aqueous HCl solution (200 mL) and further stirred for 10 h at this temperature. The reaction contents were then transferred to a separatory funnel, diluting with EtOAc (500 mL) and hexanes (500 mL). The organic layer was separated and the aqueous layer was extracted with EtOAc (3 × 400 mL). The organic layers

were combined, washed with saturated aqueous $NaHCO_3$ solution (500 mL), dried with $MgSO_4$, filtered and concentrated. The resulting crude product was purified by flash column chromatography (silica gel, hexanes/EtOAc, 50:1 to 10:1) to give ketoaldehyde **50** (5.79 g, 63% yield over two steps) as a yellowish oil.

Next, this product (**50**, 5.79 g, 14.2 mmol, 1.0 equiv) was dissolved in THF (500 mL) and cooled to 0 °C. A freshly made solution of SmI_2 in THF (0.1 M, 71.0 mmol, 710 mL, 5.0 equiv) was added dropwise through a cannula. After 10 min, the ice-water bath was removed and the reaction mixture was allowed to warm to 23 °C for 16 h. Upon completion, the reaction contents were quenched by saturated aqueous Rochelle's Salt (500 mL) and transferred to a separatory funnel. The organic layer was separated and the aqueous layer was extracted with EtOAc (3 × 500 mL). The organic layers were combined, washed by saturated aqueous NaCl (500 mL), dried with $MgSO_4$, filtered and concentrated. The resulting crude product was purified by flash column chromatography (silica gel, hexanes/EtOAc, 10:1 to 4:1) to give diol **51** (4.75 g, 82% yield) as a white solid. **51**: ^{1}H NMR (400 MHz, $CDCl_3$) δ 5.79 (m, 1 H), 3.94 (d, *J* = 9.8 Hz, 1 H), 3.72 (s, 1 H), 3.61 (d, *J* = 9.8 Hz, 1 H), 2.31 (m, 1 H), 2.07–1.91 (m, 2 H), 2.02 (br, 3 H), 1.73–1.52 (m, 3 H), 1.48 (m, 1 H), 1.42 (m, 1 H), 1.16–0.98 (m, 27 H); ^{13}C NMR (100 MHz, $CDCl_3$) δ 139.1, 127.3, 85.8, 83.5, 73.2, 47.0, 46.7, 45.6, 38.1, 35.8, 23.0, 22.8, 21.2, 18.0, 17.9, 16.5, 16.3, 11.6.

Carboxylic acid 53. To a solution of oxalyl chloride (0.60 mL, 6.80 mmol, 1.5 equiv) in CH_2Cl_2 (50 mL) at –78 °C was added DMSO (1.65 mL, 22.7 mmol, 5.0 equiv) dropwise. After stirring for 30 min, a solution of diol **51** (1.85 g, 4.53 mmol, 1.0 equiv) in CH_2Cl_2 (100 mL) was slowly added at –78 °C. The reaction solution was further stirred at –78 °C for 1 h, whereafter

Et_3N (6.5 mL, 45.3 mmol, 10 equiv) was added at the same temperature, and the reaction contents were slowly warmed to 23 °C over 6 h. The yellow solution was then quenched by water (100 mL) and transferred to a separatory funnel. The organic layer was separated and the aqueous layer was extracted with CH_2Cl_2 (3 × 50 mL). The organic layers were combined, dried with $MgSO_4$, filtered and concentrated. The resulting crude product was purified by flash column chromatography (silica gel, hexanes/EtOAc, 30:1 to 10:1) to give the resulting ketone (1.64 g, 89% yield) as a yellowish oil.

Next, this ketone product (1.73 g, 4.26 mmol, 1.0 equiv) was dissolved in THF (100 mL) and cooled to 0 °C. Pyridine (1.6 mL, 21.3 mmol, 5.0 equiv) followed by a solution of Tebbe reagent in toluene (0.5 M, 21.3 mL, 5.0 equiv) was added dropwise. After 10 min, the ice-water bath was removed and the dark-brown solution was heated to 50 °C for 16 h. Upon completion (determined by TLC analysis), the reaction contents were quenched by saturated aqueous Rochelle's Salt (500 mL) and transferred to a separatory funnel. The organic layer was separated and the aqueous layer was extracted with EtOAc (3 × 50 mL). The organic layers were combined, washed by saturated aqueous NaCl (500 mL), dried with $MgSO_4$, filtered and concentrated. The resulting crude product was purified by flash column chromatography (silica gel, hexanes/EtOAc, 50:1 to 30:1) to give alkene **52** (1.00 g, 58% yield) as a colorless oil.

To a solution of alkene **52** (1.00 g, 2.47 mmol, 1.0 equiv) in THF (50 mL) at 0 °C was added borane THF complex solution (1.0 M, 6.18 mmol, 2.5 equiv). After 10 min, the ice-water bath was removed and the reaction solution was heated to 35 °C for 3 h. Upon completion, the reaction was cooled to 0 °C and quenched by water (5 mL), followed by addition of $NaBO_3$-H_2O (494 mg, 4.94 mmol, 2.0 equiv) in one portion. After stirring at 23 °C for 5 h, the reaction

mixture was diluted with tBuOH (50 mL) and 2-Methyl-2-butene (20 mL). Next, TEMPO (385 mg, 2.47 mmol, 1.0 equiv) followed by a solution of $NaClO_2$ (4.47 g, 49.44 mmol, 20 equiv) and NaH_2PO_4-$2H_2O$ (7.71 g, 49.4 mmol, 20 equiv) in water (40 mL) was added into reaction mixture at 0 °C. After 10 min, the ice-water bath was removed and the reaction mixture was allowed to warm to 23 °C for 6 h. Upon completion, the reaction contents were diluted with water (50 mL) and transferred to a separatory funnel. The organic layer was separated and the aqueous layer was extracted with EtOAc (3 × 50 mL). The organic layers were combined, washed by saturated aqueous NaCl (50 mL), dried with $MgSO_4$, filtered and concentrated. The resulting crude product was purified by flash column chromatography (silica gel, hexanes/EtOAc, 20:1 to 10:1, with 0.1% AcOH) to give carboxylic acid **53** (702 mg, 65% yield) as a colorless oil. **53**: ^{1}H NMR (400 MHz, $CDCl_3$) δ 9.93 (br, 1 H), 6.09 (br, 1 H), 5.79 (m, 1 H), 3.98 (d, *J* = 10.4 Hz, 1 H), 3.58 (d, *J* = 10.4 Hz, 1 H), 2.33 (s, 1 H), 2.07 (br, 3 H), 2.06–1.92 (m, 3 H), 1.86 (m, 1 H), 1.74–1.53 (m, 4 H), 1.29 (s, 3 H), 1.15–0.98 (m, 24 H); ^{13}C NMR (100 MHz, $CDCl_3$) δ 173.1, 139.1, 127.5, 88.0, 73.2, 61.4, 48.6, 46.7, 46.4, 41.2, 40.8, 23.5, 22.9, 17.8, 17.7, 17.4, 16.9, 11.6.

Carboxylic acid 54. To a solution of carboxylic acid **53** (538 mg, 1.23 mmol, 1.0 equiv) in THF (10 mL) at 0 °C was added a solution of TBAF in THF (1.0 M, 1.35 mL, 1.1 equiv). After 10 min, the ice-water bath was removed and the reaction mixture was allowed to warm to 23 °C for 4 h. The resultant solution was slowly transferred into a vigorously-stirred solution of acetic anhydride (0.26 mL, 2.71 mmol, 2.2 equiv) and DMAP (480 mg, 3.94 mmol, 3.2 equiv) in THF (10 mL) at 0 °C through a cannula. After stirring at 0 °C for an additional 30 min, the reaction was quenched by 10% aqueous AcOH solution (20 mL) and further stirred for 30 min at

this temperature. The reaction contents were then transferred to a separatory funnel, diluting with EtOAc (20 mL) and hexanes (20 mL). The organic layer was separated and the aqueous layer was extracted with EtOAc (3 × 30 mL). The organic layers were combined, dried with $MgSO_4$, filtered and concentrated. The resulting crude product was purified by flash column chromatography (silica gel, hexanes/EtOAc, 3:1 to 1:1, with 0.1% AcOH) to give acetate product **37** (337 mg, 85% yield) as a colorless oil.

Next, this acetate product (337 mg, 1.05 mmol, 1.0 equiv) was dissolved in CH_2Cl_2 (10 mL) and cooled to 0 °C. 2,6-Lutidine (0.36 mL, 3.15 mmol, 3.0 equiv) followed by TESOTf (0.47 mL, 2.10 mmol, 2.0 equiv) was added dropwise. After 10 min, the ice-water bath was removed and the reaction was allowed to warm to 23 °C for 5 h. Upon completion (determined by TLC analysis), the reaction contents were quenched by MeOH (1 mL) and AcOH (1 mL) and further stirred at 23 °C for 2 h. The reaction contents were then transferred to a separatory funnel, diluting with EtOAc (40 mL), hexanes (40 mL) and water (100 mL). The organic layer was separated and the aqueous layer was extracted with EtOAc (3 × 50 mL). The organic layers were combined, dried with $MgSO_4$, filtered and concentrated. The resulting crude product was purified by flash column chromatography (silica gel, hexanes/EtOAc, 5:1 to 3:1, with 0.1% AcOH) to give carboxylic acid **54** (440 mg, 96% yield) as a white solid. **54**: ^{1}H NMR (400 MHz, $CDCl_3$) δ 5.70 (br, 1 H), 4.46 (d, *J* = 11.5 Hz, 1 H), 3.94 (d, *J* = 11.5 Hz, 1 H), 2.81 (t, *J* = 9.2 Hz, 1 H), 2.38 (s, 1 H), 2.05–1.90 (m, 2 H), 1.97 (s, 3 H), 1.82 (m, 1 H), 1.77 (br, 3 H), 1.74–1.65 (m, 2 H), 1.60 (m, 1 H), 1.31 (m, 1 H), 1.21 (s, 3 H), 1.05 (d, *J* = 7.8 Hz, 3 H), 0.98 (m, 9 H), 0.73 (m, 6 H).

Advanced intermediate 56. To a suspension of carboxylic acid **54** (56.2 mg, 0.128 mmol, 1.0 equiv) in CH_3CN (3 mL) at 10 ^oC was added a solution of Fe(PDP) (2.4 mg, 2 mol%) in CH_3CN (3 mL) and a solution of H_2O_2 (30%, 17 uL, 0.154 mmol, 1.2 equiv) in CH_3CN (3 mL) simultaneously over 1 h using syringe pump. After stirring for an additional 10 min at 23 °C, the yellowish solution was quenched by saturated aqueous Na_2SO_3 solution (20 mL) and diluted with Et_2O (20 mL). The reaction contents were then transferred to a separatory funnel, diluting with hexanes (20 mL) and water (20 mL). The organic layer was separated and the aqueous layer was extracted with Et_2O (3 × 20 mL). The organic layers were combined, washed by saturated aqueous NaCl (20 mL), dried with $MgSO_4$, filtered and concentrated. The resulting crude product was purified by flash column chromatography (silica gel, hexanes/EtOAc, 10:1 to 4:1) to give advanced intermediate **56** (23.9 mg, 43% yield) and epoxide **55** (16.2 mg, 28% yield). **56**: ^{1}H NMR (400 MHz, $CDCl_3$) δ 5.61 (br, 1 H), 4.63 (d, *J* = 12.4 Hz, 1 H), 3.90 (d, *J* = 12.4 Hz, 1 H), 2.51 (s, 1 H), 2.27–2.14 (m, 2 H), 2.14–2.01 (m, 3 H), 1.99 (s, 3 H), 1.82 (br, 3 H), 1.82 (m, 1 H), 1.69 (m, 1 H), 1.10 (s, 3 H), 0.97 (m, 12 H), 0.67 (m, 6 H); ^{13}C NMR (100 MHz, $CDCl_3$) δ 174.4, 170.2, 132.8, 126.9, 94.3, 87.3, 66.7, 63.2, 62.3, 52.2, 39.5, 36.3, 22.2, 21.0, 20.7, 20.0, 13.7, 13.6, 6.8, 6.0.

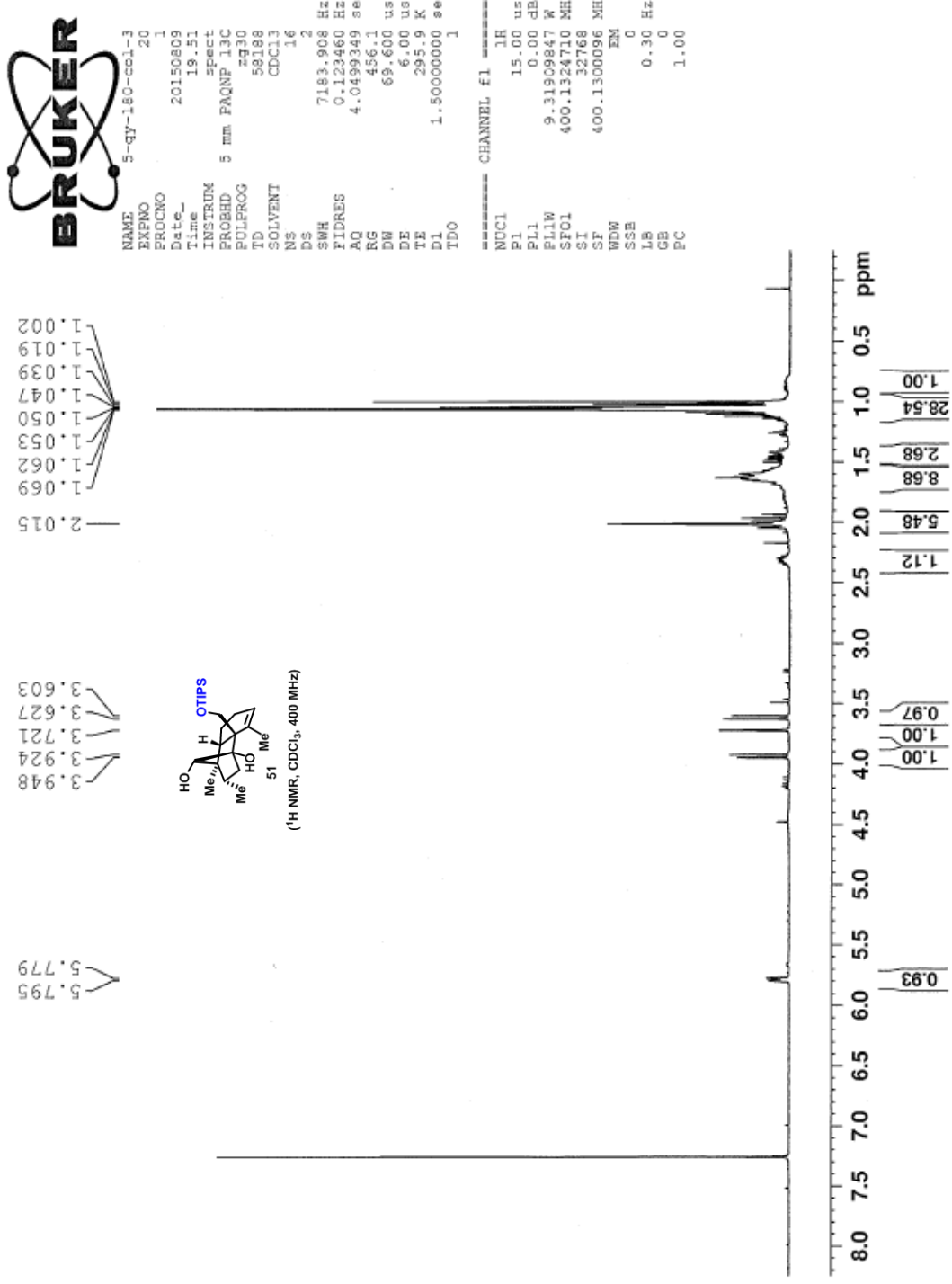
NAME 5-qy-180-col-3
EXPNO 20
PROCNO 1
Date_ 20150809
Time 19.51
INSTRUM spect
PROBHD 5 mm PAQNP 13C
PULPROG zg30
TD 58188
SOLVENT CDCl3
NS 16
DS 2
SWH 7183.908 Hz
FIDRES 0.123460 Hz
AQ 4.04999349 sec
RG 456.1
DW 69.600 usec
DE 6.00 usec
TE 295.9 K
D1 1.50000000 sec
TDO 1
CHANNEL f1
NUC1 1H
P1 15.00 usec
PL1 0.00 dB
PL1W 9.31909847 W
SFO1 400.1324710 MHz
SI 32768
SF 400.1300096 MHz
WDW EM
SSB 0
LB 0.30 Hz
GB 0
PC 1.00
OTIPS
HO
Me
Me
HO
Me
51
(1H NMR, CDCl3, 400 MHz)
ppm

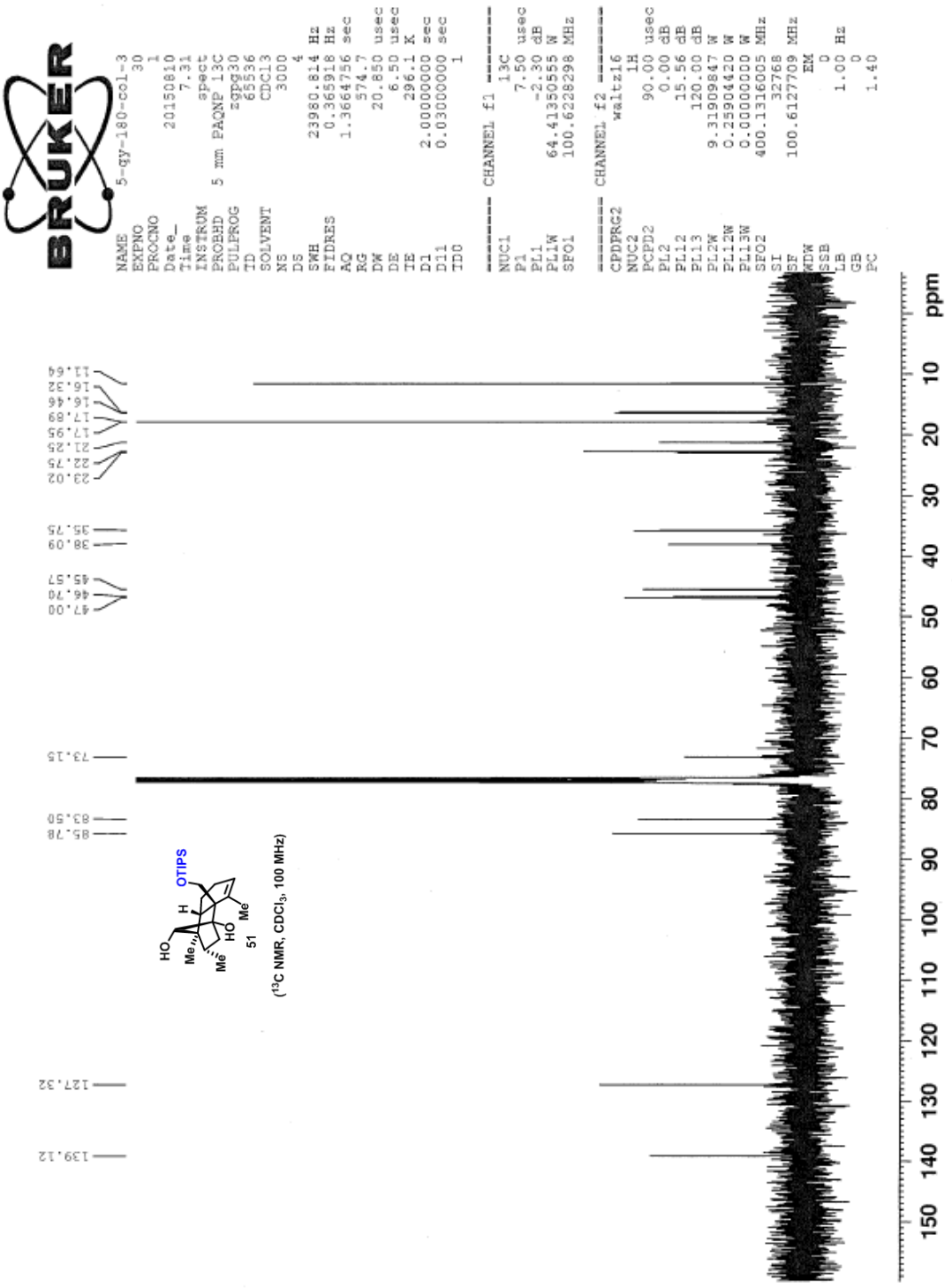
BRUKER
NAME 5-gy-180-col-3
EXPNO 30
PROCNO 1
Date_ 20150810
Time 7.31
INSTRUM spect
PROBHD 5 mm PAQNP 13C
PULPROG zgpg30
TD 65536
SOLVENT CDCl3
NS 3000
DS 4
SWH 23980.814 Hz
FIDRES 0.365918 Hz
AQ 1.3664756 sec
RG 574.7
DW 20.850 usec
DB 6.50 usec
TE 296.1 K
D1 2.00000000 sec
D11 0.03000000 sec
TD0 1
CHANNEL f1
NUC1 13C
P1 7.50 usec
PL1 -2.30 dB
PL1W 64.41350555 W
SFO1 100.6228298 MHz
CHANNEL f2
CPDPRG2 waltz16
NUC2 1H
PCPD2 90.00 usec
PL2 0.00 dB
PL12 15.56 dB
PL13 120.00 dB
PL2W 9.31909847 W
PL12W 0.25904420 W
PL13W 0.00000000 W
SFO2 400.1316005 MHz
SI 32768
SF 100.6127709 MHz
WDW EM
SSB 0
LB 1.00 Hz
GB 0
PC 1.40
11.64
16.32
16.46
17.89
17.95
21.25
22.75
23.02
35.75
38.09
45.57
46.70
47.00
73.15
83.50
85.78
127.32
139.12
OTIPS
H
HO
Me
Me
Me
HO
51
(13C NMR, CDCl3, 100 MHz)
150 140 130 120 110 100 90 80 70 60 50 40 30 20 10 ppm

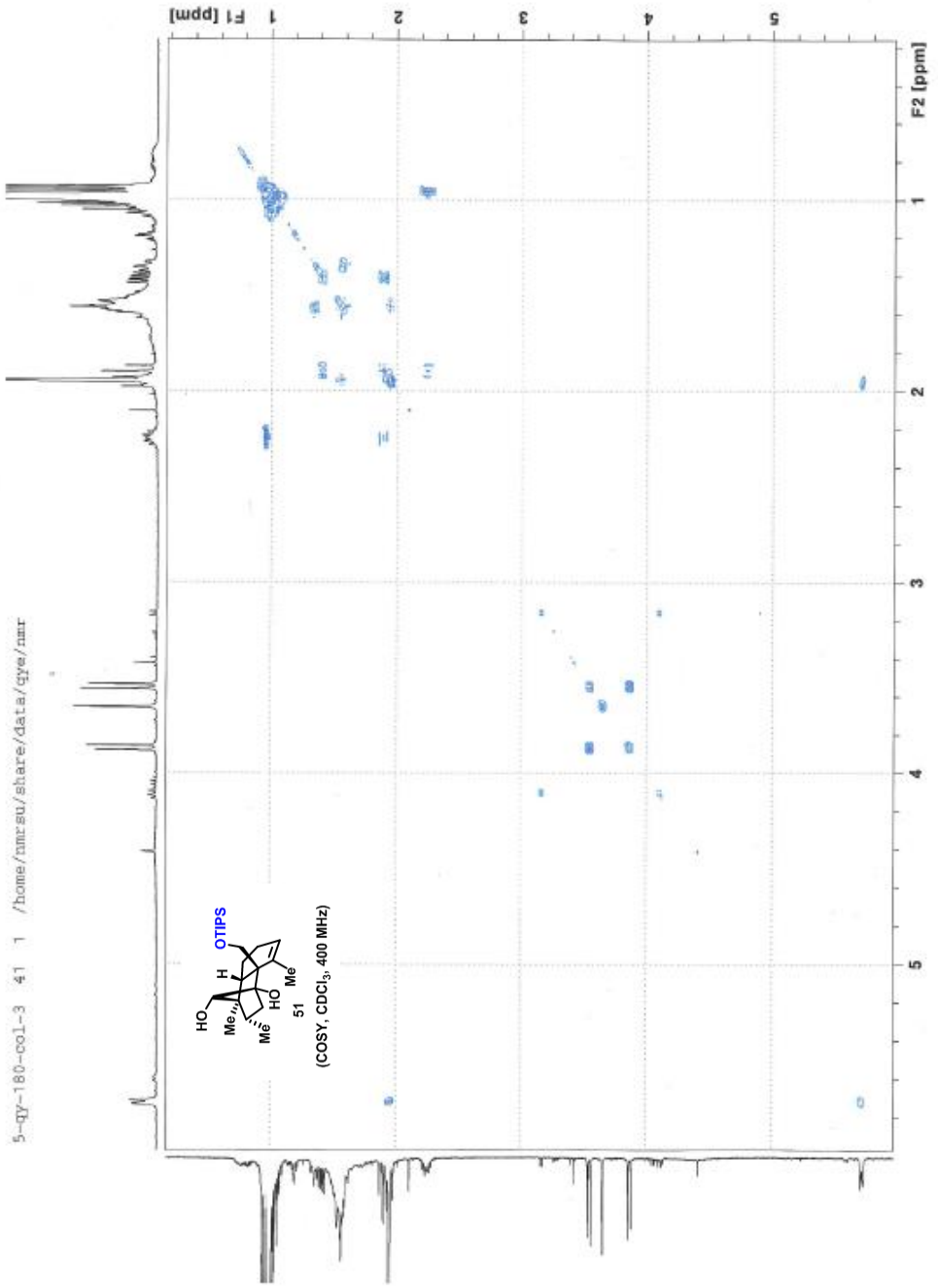
5-qy-180-col-3 41 1 /home/nmrsu/share/data/qye/nmr
F1 [ppm]
F2 [ppm]
1
2
3
4
5
OTIPS
H
HO
Me
Me
Me
HO
51
(COSY, CDCl3, 400 MHz)

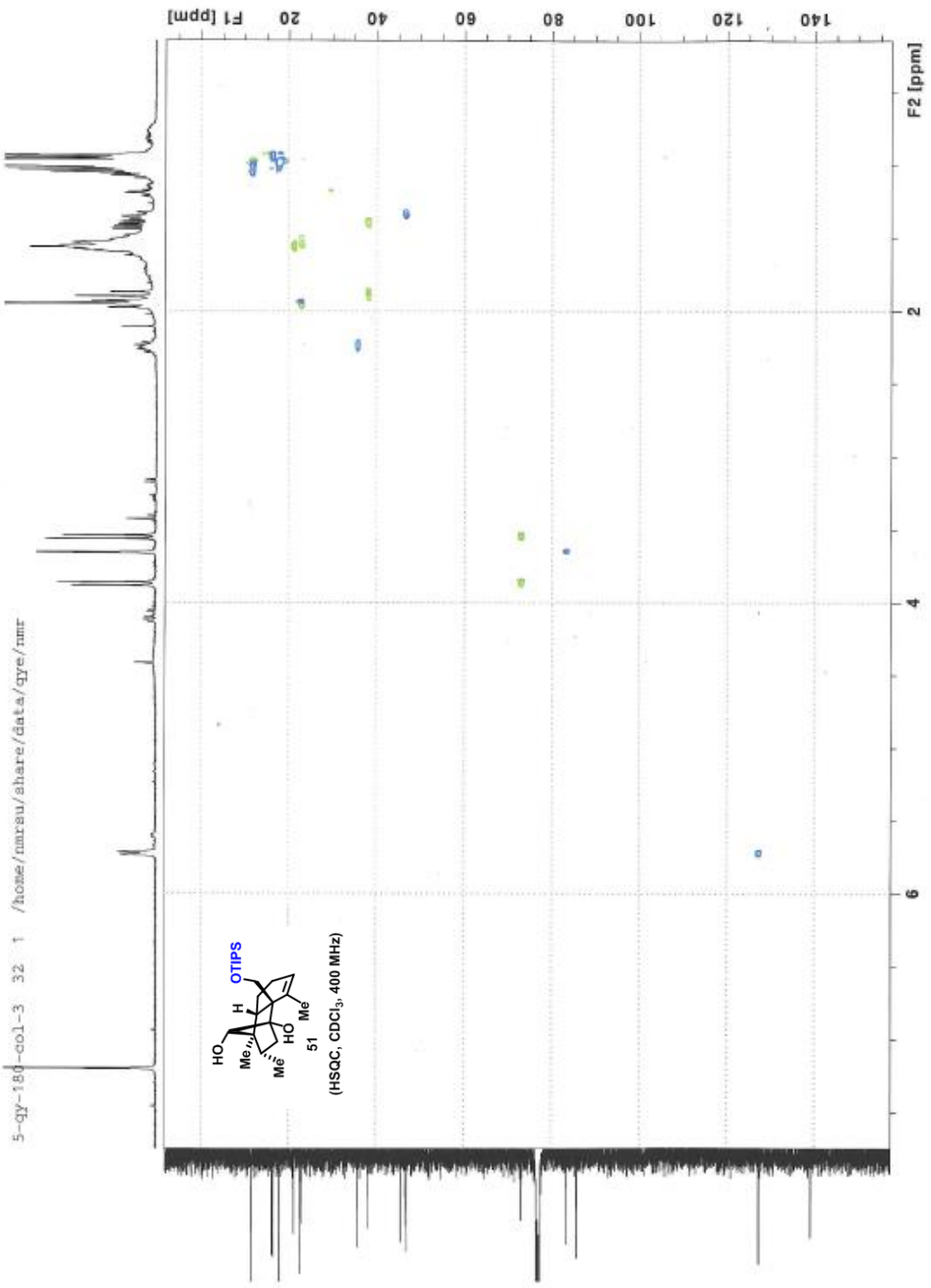
5-qy-180-col-3 32 1 /home/nmrau/share/data/qye/nmr
F1 [ppm]
F2 [ppm]
OTIPS
HO
Me
Me
HO
Me
51
(HSQC, CDCl3, 400 MHz)

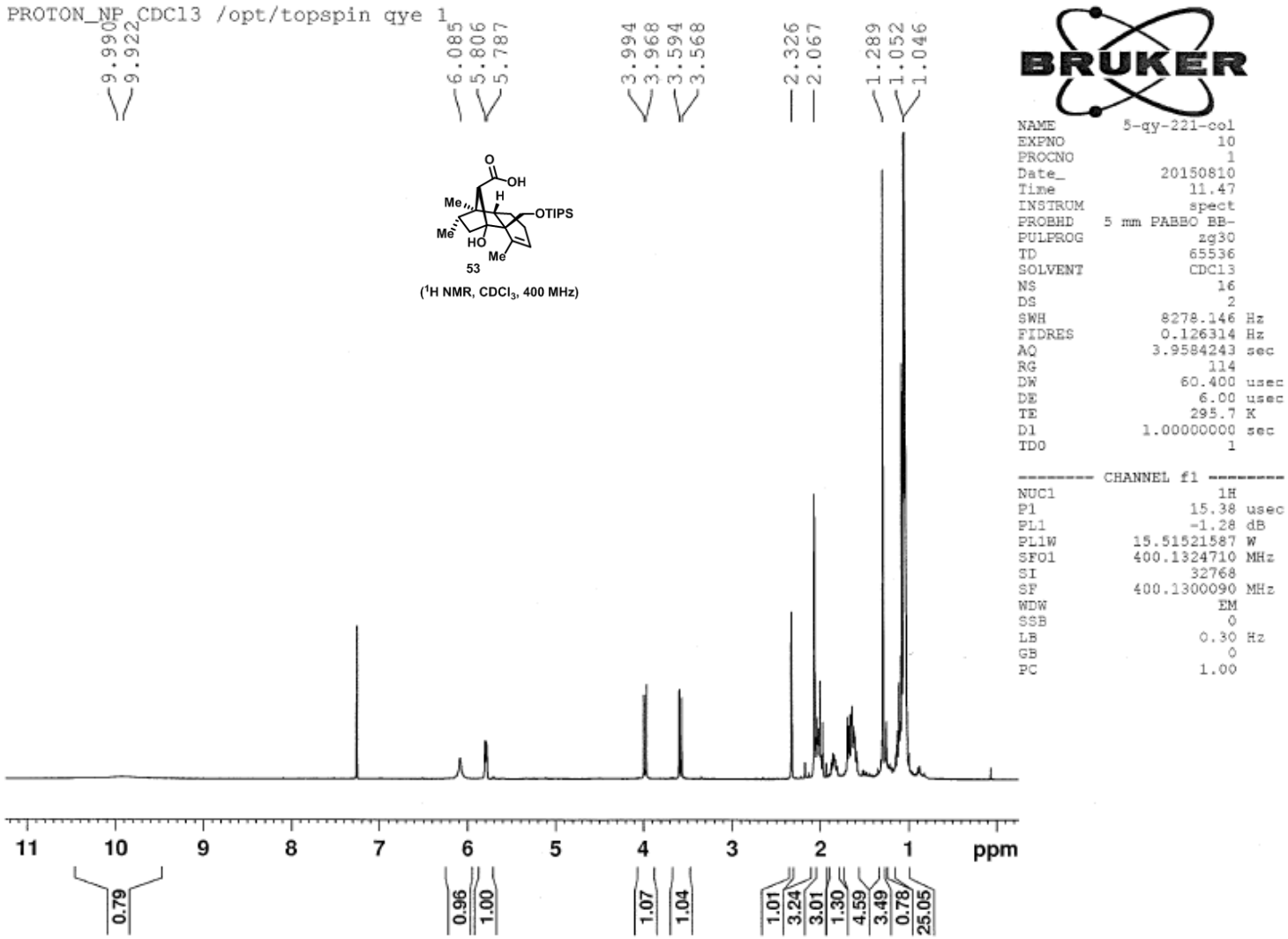


```
NAME            5-qy-221-col
EXPNO                    10
PROCNO                    1
Date_              20150810
Time                  11.47
INSTRUM               spect
PROBHD    5 mm PABBO BB-
PULPROG                zg30
TD                    65536
SOLVENT               CDCl3
NS                       16
DS                        2
SWH                8278.146 Hz
FIDRES            0.126314 Hz
AQ               3.9584243 sec
RG                      114
DW                   60.400 usec
DE                    6.00 usec
TE                   295.7 K
D1              1.00000000 sec
TD0                       1

-------- CHANNEL f1 --------
NUC1                     1H
P1                    15.38 usec
PL1                   -1.28 dB
PL1W           15.51521587 W
SFO1           400.1324710 MHz
SI                    32768
SF             400.1300090 MHz
WDW                      EM
SSB                       0
LB                     0.30 Hz
GB                        0
PC                     1.00
```

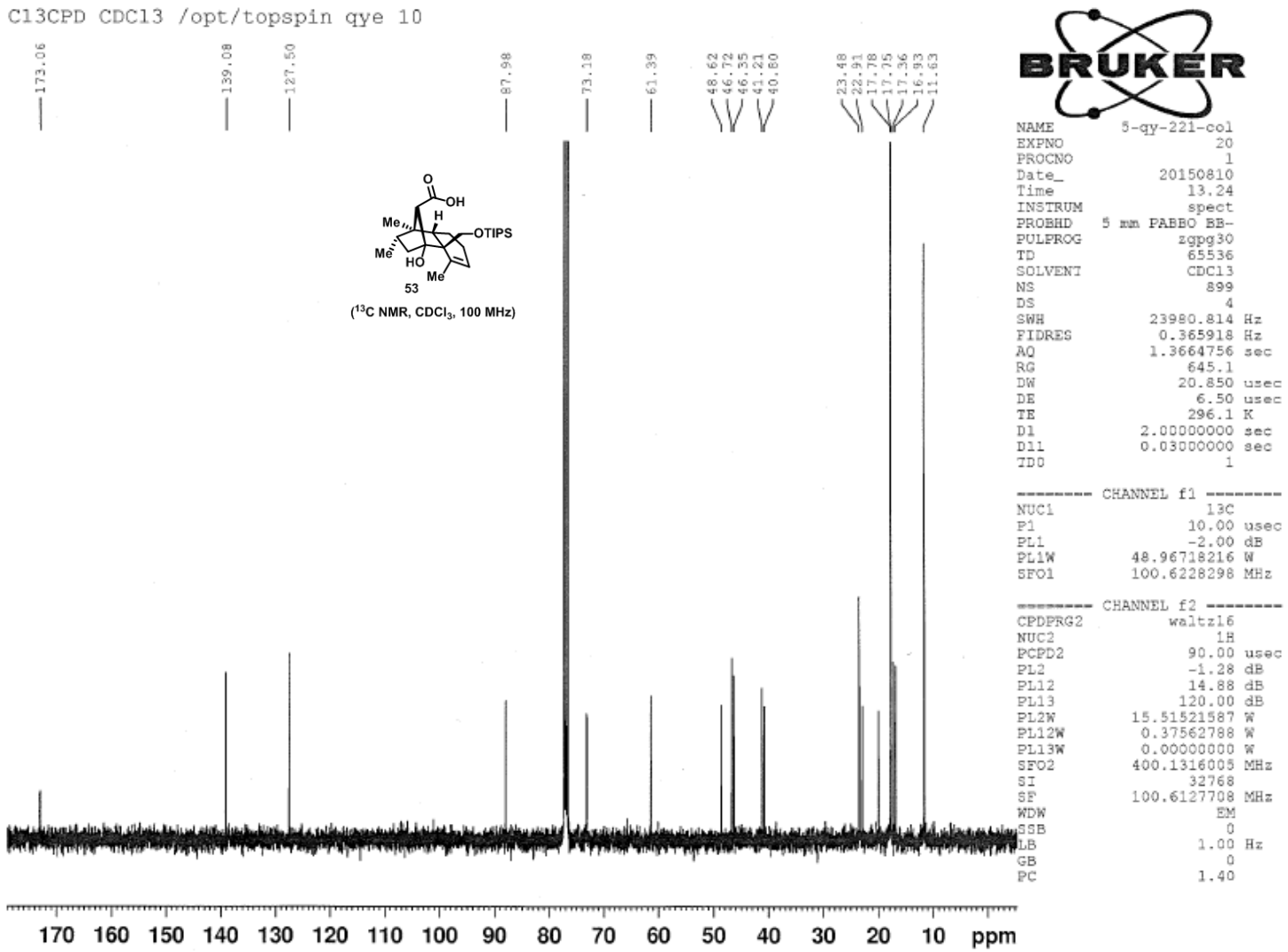
C13CPD CDCl3 /opt/topspin qye 10
173.06
139.08
127.50
87.98
73.18
61.39
48.62
46.72
46.35
41.21
40.80
23.48
22.91
17.78
17.05
17.36
16.93
11.63
O
OH
H
Me
OTIPS
Me
HO
Me
53
(13C NMR, CDCl3, 100 MHz)
BRUKER
NAME 5-qy-221-col
EXPNO 20
PROCNO 1
Date_ 20150810
Time 13.24
INSTRUM spect
PROBHD 5 mm PABBO BB-
PULPROG zgpg30
TD 65536
SOLVENT CDCl3
NS 899
DS 4
SWH 23980.814 Hz
FIDRES 0.365918 Hz
AQ 1.3664756 sec
RG 645.1
DW 20.850 usec
DE 6.50 usec
TE 296.1 K
D1 2.00000000 sec
D11 0.03000000 sec
TD0 1
======== CHANNEL f1 ========
NUC1 13C
P1 10.00 usec
PL1 -2.00 dB
PL1W 48.96718216 W
SFO1 100.6228298 MHz
======== CHANNEL f2 ========
CPDPRG2 waltz16
NUC2 1H
PCPD2 90.00 usec
PL2 -1.28 dB
PL12 14.88 dB
PL13 120.00 dB
PL2W 15.51521587 W
PL12W 0.37562788 W
PL13W 0.00000000 W
SFO2 400.1316005 MHz
SI 32768
SF 100.6127708 MHz
WDW EM
SSB 0
LB 1.00 Hz
GB 0
PC 1.40
170 160 150 140 130 120 110 100 90 80 70 60 50 40 30 20 10 ppm

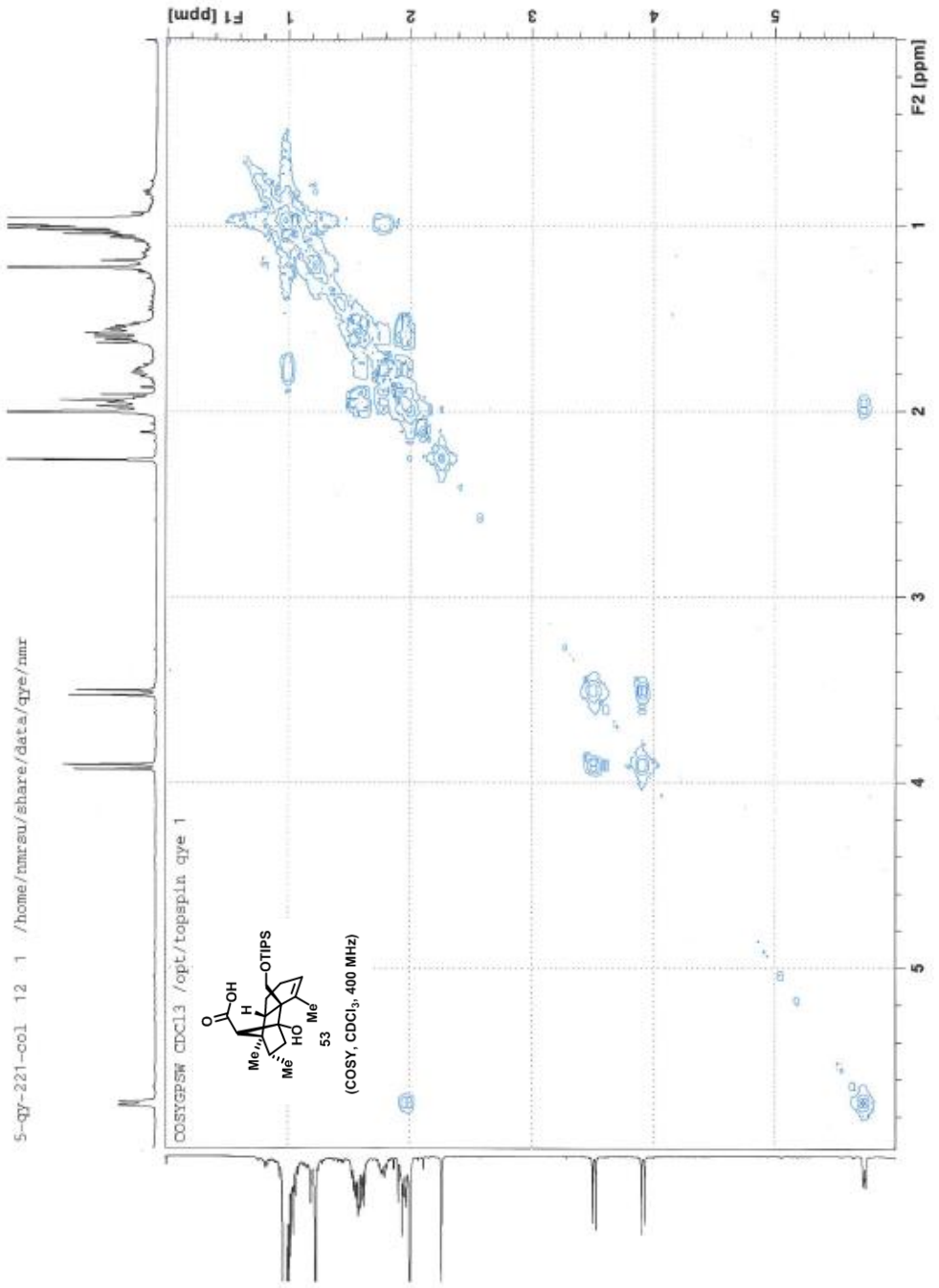
5-qy-221-col 12 1 /home/nmrsu/share/data/qye/nmr
COSYGPSW CDCl3 /opt/topspin qye 1
F1 [ppm]
F2 [ppm]
OTIPS
OH
O
H
Me
HO
Me
Me
53
(COSY, CDCl3, 400 MHz)

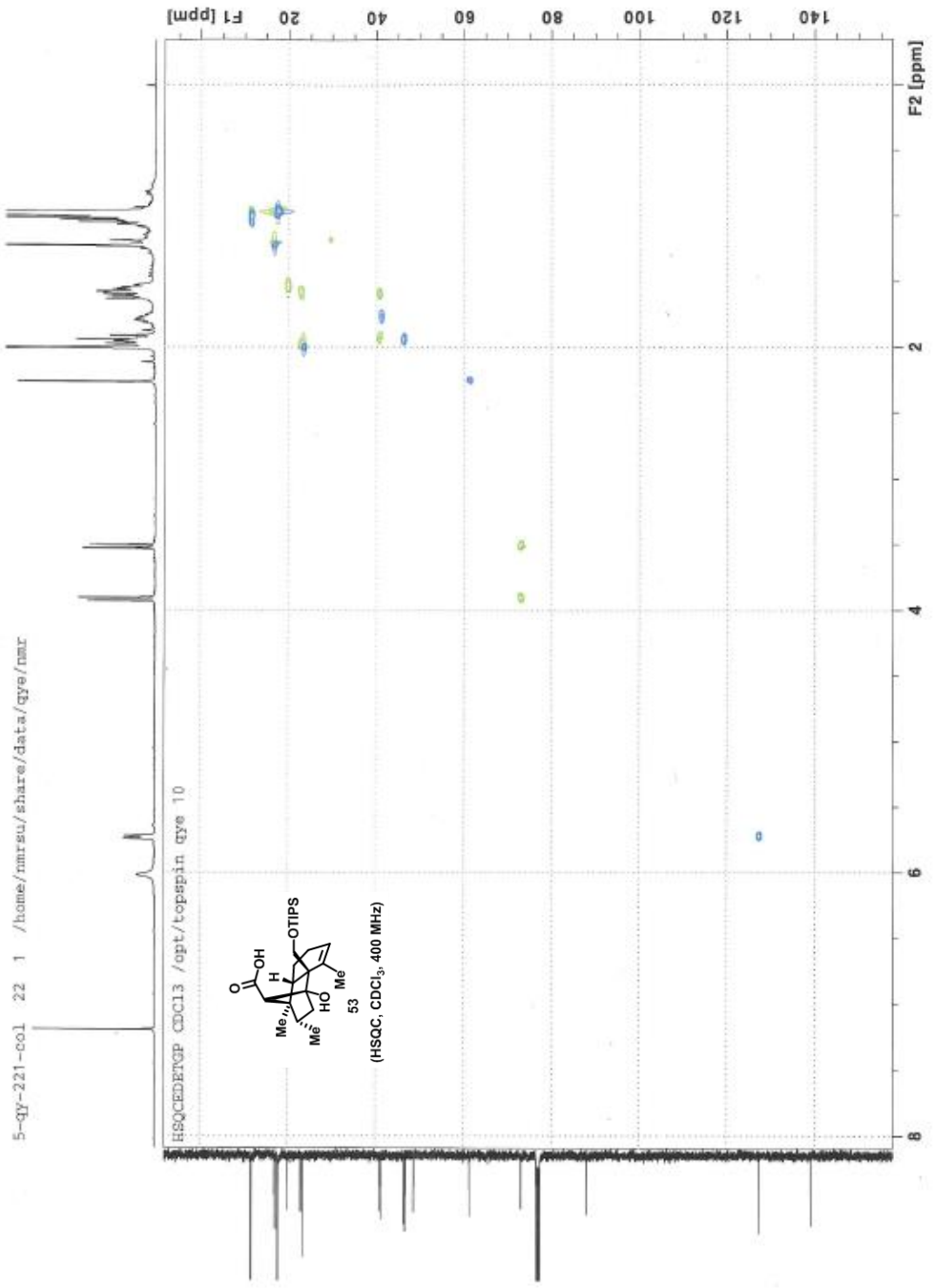
5-qy-221-col 22 1 /home/nmrsu/share/data/qye/nmr
HSQCEDETGP CDCl3 /opt/topspin qye 10
F1 [ppm]
F2 [ppm]
OTIPS
OH
O
H
HO
Me
Me
Me
53
(HSQC, CDCl3, 400 MHz)

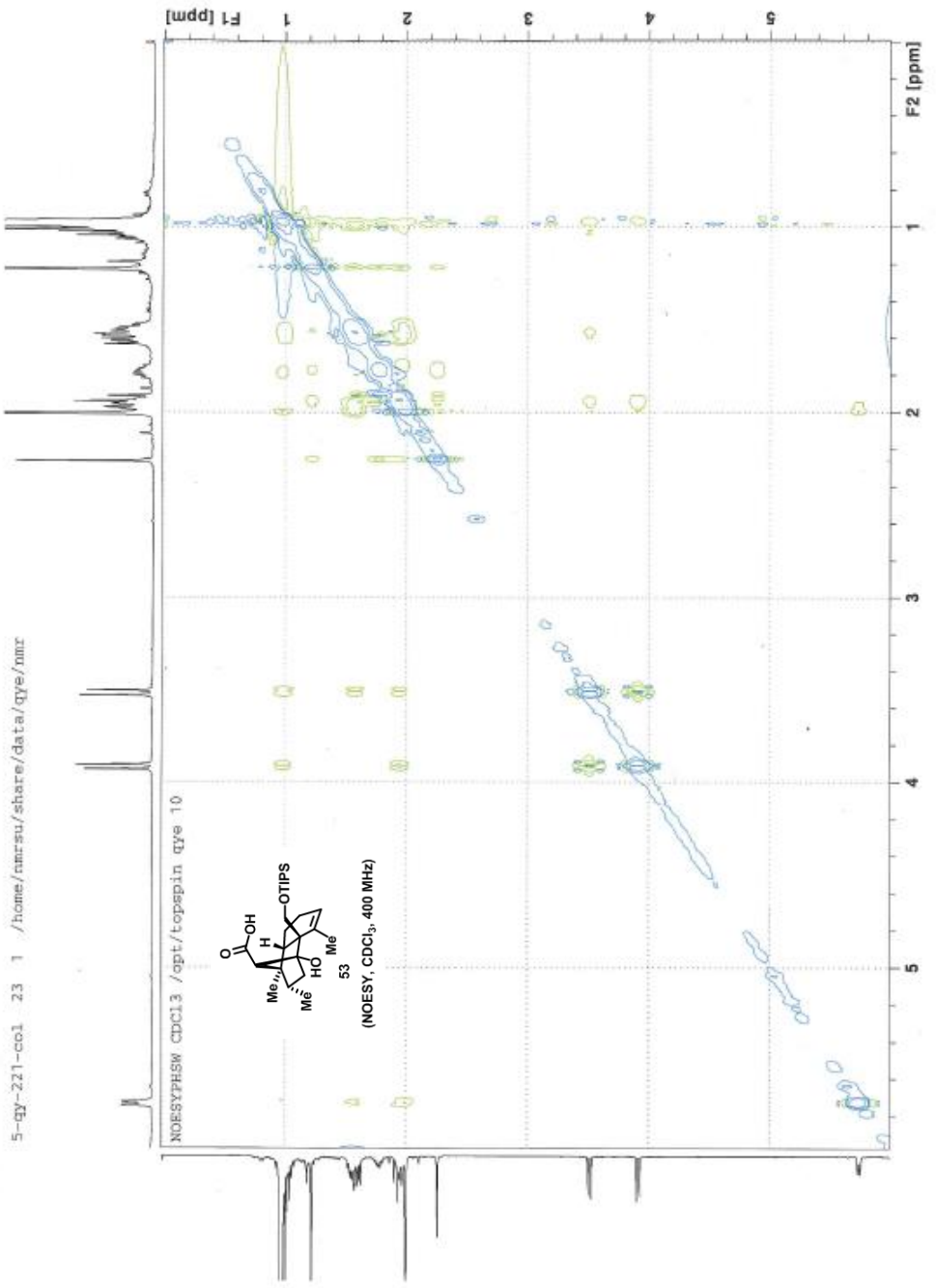
5-qy-221-col 23 1 /home/nmrsu/share/data/qye/nmr
NOESYPHSW CDCl3 /opt/topspin qye 10
F1 [ppm]
F2 [ppm]
OTIPS
OH
O
H
HO
Me
Me
Me
53
(NOESY, CDCl3, 400 MHz)

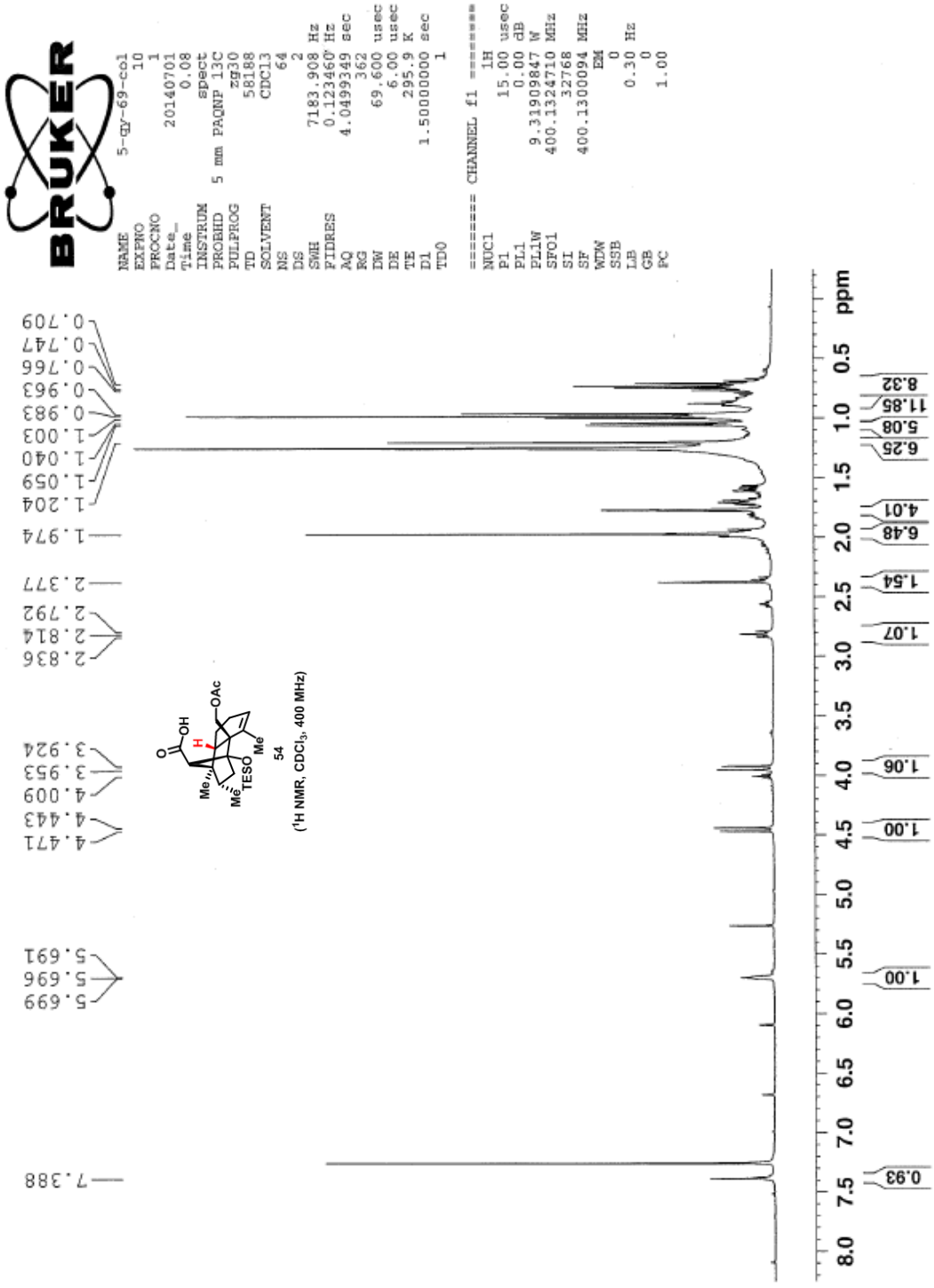
BRUKER
NAME 5-gy-69-col
EXPNO 10
PROCNO 1
Date_ 20140701
Time 0.08
INSTRUM spect
PROBHD 5 mm PAQNP 13C
PULPROG zg30
TD 58188
SOLVENT CDC13
NS 64
DS 2
SWH 7183.908 Hz
FIDRES 0.123460 Hz
AQ 4.04999349 sec
RG 362
DW 69.600 usec
DE 6.00 usec
TE 295.9 K
D1 1.50000000 sec
TD0 1
======== CHANNEL f1 ========
NUC1 1H
P1 15.00 usec
PL1 0.00 dB
PL1W 9.31909847 W
SFO1 400.1324710 MHz
SI 32768
SF 400.1300094 MHz
WDW EM
SSB 0
LB 0.30 Hz
GB 0
PC 1.00
OH
OAc
H
Me
Me
Me
TESO
54
(1H NMR, CDCl3, 400 MHz)
0.709
0.747
0.766
0.963
0.983
1.003
1.040
1.059
1.204
1.974
2.377
2.792
2.814
2.836
3.924
3.953
4.009
4.443
4.471
5.691
5.696
5.699
7.388
ppm
8.32
11.85
5.08
6.25
4.01
6.48
1.54
1.07
1.06
1.00
1.00
0.93

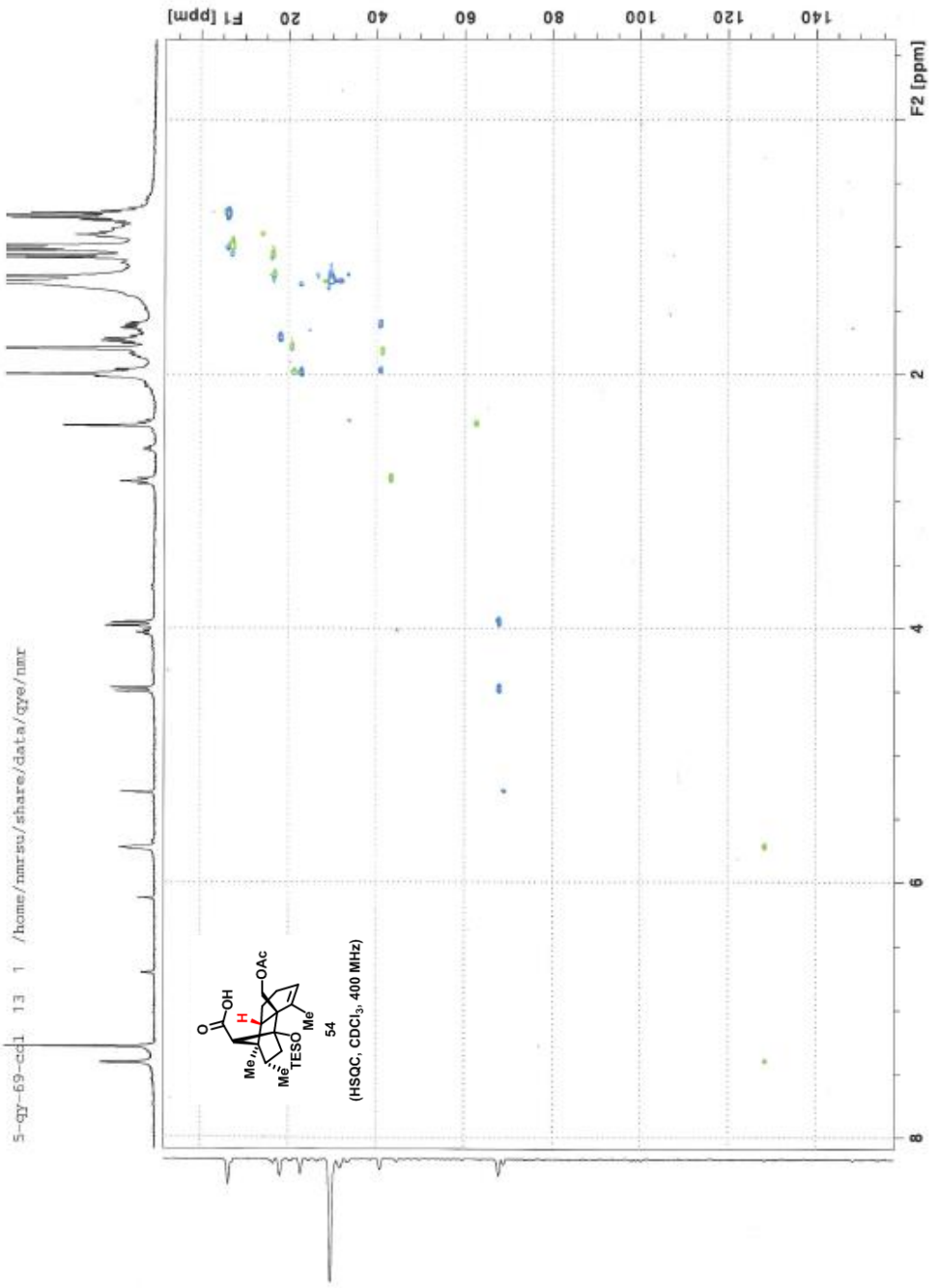
F1 [ppm]
F2 [ppm]
5-qy-69-cd1 13 1 /home/nmrsu/share/data/qye/nmr
OAc
OH
H
Me
TESO
Me
54
(HSQC, CDCl3, 400 MHz)

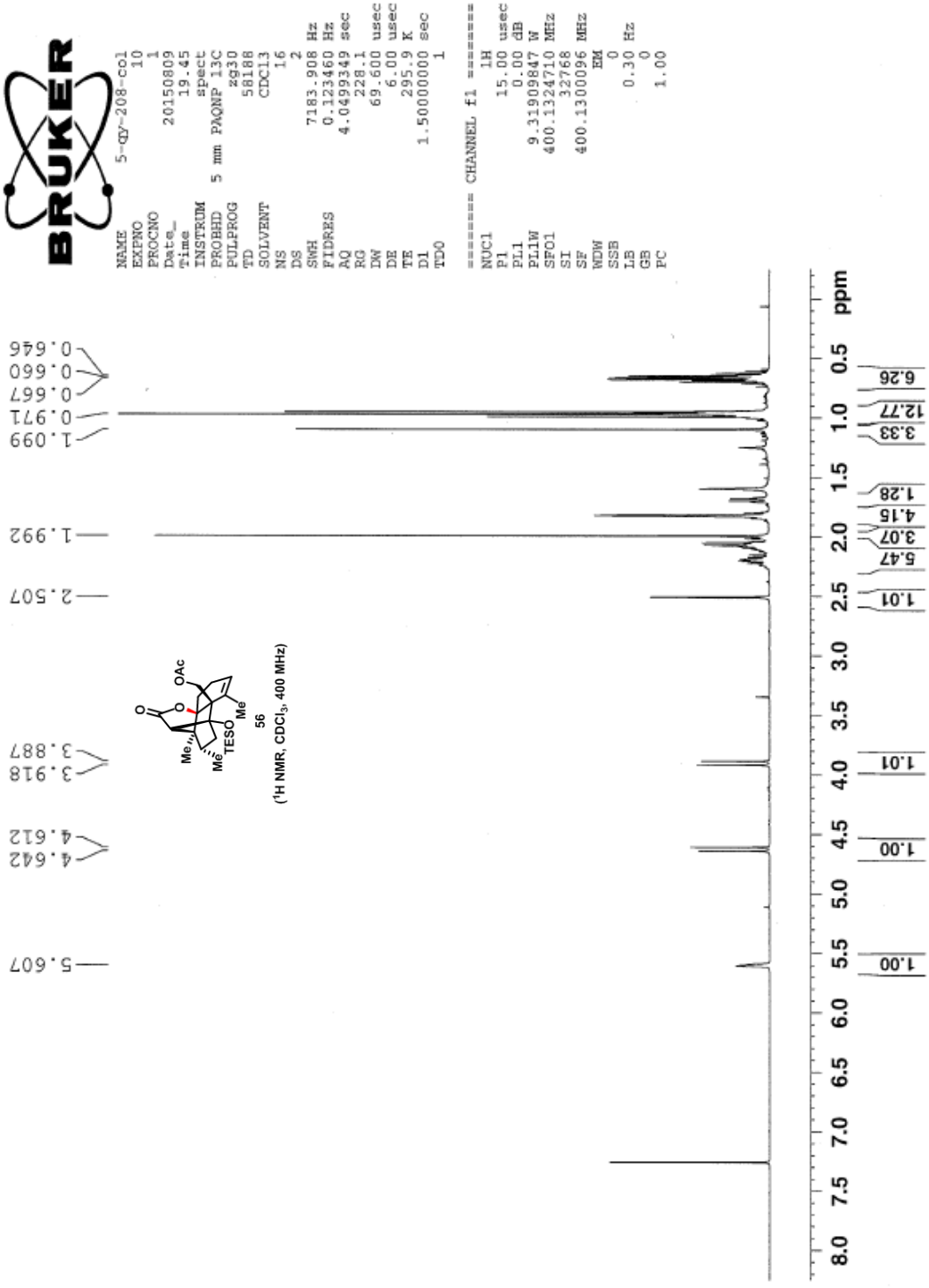
BRUKER
NAME 5-qy-208-col
EXPNO 10
PROCNO 1
Date_ 20150809
Time 19.45
INSTRUM spect
PROBHD 5 mm PAQNP 13C
PULPROG zg30
TD 58188
SOLVENT CDCl3
NS 16
DS 2
SWH 7183.908 Hz
FIDRES 0.123460 Hz
AQ 4.0499349 sec
RG 228.1
DW 69.600 usec
DE 6.00 usec
TE 295.9 K
D1 1.50000000 sec
TD0 1
======== CHANNEL f1 ========
NUC1 1H
P1 15.00 usec
PL1 0.00 dB
PL1W 9.31909847 W
SFO1 400.1324710 MHz
SI 32768
SF 400.1300096 MHz
WDW EM
SSB 0
LB 0.30 Hz
GB 0
PC 1.00
0.646
0.660
0.667
0.971
1.099
1.992
2.507
3.887
3.918
4.612
4.642
5.607
6.26
12.77
3.33
1.28
4.15
3.07
5.47
1.01
1.01
1.00
1.00
ppm
OAc
O
O
Me
Me
TESO
Me
56
(1H NMR, CDCl3, 400 MHz)

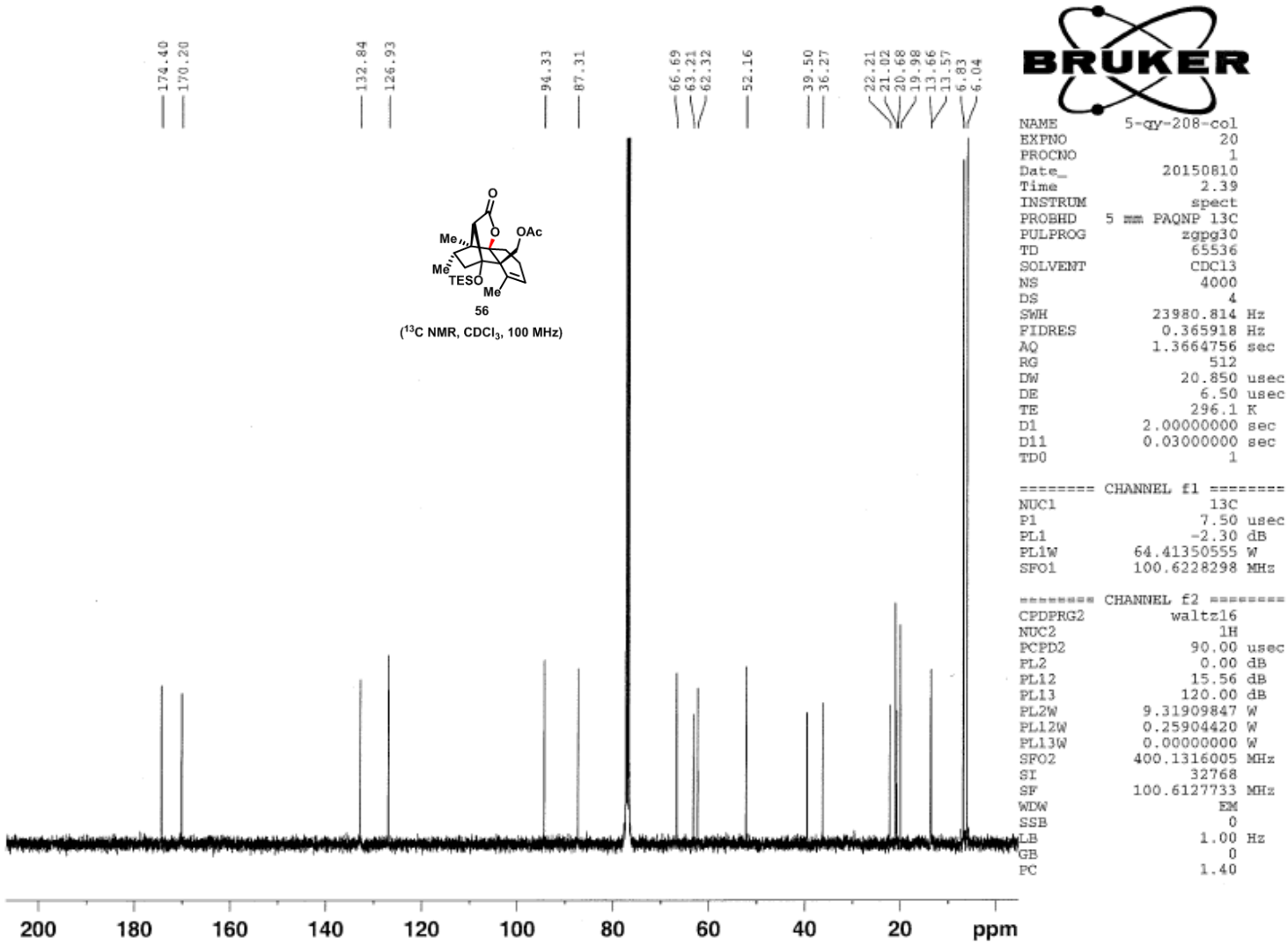

BRUKER

NAME	5-qy-208-col	
EXPNO	20	
PROCNO	1	
Date_	20150810	
Time	2.39	
INSTRUM	spect	
PROBHD	5 mm PAQNP 13C	
PULPROG	zgpg30	
TD	65536	
SOLVENT	CDCl3	
NS	4000	
DS	4	
SWH	23980.814	Hz
FIDRES	0.365918	Hz
AQ	1.3664756	sec
RG	512	
DW	20.850	usec
DE	6.50	usec
TE	296.1	K
D1	2.00000000	sec
D11	0.03000000	sec
TD0	1	
======== CHANNEL f1 ========		
NUC1	13C	
P1	7.50	usec
PL1	-2.30	dB
PL1W	64.41350555	W
SFO1	100.6228298	MHz
======== CHANNEL f2 ========		
CPDPRG2	waltz16	
NUC2	1H	
PCPD2	90.00	usec
PL2	0.00	dB
PL12	15.56	dB
PL13	120.00	dB
PL2W	9.31909847	W
PL12W	0.25904420	W
PL13W	0.00000000	W
SFO2	400.1316005	MHz
SI	32768	
SF	100.6127733	MHz
WDW	EM	
SSB	0	
LB	1.00	Hz
GB	0	
PC	1.40	

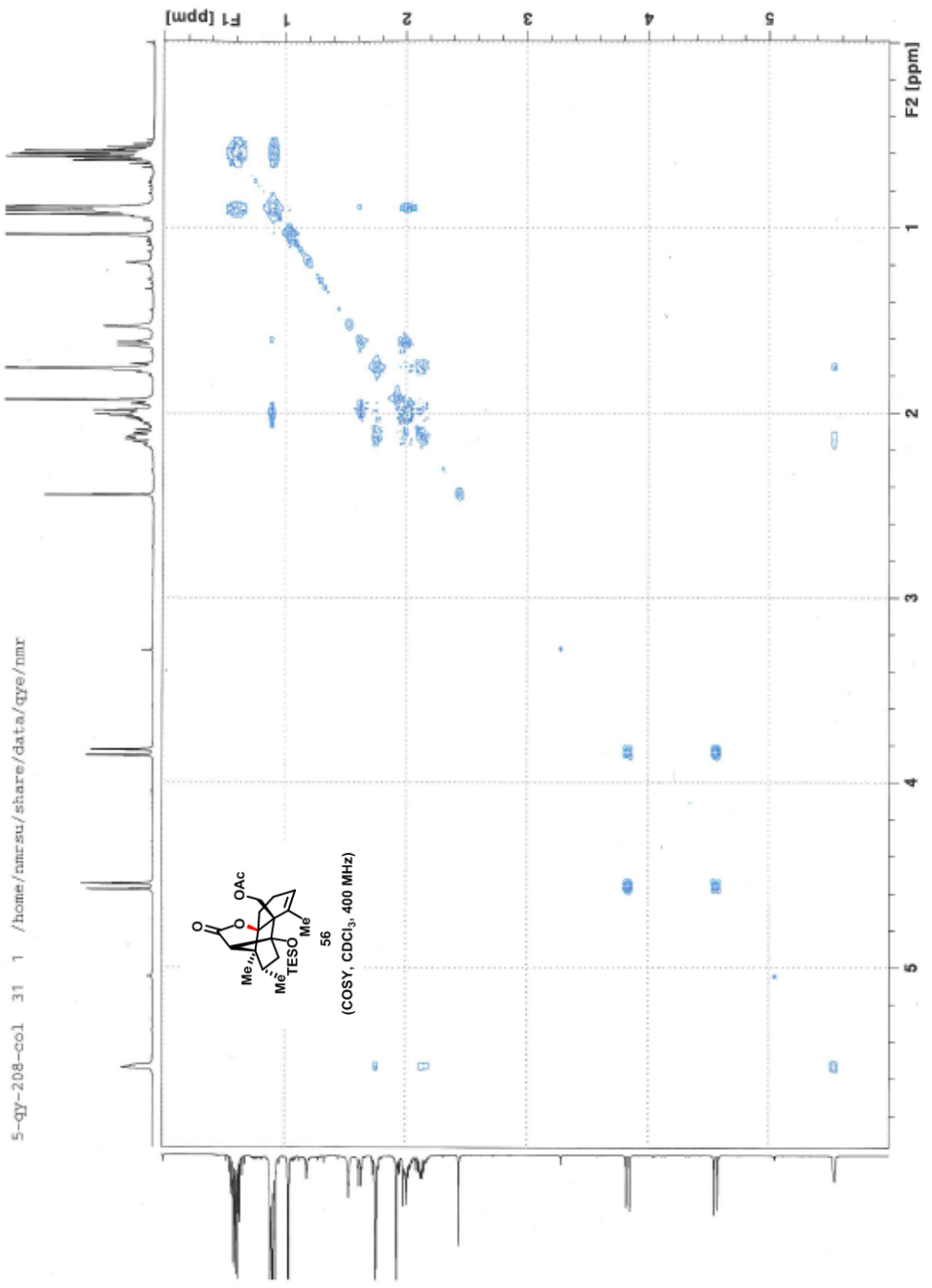
5-qy-208-col 31 1 /home/nmrsu/share/data/qye/nmr
F1 [ppm]
F2 [ppm]
OAc
O
O
Me
Me
TESO
Me
56
(COSY, CDCl3, 400 MHz)

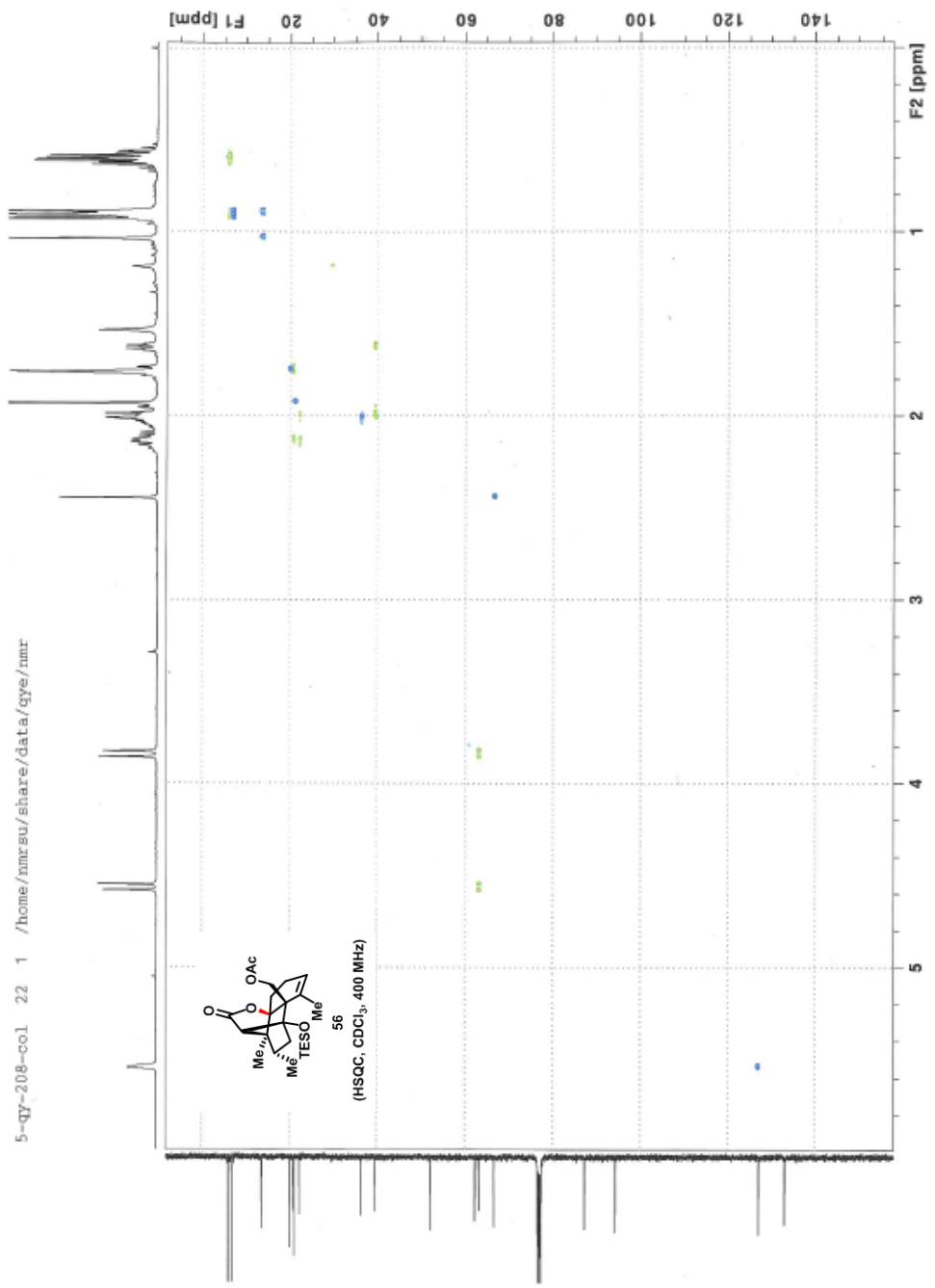
5-qy-208-col 22 1 /home/nmrsu/share/data/qye/nmr
F1 [ppm]
F2 [ppm]
OAc
O
Me
Me
TESO
Me
56
(HSQC, CDCl3, 400 MHz)

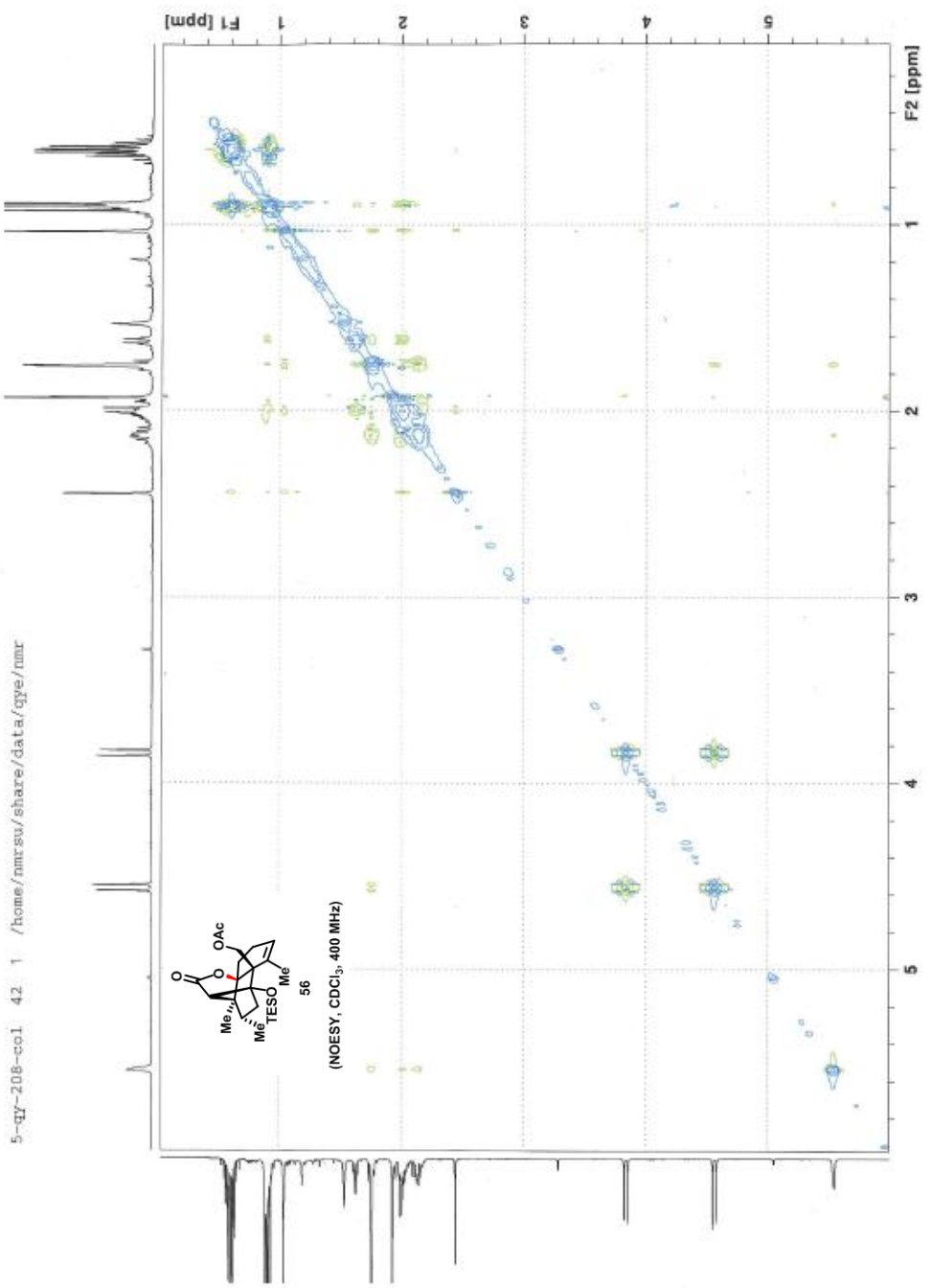
5-qy-208-col 42 1 /home/nmrsu/share/data/qye/nmr
F1 [ppm]
F2 [ppm]
1
2
3
4
5
OAc
O
O
Me
Me
Me
TESO
56
(NOESY, CDCl3, 400 MHz)

CHAPTER 5

INSTALLATION OF THE FURAN MOIETY TO ACHIEVE

TOTAL SYNTHESES OF CLERODANE TERPENOIDS

5.1 Introduction

With a reliable synthetic route towards advanced intermediate **1**, we then turned our attention to the final tailoring needed to achieve total syntheses of the scaparvin terpenoids (Scheme 1). The two key remaining tasks are the installation of the 3-furanyl moiety and intramolecular formation of ketal, events which could potentially be achieved in a single pot. This chapter will describe the final stages leading to a completed total synthesis of scaparvin C as well as a detailed evolution of our approach towards scaparvin A.

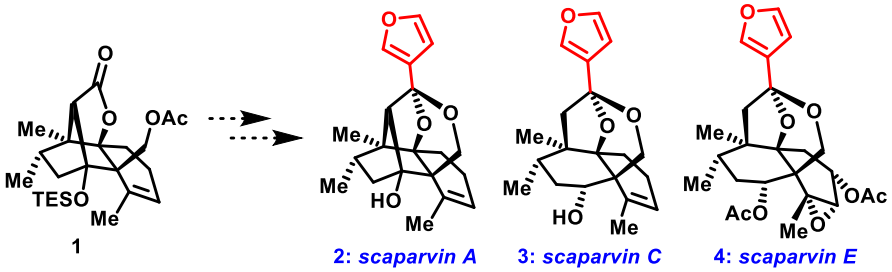

Scheme 1. Installation of furan moiety for total synthesis of scaparvin terpenoids.

5.2 Total Synthesis of Scaparvin C

Retrosynthetically, scaparvin C (**3**) can be viewed as the thermodynamic product of transketalization from compound **5**, a material which in turn could arise from lactone **6** via the nucleophilic addition of 3-furyllithium. Lactone **6** could be then traced back to **7** through several straightforward chemical transformations. Finally, compound **7** could be obtained from a retro-aldo-type ring opening of advanced intermediate **1** due to the release of ring strain.

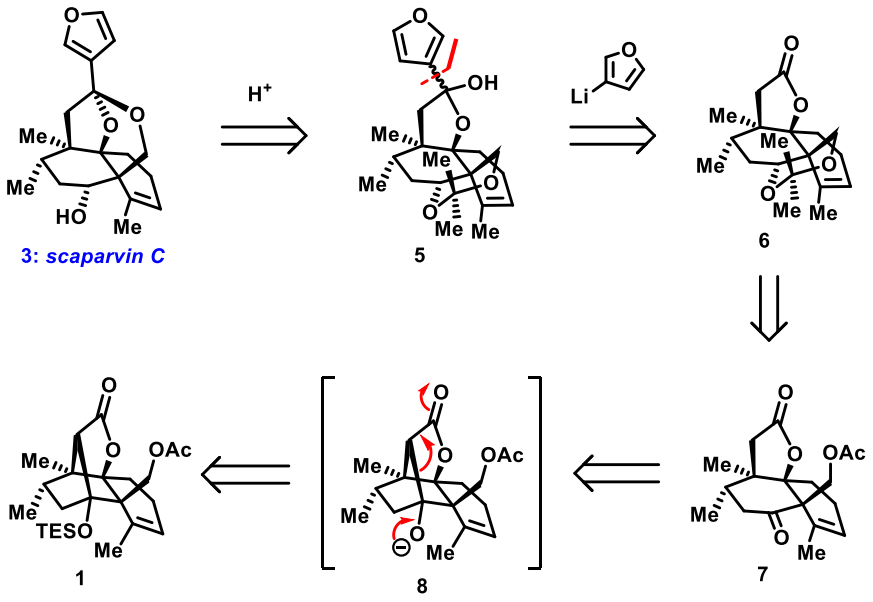

Scheme 2. Retrosynthetic analysis of scaparvin C (**3**) from advanced intermediate **1**.

In the forward sense, treating advanced intermediate **1** with TBAF in THF succeeded in deprotecting the tertiary TES ether selectively, with the resulting anion (**8**) converting to ketoester **7** quantitatively with prolonged reaction times. Surprisingly, mixing **7** with $NaBH_4$ in MeOH not only reduced the ketone group, but also deprotected the acetate group (likely due to the basic reaction condition). The resulting 1,3-diol **9** was then protected *in situ* as the base-stable acetonide **6** in a single pot operation which proceeded in 89% yield from **7**.

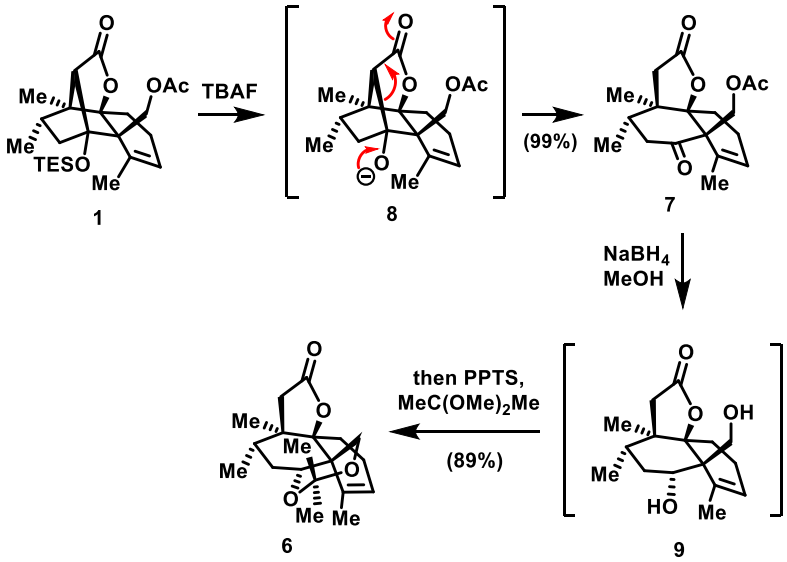

Scheme 3. Synthesis of lactone **6** from advanced intermediate **1.**

Our initial attempts to install the furan moiety focused on the nucleophilic addition of 3-furyllithium (Scheme 4). Monoaddition to lactone **6** at low temperature (<–40 °C) seemed promising to deliver hemiketal **5**. Unfortunately, despite being effective on simple five-membered lactones, a screen of various conditions (temperature, Lewis acid, solvent, etc.) consistently afforded no conversion at low temperature (<–20 °C) and occasionally the formation of several uncharacterizable by-products at high temperature (>23 °C). In addition, the hemiacetal variant (**10**), which was obtained from DIBAL-H reduction of **6**, showed a similar reactivity profile as lactone **6**. Our analysis of these outcomes was that the hindered nature of the lactone group renders it exceptionally unreactive, likely because the preferred attack trajectory (Bürgi–Dunitz angle) may be sterically obstructed by the presence of the C-20 methyl, a domain absent in all of our model systems.

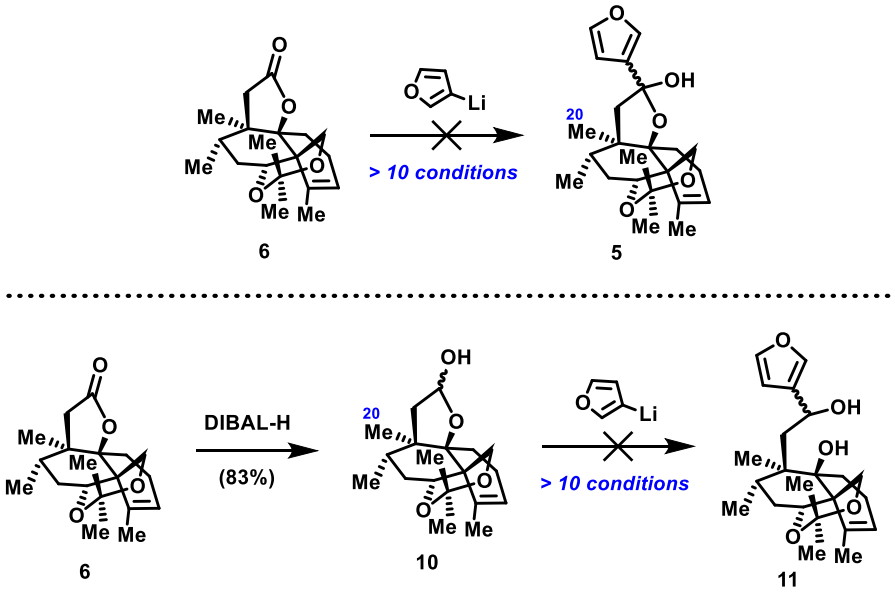

Scheme 4. The failed nucleophilic addition of 3-furyllithium.

In light of these consistent failures, we contemplated installing the furan moiety through a cross-coupling strategy. Specifically, we hoped that triflate **12**, derived from lactone **6**, could couple with 3-furyltin compound **14** via a Stille coupling,[1] thus resulting in the formal installation of furan moiety and affording a new material whose oxidation state is consistent with that of the final targets.

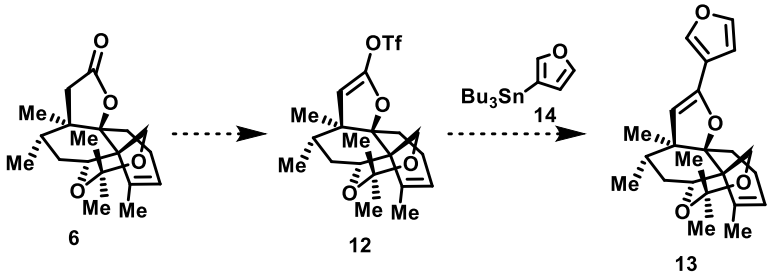

Scheme 5. Installation of furan moiety employing a cross-coupling strategy.

Executing this idea started by subjecting lactone **6** to KHMDS, followed by the addition of Comin's reagent[2] at low temperature (–78 °C). Although the resulting vinyl triflate **12** proved to be very labile to mildly acidic conditions (it slowly decomposed on silica gel, for example), it

was stable (at least for 1 d) under neutral or basic condition to utilize in the subsequent Stille coupling reaction. For this key event, after a small amount of screening, we discovered that the Nicolaou conditions used in their syntheses of maitotoxin fragments gave the best results.[3]

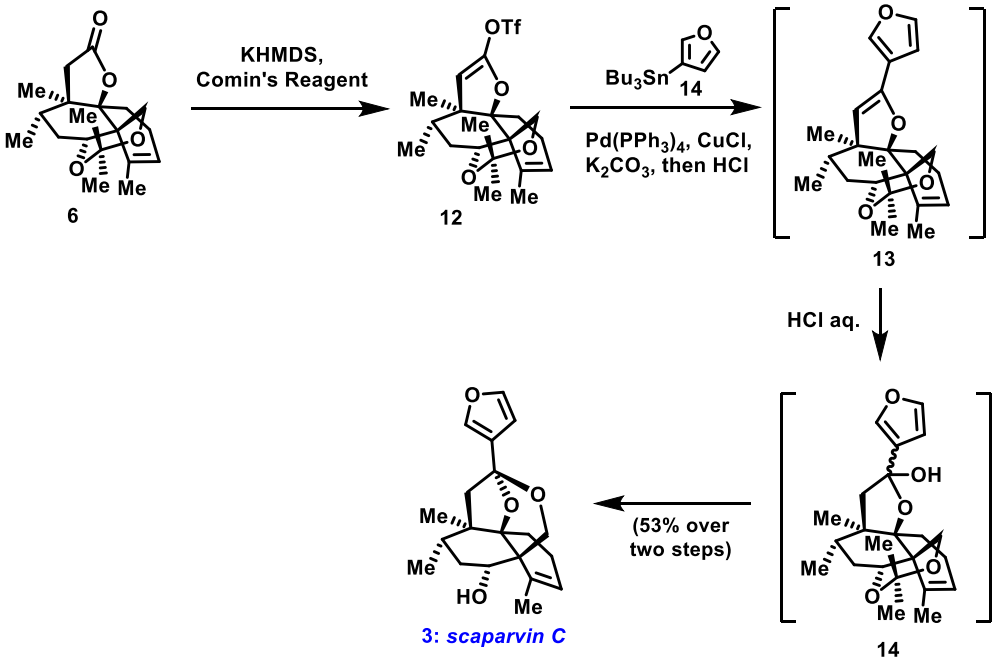

Scheme 6. Total synthesis of scaparvin C (**3**).

In this operation, the Pd-catalyzed cross-coupling of enol triflate **12** and 3-furyltin **14** was carried out in the presence of CuCl (2.0 equiv) and K_2CO_3 (2.0 equiv) in THF at 25 °C, affording vinyl furan **13** after 2 h of reaction time. Upon acidic work-up, the proposed transketalization occurred cleanly using aqueous HCl in THF/MeOH at room temperature, thus completing our total synthesis of scaparvin C (**3**). The spectral properties of synthetic **3** fully agree with the naturally isolated material reported by Lou,[4] as shown in Table 1 and 2.

Table 1. Comparison of ^{1}H NMR shifts (δ) of synthetic **3** and natural **3**.

Natural **3**	Synthetic **3**
7.46 (br, 1 H)	7.45 (br, 1 H)
7.33 (t, *J* = 1.5 Hz, 1 H)	7.33 (t, *J* = 1.7 Hz, 1 H)

6.39 (br, 1 H)	6.39 (br, 1 H)
6.06 (br, 1 H)	6.06 (br, 1 H)
4.20 (d, *J* = 12.8 Hz, 1 H)	4.20 (d, *J* = 12.7 Hz, 1 H)
3.89 (d, *J* = 12.8 Hz, 1 H)	3.89 (d, *J* = 12.7 Hz, 1 H)
3.45 (t, *J* = 7.0 Hz, 1 H)	3.45 (dt, *J* = 1.8, 6.8 Hz, 1 H)
2.41 (d, *J* = 14.1 Hz, 1 H)	2.41 (d, *J* = 14.0 Hz, 1 H)
2.33 (m, 1 H), 2.27 (ddq, *J* = 4.2, 6.8, 10.8 Hz, 1 H)	2.38–2.20 (m, 2 H)
2.21 (ddd, *J* = 4.2, 6.5, 14.3 Hz, 1 H)	2.12 (m, 1 H)
2.08 (d, *J* = 14.1 Hz, 1 H)	2.08 (d, *J* = 14.0 Hz, 1 H)
2.06 (m, 1 H)	2.06 (m, 1 H)
1.93 (dd, *J* = 6.4, 13.6 Hz, 1 H)	1.94 (m, 1 H)
1.82 (br, 3 H)	1.82 (br, 3 H)
1.73 (ddd, *J* = 6.7, 11.8, 13.4 Hz, 1 H)	1.73 (m, 1 H)
1.47 (ddd, *J* = 7.4, 10.8, 14.3 Hz, 1 H)	1.47 (m, 1 H)
1.07 (s, 3 H)	1.07 (s, 3 H)
1.07 (d, *J* = 6.8 Hz, 3 H)	1.06 (d, *J* = 7.0 Hz, 3 H)

Table 2. Comparison of ^{1}C NMR shifts (δ) of synthetic **3** and natural **3**.

Natural **3**	Synthetic **3**
142.9	142.9
139.5	139.5
131.3	131.2
130.9	130.8
127.4	127.3
108.4	108.4
101.6	101.5
84.8	84.8
67.6	67.6
65.3	65.3
55.4	55.3
45.5	45.5
45.1	45.0
35.1	35.1
34.1	34.1
26.8	26.8
23.5	23.5
22.5	22.5
20.5	20.5
19.3	19.2

Globally, we had succeeded in preparing scaparvin C (**3**) in 16 steps from Rawal's diene. With this exciting result in hand, we next set our sights on achieving a total synthesis of scaparvin A with the [2.2.1]-bicycle structure needing to remain intact.

5.3 Studies towards the Total Synthesis of Scaparvin A

Despite the success of the Stille coupling strategy towards scaparvin C (**3**) noted above, its use for scaparvin A in the form of vinyl triflate **15** with its bridge system intact was anticipated to be hard, if not impossible, to synthesize, thus preventing the use of this approach to access of scaparvin A (**1**). In addition, similar to the previous results described above in terms of nucleophilic additions of 3-furyllithium, all attempts to achieve this process with **1** and other protected variants of this key compound failed to deliver the desired hemiketal **17**. As a result, we needed a unique strategy, and contemplated the potential of radical-based approaches.

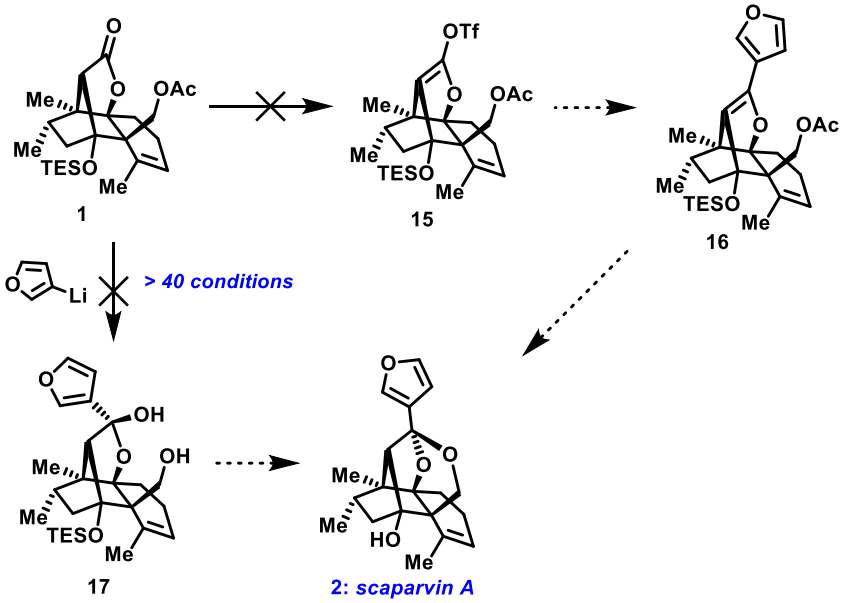

Scheme 7. The failed approach towards scaparvin A (**2**).

As shown in Scheme 8, if a radical-generating group could be attached to the C-12 bridge head position, the resulting radical (**19**) could potentially attack a radical acceptor such as α,β-unsaturated lactone **20** and give **21**. Although not a direct formation of the furyl ring system, if this coupling could be achieved it was anticipated that the furan moiety in scaparvin A (**2**) could be derived readily through several straightforward reactions. Literature precedents supported this radical-based coupling idea in general terms, as there were a few examples of productive bridgehead radicals, particularly as demonstrated by the Inoue group at the University of Tokyo.[5] While these precedents were certainly encouraging, however, none matched our exact system, and we uncertain just what the stability and electronic profile our bridgehead radical would have if it could be formed.

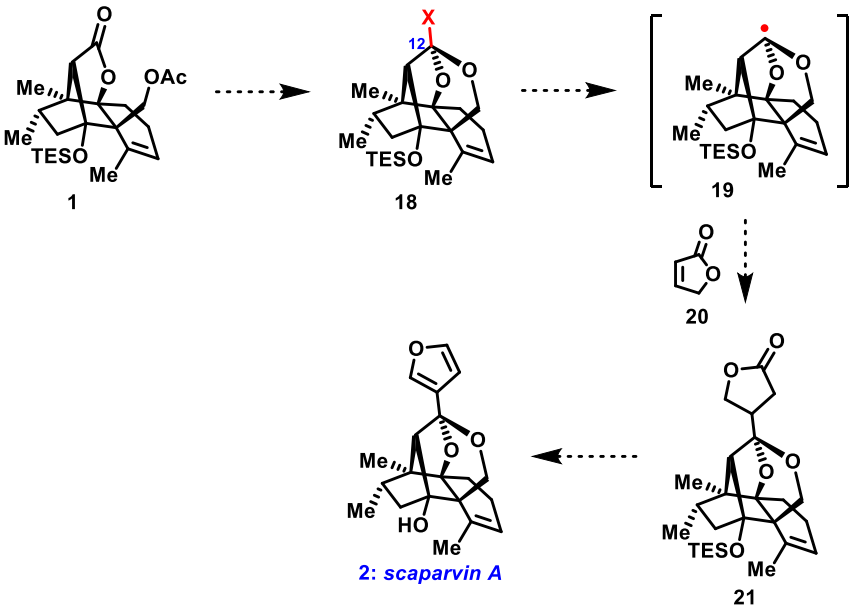

Scheme 8. The radical-based approach towards scaparvin A (**2**).

Given our concerns, we felt that the most prudent course of action was to identify an initial model for the desired transformation. The most readily accessible and comparable model compound in our opinion was **24**. This material was prepared in two steps through mono-

reduction of commercially available diketone **22** and subsequent thiocarbonate formation. Pleasingly, treatment of **24** with 5 equivalents of radical acceptor **20** using Et_3B and O_2 as the radical initiators at room temperature, afforded the desired coupling product **26** in 93% yield. Finally, formation of the furan moiety was accomplished through a sequence involving oxidative selenoxide elimination[6] and DIBAL-H reduction.

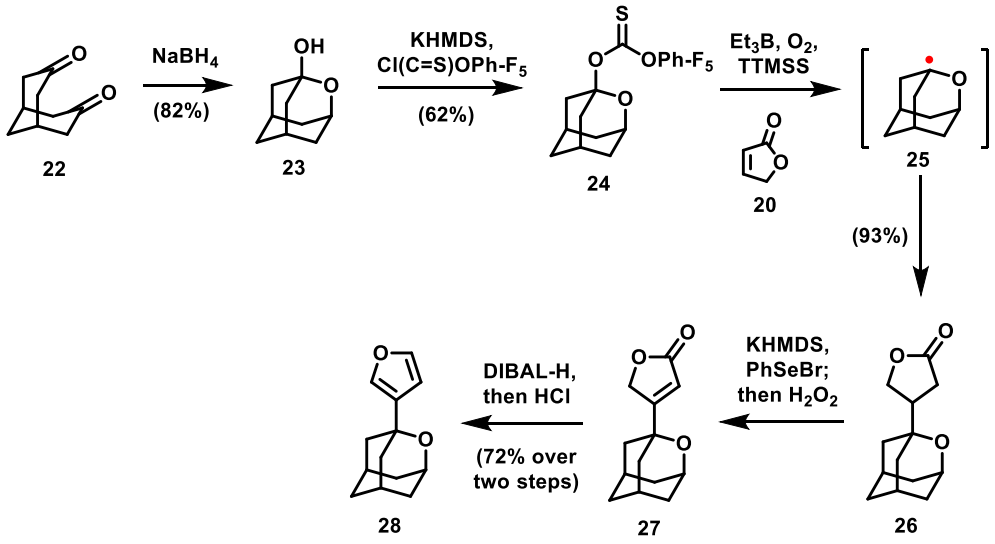

Scheme 9. Model study of installation of furan moiety employing the radical-based approach.

Encouraged by this result, we set about applying these conditions to fully functionalized materials for scaparvin A (**2**). Thus, advanced intermediate **1** was therefore hydrolyzed under neutral condition of Me_3SnOH,[7] affording translactonization product **29**. After installing the thiocarbonate group, radical **19** was generated by using Et_3B and O_2 as radical initiators just as described earlier. However, instead of forming lactone **21** through radical addition, only six-membered lactone **32** was observed. Evidently, the bridge head radical **19** in this case is not stable enough for the intermolecular addition, but prefers to break the cage structure in what would then release of ring strain. Because it is an intramolecular process, we felt that this approach was likely a dead end since its kinetics could not be countermanded.

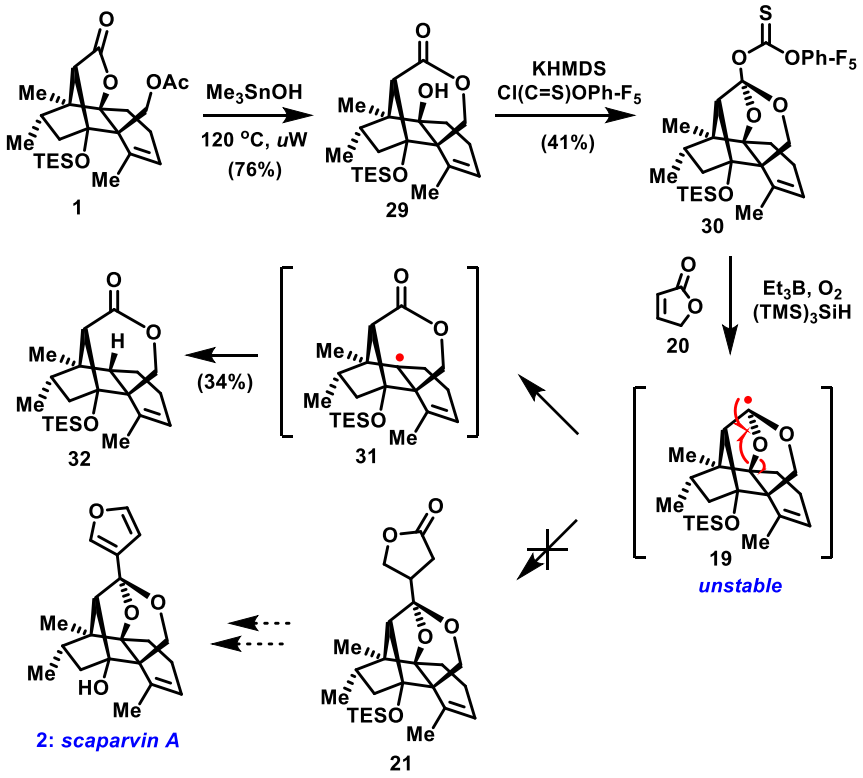

Scheme 10. Installation of furan moiety employing the radical-based approach.

With this failure, we believe that future efforts should revisit the original nucleophilic addition approach, but do so using oxonium ion **35** as the electrophile (Scheme 11). If acetal **33** could be synthesized from advanced intermediate **1**, treatment with 3-furyltitanium reagent may give oxonium ion **35** and, in turn, facilitate the nucleophilic addition of furan moiety. This mode of nucleophilic addition is believed to be promising for two reasons. First, the oxonium ion is more electrophilic than the previously used lactone, and thus should be more reactive towards addition of furan moiety. Second, and which is more important, the preferred attack trajectory of the oxonium ion (i.e. the Bürgi–Dunitz angle) is different from the lactone counterpart and would appear to not be sterically obstructed by the C-20 methyl. If true, a subsequent benzylic oxidation could complete the synthesis of scaparvin A. Future efforts will explore this idea.

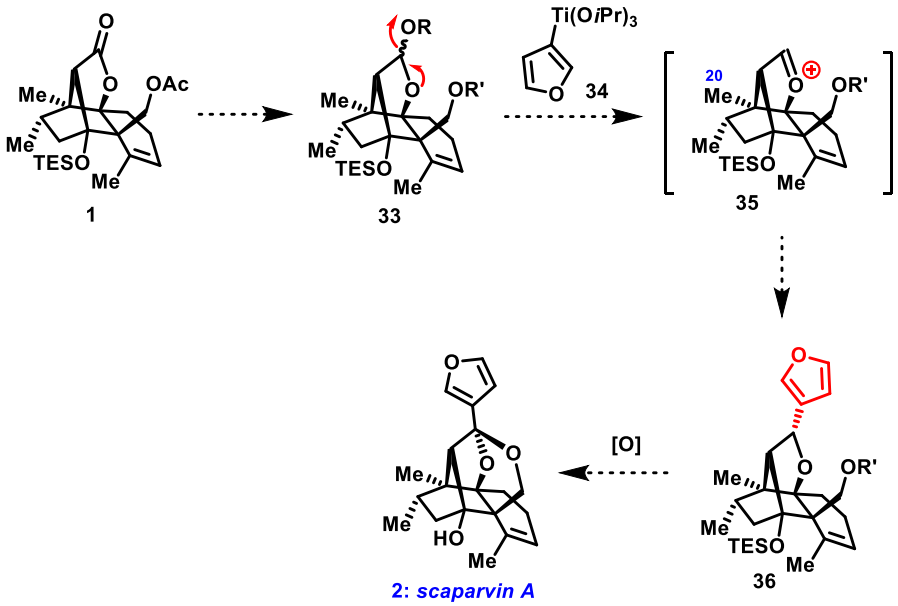

Scheme 11. Installation of furan moiety via oxonium ion (**36**).

5.4 Conclusion

Globally, through the work delineated in this chapter, the total synthesis of scaparvin C (**3**) has been accomplished in 16 steps from Rawal's diene (Scheme 12). Also, we are confident that an effective synthetic solution for scaparvin A (**2**) will be available in the near future. From these initial advances, an effective course for accessing the full diversity represented by clerodane terpenoids family can be confidently plotted.

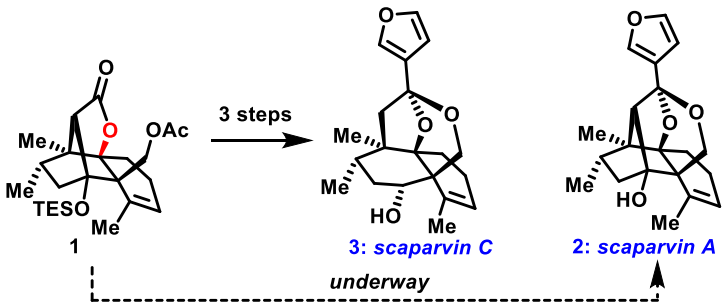

Scheme 12. Syntheses of scaparvin terpenoids from advanced intermediate **1**.

5.5 References

(1) Stille, J. K. *Angew. Chem. Int. Ed. Engl.* **1986**, *25*, 508.

(2) Comins, D. L.; Dehghani, A. *Tetrahedron Lett.* **1992**, *33*, 6299.

(3) Nicolaou, K. C.; Sato, M.; Miller, N. D.; Gunzner, J. L.; Renaud, J.; Untersteller, E. *Angew. Chem. Int. Ed. Engl.* **1996**, *35*, 889.

(4) Guo, D.-X.; Zhu, R.-X.; Wang, X.-N.; Wang, L.-N.; Wang, S.-Q.; Lin, Z.-M.; Lou, H.-X. *Org. Lett.* **2010**, *12*, 4404.

(5) (a) Nagatomo, M.; Koshimizu, M.; Masuda, K.; Tabuchi, T.; Urabe, D.; Inoue, M. *J. Am. Chem. Soc.* **2014**, *136*, 5916. (b) Kamimura, D.; Urabe, D.; Nagatomo, M.; Inoue, M. *Organic Letters* **2013**, *15*, 5122. (c) Murai, K.; Katoh, S.-i.; Urabe, D.; Inoue, M. *J. Am. Chem. Soc.* **2013**, *4*, 2364.

(6) Reich, H. J.; Renga, J. M.; Reich, I. L. *J. Am. Chem. Soc.* **1975**, *97*, 5434.

(7) Nicolaou, K. C.; Estrada, A. A.; Zak, M.; Lee, S. H.; Safina, B. S. *Angew. Chem. Int. Ed.* **2005**, *44*, 1378.

5.6 Experimental Section

General Methods: All reactions were carried out under an argon atmosphere with dry solvents under anhydrous conditions, unless otherwise stated. Dry methylene chloride (CH_2Cl_2), diethyl ether (Et_2O), tetrahydrofuran (THF), benzene and toluene were obtained by passing commercially available pre-dried, oxygen-free formulations through activated alumina columns; triethylamine (Et_3N) was distilled from KOH; dichloroethane (DCE), acetonitrile (CH_3CN) and methanol (MeOH) were purchased in anhydrous form from Sigma-Aldrich and used as received. Yields refer to chromatographically and spectroscopically (^1H and ^{13}C NMR) homogeneous materials, unless otherwise stated. Reagents were purchased at the highest commercial quality and used without further purification, unless otherwise stated. Reactions were magnetically stirred and monitored by thin-layer chromatography (TLC) carried out on 0.25 mm E. Merck silica gel plates (60F-254) using UV light and an aqueous solution of cerium ammonium sulfate and ammonium molybdate and heat as visualizing agents. Preparative TLC was carried out on 0.50 mm E. Merck silica gel plates (60F-254). SiliCycle silica ge (60 A, academic grade, particle size 40-63 μm) was used for flash column chromatography. NMR spectra were recorded on Bruker DRX-300, DRX-400, DRX-500 and DRX-700 instruments and calibrated using residual undeuterated solvent as an internal reference. The following abbreviations are used to explain multiplicities: s = singlet, d = doublet, t = triplet, q = quartet, m = multiplet, br = broad, app = apparent. IR spectra were recorded on a Perkin-Elmer Spectrum Two FT-IR spectrometer. High resolution mass spectra (HRMS) were recorded in the Columbia University Mass Spectral Core facility on a JOEL HX110 mass spectrometer using FAB (Fast Atom Bombardment).

Lactone 6. To a solution of advanced intermediate **1** (20.2 mg, 0.0464 mmol, 1.0 equiv) in THF (2 mL) at 0 °C was added a solution of TBAF in THF (1.0 M, 0.070 mL, 1.5 equiv). The reaction contents were then concentrated in vacuum and diluted with MeOH (2 mL). $NaBH_4$ (8.8 mg, 0.232 mmol, 5.0 equiv) was added in three portions into the reaction solution at 0 °C over 1 h. Then, the reaction contents were slowly warmed to 23 °C over 10 h. Upon full conversion to the resultant diol (determined by TLC analysis), the reaction mixture was concentrated again and diluted with 2,2-dimethoxypropane (10 mL). *p*TSA-H_2O (265 mg, 1.39 mmol, 30.0 equiv) was added in one portion to the solution at 23 °C. After stirring for an additional 2 h at 23 °C, the reaction was quenched by saturated aqueous $NaHCO_3$ solution (20 mL). The reaction contents were then transferred to a separatory funnel, diluting with EtOAc (10 mL) and hexanes (10 mL). The organic layer was separated and the aqueous layer was extracted with EtOAc (3 × 10 mL). The organic layers were combined, washed by saturated aqueous NaCl (10 mL), dried with $MgSO_4$, filtered and concentrated. The resulting crude product was purified by flash column chromatography (silica gel, hexanes/EtOAc, 20:1 to 6:1) to give lactone **6** (13.2 mg, 89% yield) as a white solid. **6**: ^{1}H NMR (400 MHz, $CDCl_3$) δ 5.46 (br, 1 H), 4.31 (d, *J* = 10.6 Hz, 1 H), 4.22 (dd, *J* = 3.3, 11.2 Hz, 1 H), 3.62 (d, *J* = 10.6 Hz, 1 H), 2.46 (d, *J* = 17.2 Hz, 1 H), 2.24 (d, *J* = 17.2 Hz, 1 H), 2.29–2.14 (m, 2 H), 2.10 (br, 3 H), 1.98–1.71 (m, 3 H), 1.69–1.45 (m, 2 H), 1.45 (s, 3 H), 1.36 (s, 3 H), 0.99 (s, 3 H), 0.85 (d, *J* = 6.7 Hz, 3 H); ^{13}C NMR (100 MHz, $CDCl_3$) δ 175.1, 137.2, 125.9, 99.0, 91.8, 70.6, 70.5, 46.8, 42.7, 42.3, 37.3, 33.1, 29.3, 25.6, 24.9, 24.3, 19.1, 16.7, 14.0.

Scaparvin C (3). To a solution of lactone **6** (3.5 mg, 0.0109 mmol, 1.0 equiv) in THF (2 mL) at –78 °C was added a solution of KHMDS in toluene (0.5 M, 0.066 mL, 3.0 equiv). After stirring at –78 °C for 45 min, a solution of Comin's reagent (17.0 mg, 0.0436 mmol, 4.0 equiv)

in THF (2 mL) was added dropwise at the same temperature. After stirring for an additional 1 h at –78 °C, the reaction was quenched by saturated aqueous $NaHCO_3$ solution (5 mL) at –78 °C, whereafter the reaction mixture was slowly warmed to 23 °C over 30 min. The reaction contents were then transferred to a separatory funnel, diluting with EtOAc (5 mL) and hexanes (5 mL). The organic layer was separated and the aqueous layer was extracted with EtOAc (3 × 5 mL). The organic layers were combined, dried with Na_2SO_4, filtered and concentrated. The resulting crude product was roughly purified by a quick flash column chromatography (silica gel, hexanes/EtOAc, 10:1) to give triflate **12** as a yellowish foam. This material was immediately carried forward in the following reaction.

Triflate **12** was then dissolved in THF (1 mL) at 23 °C. Then, a solution of 3-furyltin compound **14** (7.8 mg, 0.0218 mmol, 2.0 equiv) in THF was added to the resultant solution, followed by consecutive additions of CuCl (2.2 mg, 0.0218 mmol, 2.0 equiv), K_2CO_3 (3.0 mg, 0.0218 mmol, 2.0 equiv) and $Pd(PPh_3)_4$ (1.3 mg, 0.00109 mmol, 10 mol%). The reaction mixture quickly turned brown over 10 min. After stirring at 23 °C for 2 h, the reaction was quenched by ~1.25 M HCl in MeOH (1 mL). The reaction mixture was vigorously stirred at 23 °C for 10 h, whereafter the reaction contents were transferred to a separatory funnel, diluting with Et_2O (5 mL) and aqueous $NaHCO_3$ solution (5 mL). The organic layer was separated and the aqueous layer was extracted with Et_2O (3 × 5 mL). The organic layers were combined, washed with 5% aqueous KF solution (10 mL), dried with $MgSO_4$, filtered and concentrated. The resulting crude product was purified by flash column chromatography (silica gel, hexanes/EtOAc, 10:1 to 4:1) to give scaparvin C (**3**) (1.9 mg, 53% yield over two steps) as white solid. **3**: ^{1}H NMR (400 MHz, $CDCl_3$) δ 7.45 (br, 1 H), 7.33 (t, *J* = 1.7 Hz, 1 H), 6.39 (br, 1 H), 6.06 (br, 1 H), 4.20 (d, *J* = 12.7 Hz, 1 H), 3.89 (d, *J* = 12.7 Hz, 1 H), 3.45 (dt, *J* = 1.8, 6.8 Hz, 1 H), 2.41 (d, *J* = 14.0 Hz, 1 H),

2.38–2.20 (m, 2 H), 2.12 (m, 1 H), 2.08 (d, *J* = 14.0 Hz, 1 H), 2.06 (m, 1 H), 1.94 (m, 1 H), 1.82 (br, 3 H), 1.73 (m, 1 H), 1.47 (m, 1 H), 1.07 (s, 3 H), 1.06 (d, *J* = 7.0 Hz, 3 H); ^{13}C NMR (175 MHz, $CDCl_3$) δ 142.9, 139.5, 131.2, 130.8, 127.3, 108.4, 101.5, 84.8, 67.6, 65.3, 55.3, 45.5, 45.0, 35.1, 34.1, 26.8, 23.5, 22.5, 20.5, 19.2.

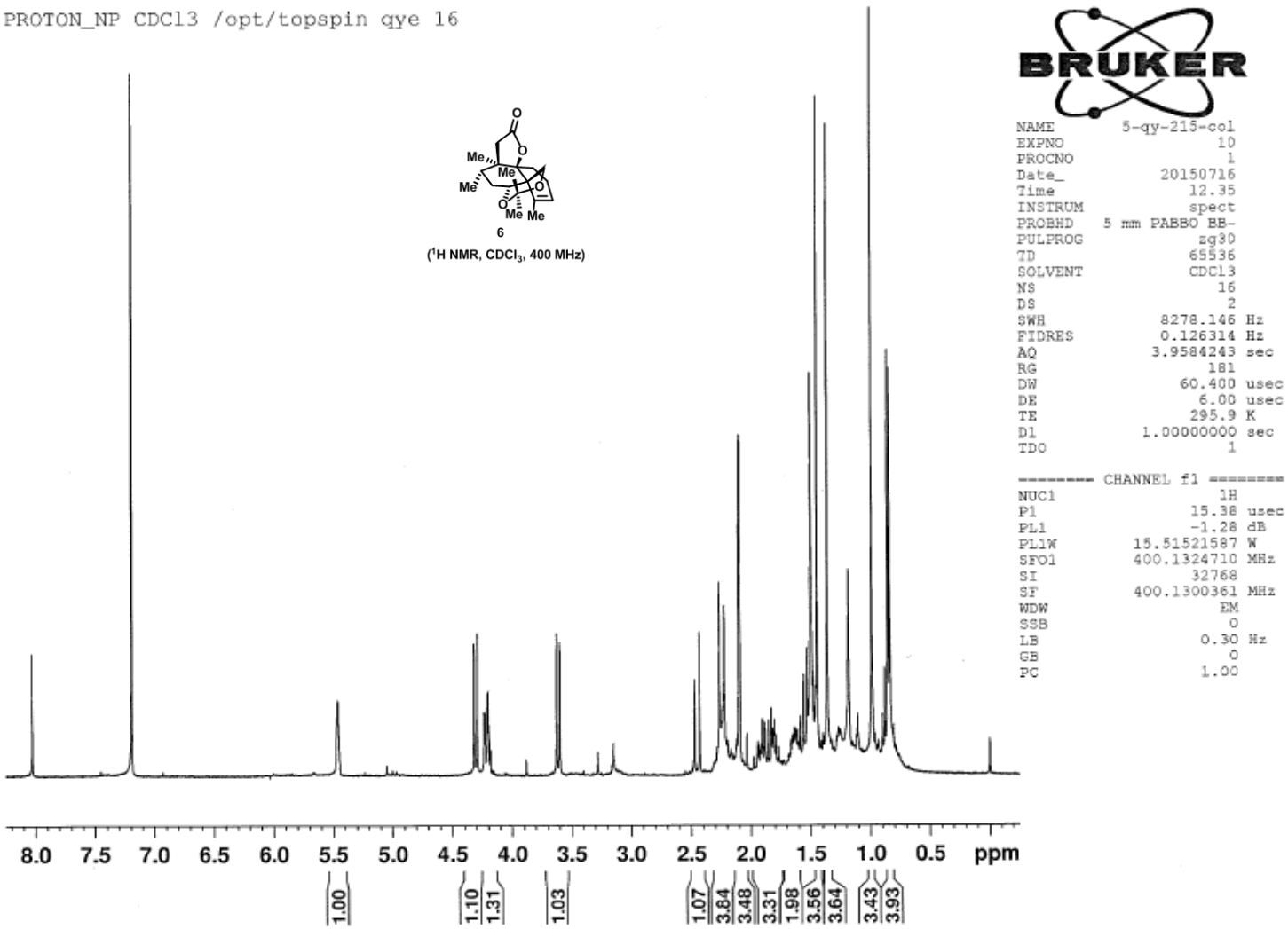
PROTON_NP CDCl3 /opt/topspin qye 16
Me
Me
Me
O
O
O
Me
Me
6
(1H NMR, CDCl3, 400 MHz)
BRUKER
NAME 5-qy-215-col
EXPNO 10
PROCNO 1
Date_ 20150716
Time 12.35
INSTRUM spect
PROBHD 5 mm PABBO BB-
PULPROG zg30
TD 65536
SOLVENT CDCl3
NS 16
DS 2
SWH 8278.146 Hz
FIDRES 0.126314 Hz
AQ 3.9584243 sec
RG 181
DW 60.400 usec
DE 6.00 usec
TE 295.9 K
D1 1.00000000 sec
TD0 1
======== CHANNEL f1 ========
NUC1 1H
P1 15.38 usec
PL1 -1.28 dB
PL1W 15.51521587 W
SFO1 400.1324710 MHz
SI 32768
SF 400.1300361 MHz
WDW EM
SSB 0
LB 0.30 Hz
GB 0
PC 1.00
8.0 7.5 7.0 6.5 6.0 5.5 5.0 4.5 4.0 3.5 3.0 2.5 2.0 1.5 1.0 0.5 ppm
1.00
1.10
1.31
1.03
1.07
3.84
3.48
3.31
1.98
3.56
3.64
3.43
3.93

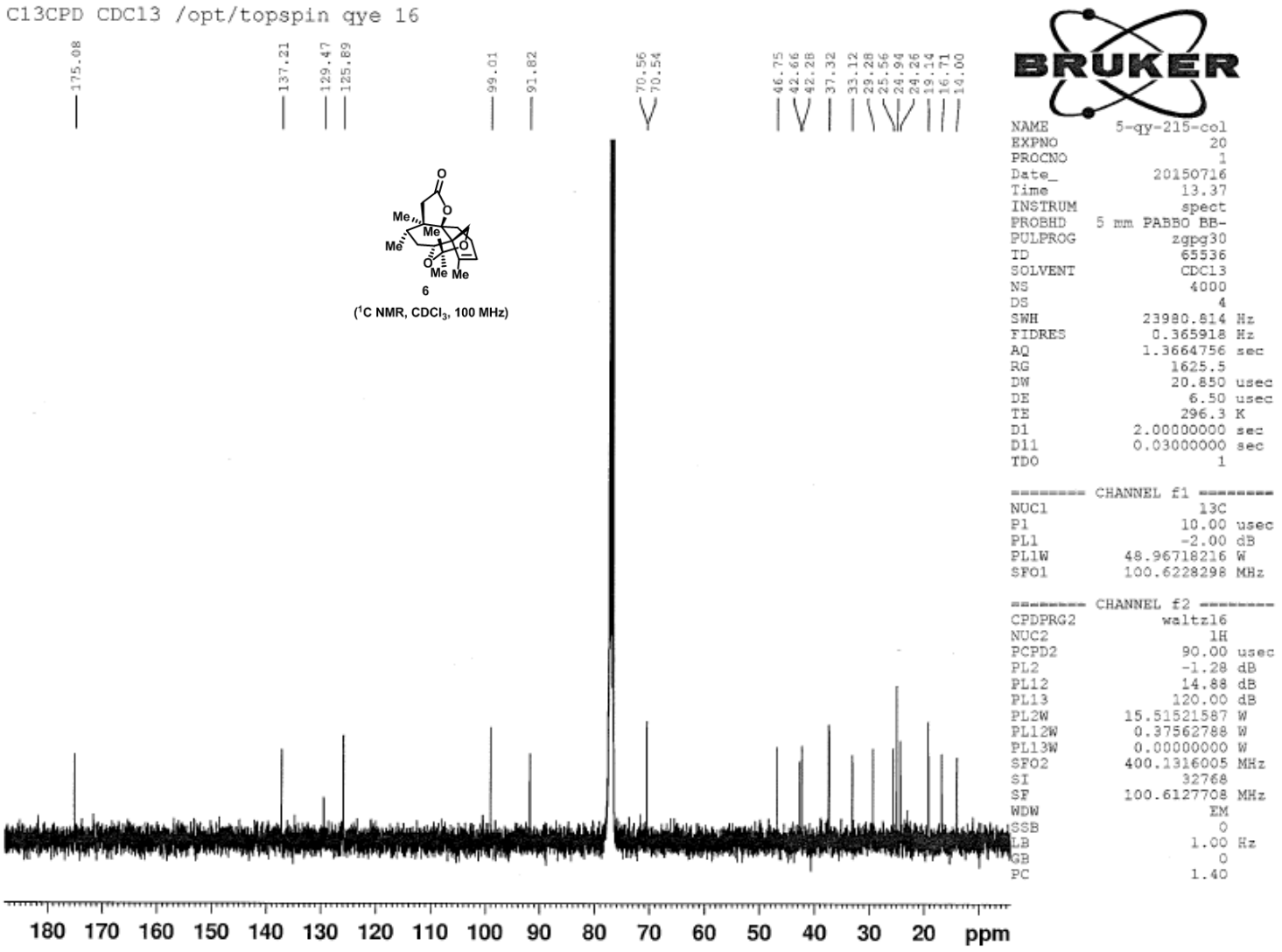
C13CPD CDCl3 /opt/topspin qye 16
175.08
137.21
129.47
125.89
99.01
91.82
70.56
70.54
46.75
42.66
42.28
37.32
33.12
29.28
25.56
24.94
24.26
19.14
16.71
14.00
Me
Me
Me
Me
Me
O
O
O
O
6
(1C NMR, CDCl3, 100 MHz)
BRUKER
NAME 5-qy-215-col
EXPNO 20
PROCNO 1
Date_ 20150716
Time 13.37
INSTRUM spect
PROBHD 5 mm PABBO BB-
PULPROG zgpg30
TD 65536
SOLVENT CDCl3
NS 4000
DS 4
SWH 23980.814 Hz
FIDRES 0.365918 Hz
AQ 1.3664756 sec
RG 1625.5
DW 20.850 usec
DE 6.50 usec
TE 296.3 K
D1 2.00000000 sec
D11 0.03000000 sec
TD0 1
======== CHANNEL f1 ========
NUC1 13C
P1 10.00 usec
PL1 -2.00 dB
PL1W 48.96718216 W
SFO1 100.6228298 MHz
======== CHANNEL f2 ========
CPDPRG2 waltz16
NUC2 1H
PCPD2 90.00 usec
PL2 -1.28 dB
PL12 14.88 dB
PL13 120.00 dB
PL2W 15.51521587 W
PL12W 0.37562788 W
PL13W 0.00000000 W
SFO2 400.1316005 MHz
SI 32768
SF 100.6127708 MHz
WDW EM
SSB 0
LB 1.00 Hz
GB 0
PC 1.40
180 170 160 150 140 130 120 110 100 90 80 70 60 50 40 30 20 ppm

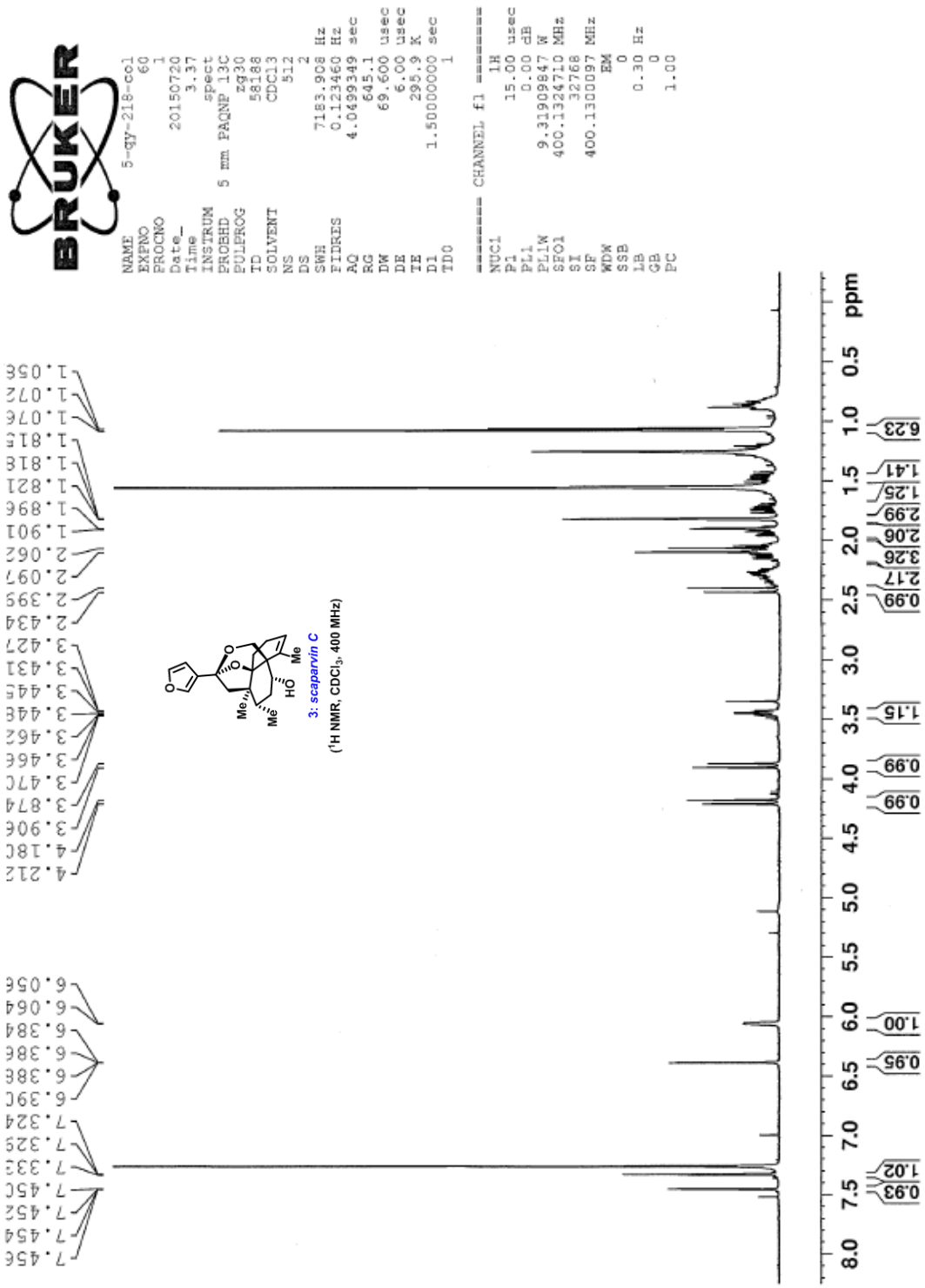
3: scaparvin C
(1H NMR, CDCl3, 400 MHz)
ppm

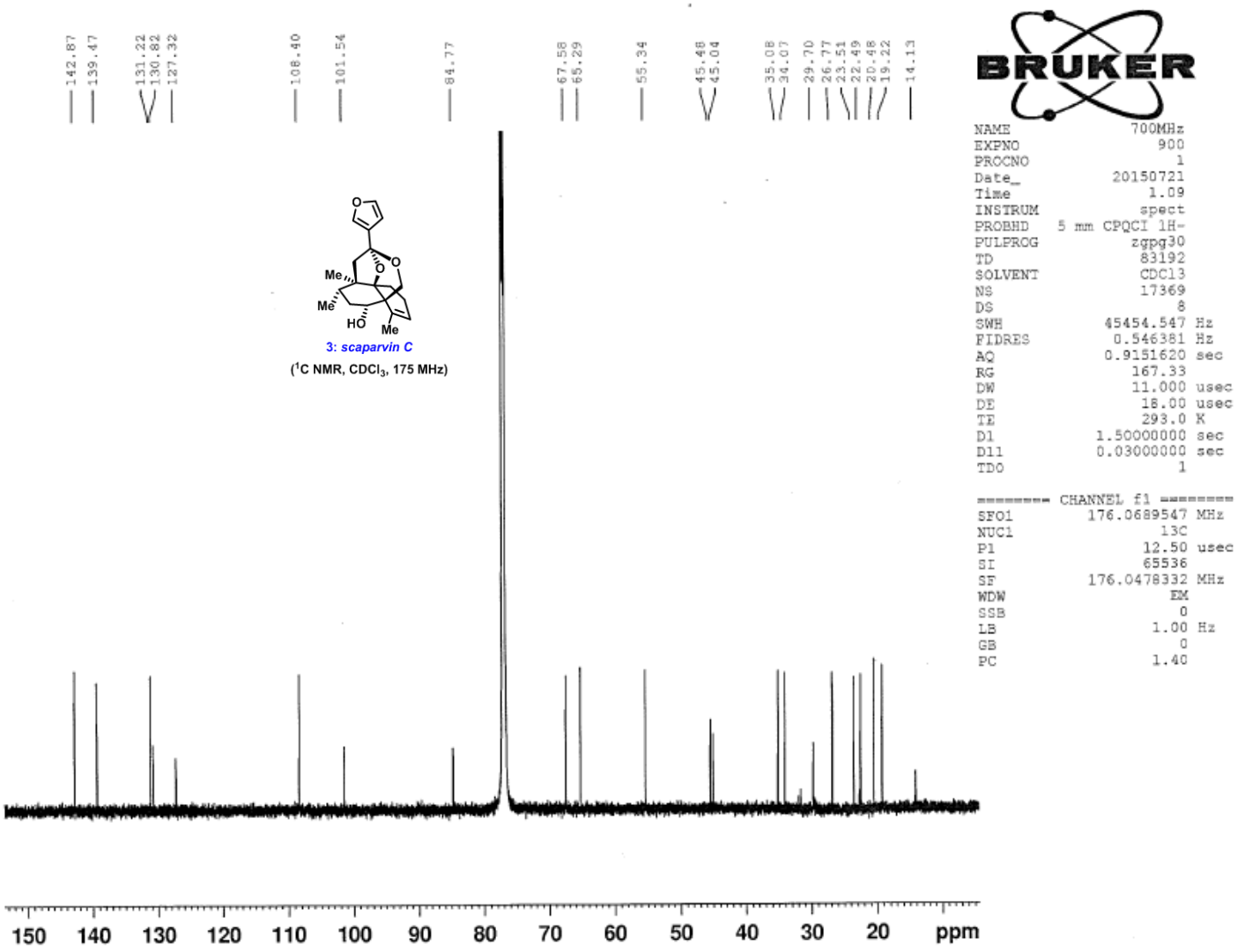

BRUKER

NAME	700MHz
EXPNO	900
PROCNO	1
Date_	20150721
Time	1.09
INSTRUM	spect
PROBHD	5 mm CPQCI 1H-
PULPROG	zgpg30
TD	83192
SOLVENT	CDCl3
NS	17369
DS	8
SWH	45454.547 Hz
FIDRES	0.546381 Hz
AQ	0.9151620 sec
RG	167.33
DW	11.000 usec
DE	18.00 usec
TE	293.0 K
D1	1.50000000 sec
D11	0.03000000 sec
TD0	1
======== CHANNEL f1 ========	
SFO1	176.0689547 MHz
NUC1	13C
P1	12.50 usec
SI	65536
SF	176.0478332 MHz
WDW	EM
SSB	0
LB	1.00 Hz
GB	0
PC	1.40

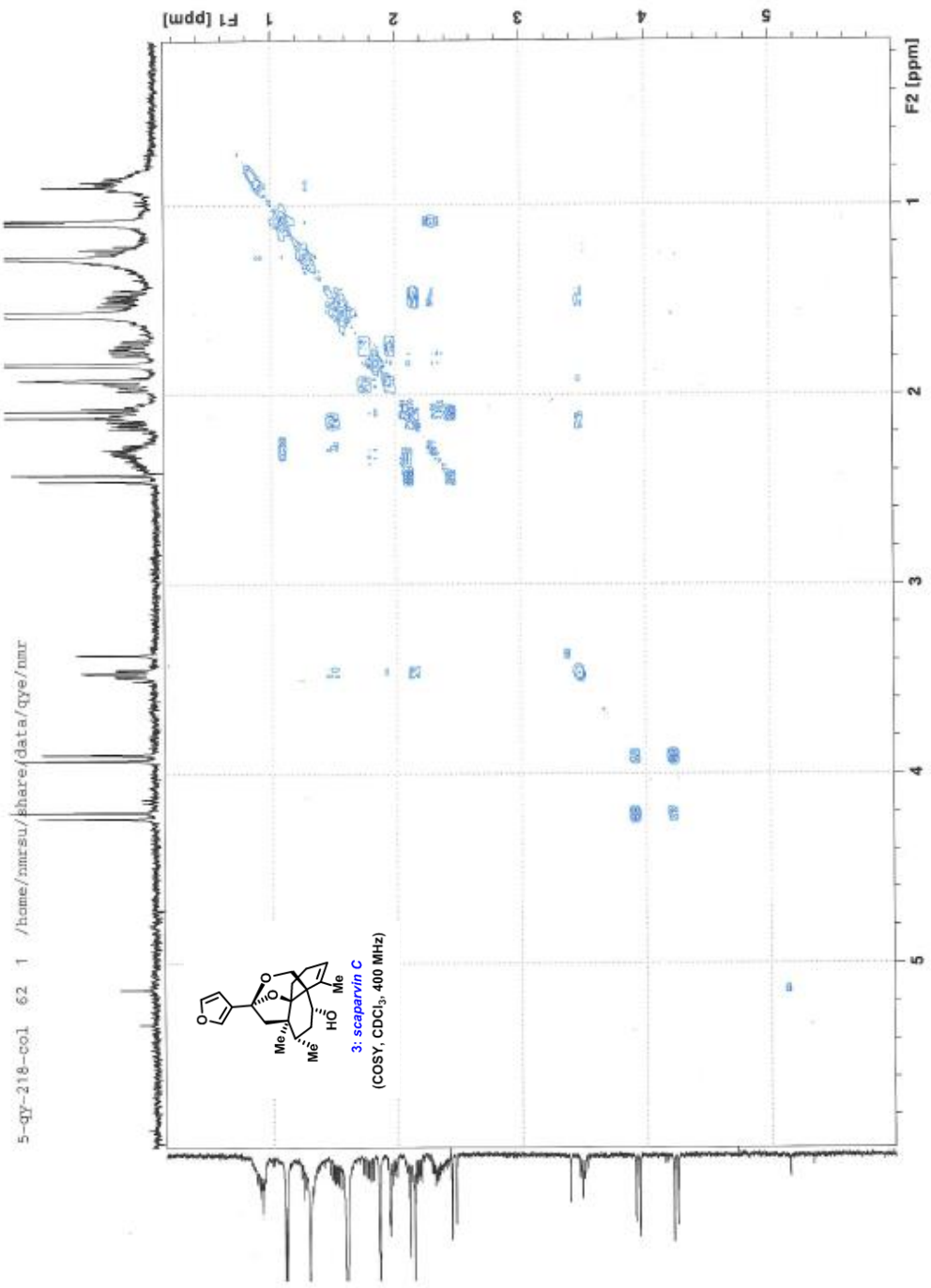
5-qy-218-col 62 1 /home/nmrsu/Bruker/data/qye/nmr
F1 [ppm]
F2 [ppm]
1
2
3
4
5
Me
Me
HO
Me
3: scaparvin C
(COSY, CDCl3, 400 MHz)